UDC 621. 039. 51

JAERI 1006—B

JAERI 1006—B

Analysis of Dynamic Characteristics of British Type Gas Cooled Reactors

研究報告No. 6—B

1959年12月

日本原子力研究所
Japan Atomic Energy Research Institute

JAERI 1006-B U. D. C. 621. 039. 51

英国型ガス冷却原子炉の動特性

要　　旨

英国型動力炉で燃焼がある程度以上進むと，反応度の温度係数が正になることは，この型の原子炉の安全性に関して重要な問題である．

正の温度係数をもつ原子炉の動特性についてアナログ計算機を用いてしらべた．コールダーホール発電所，日本原子力発電株式会社向の動力炉（英国 GEC 社設計），ハンタートストン発電所の3種の原子炉についてしらべた。（それぞれ R-Ⅰ，R-Ⅱ，R-Ⅲ と名付けた。）

R-Ⅰについて簡単なモデルによつて過渡特性をしらべたのち，R-Ⅱ，R-Ⅲについて黒鉛スリーブの影響や，放射，伝熱等も考慮したやや複雑なモデルを用いて解析した。3種の原子炉について得られた過渡特性を比較検討した。

原子炉熱系の伝達関数は複雑な形をしているが，これをみかけ上の時定数によつて近似すると，概略の動特性を求めたり，異なる原子炉の動特性を比較するのに便利であることがわかつた．

正の温度係数の大きさがどの範囲にあれば原子炉は自己平衡性を持つかについて，その限界値を求め，またその限界値を高くするにはどうすればよいかについても検討した．

1959 年 6 月

日本原子力研究所

三井田純一，原　昌雄，須田信英，

都甲泰正，望月恵一

Analysis of Dynamic Characteristics of British Type Gas Cooled Reactors.

Abstract

The positive temperature coefficient of reactivity which a British type reactor obtains over a certain irradiation level of its natural uranium fuel, has presented a new problem to the inherent safety of this type of reactors.

Decribed here in this paper is the analysis of the dynamic characteristics of three British type reactors with positive temperature coefficient of reactivity, using an analog computer. The three reactors considered are Calder Hall reactor, the power reactor proposed to the Japan Atomic Power Company by G. E. C. of Britain, and Hunterstone power reactor. Here, they are referred to as R-I, R-II and R-III, respectively.

Setting up a rather simplified model, transient characteristics of R-I has been studied at first, applying several disturbances to the reactor such as change in reactivity, coolant inlet temperature, and coolant flow. Secondly composing more complex equations of a thermal system on R-II, the same study has been made. In this case the effect of the sleeve and radiative heat transfers between the clad and sleeve, and the sleeve and moderator have been taken into consideration. Thirdly more detailed and comprehensive study has been pursued on R-III, although the same equations as those of R-II have been applied to the thermal system of this reactor.

Results obtaind on R-I, R-II and R-III were compared and analysed.

Especially virtual time constant of the thermal system and critical value of the positive temperature coefficient of moderators for these reactors have been investigated.

These investigations not only imply the possibility of anticipation of a transient behavior of some newly designed reactors without tedious calculations but also indicate the critical point of power reactor stability.

June, 1959.

Junichi Miida, Masao Hara, Nobuhide Suda,

Yasumasa Togo, Keiichi Mochizuki

Japan Atomic Energy Research Institute

PREFACE

This work has been done by one of the subgroups of the Research Project started in JAERI in October 1958, its primary objective being the pursue of the studies on a British type gas-cooled reactor with positive temperature coefficient. The project mentioned above consists of the following three major phases.

(1) Nuclear physics calculation of positive temperature coefficient as a function of burn-up of fuel and operating temperature, by Reactor Development Section. [JAERI 1006-A]

(2) Analysis of dynamic characteristics of a reactor with positive temperature coefficient, by Control and Instrumentation Section, Mechanical Engineering Section, and JPDR Construction Office. [JAERI 1006-B]

(3) Analysis of spatial oscillations of the neutron flux due to a Xe build-up, by JPDR Construction Office. [JAERI 1006-C]

TABLE OF CONTENTS

1. Introduction

It has been disclosed recently that moderator temperature coefficient of reactivity in natural uranium gas-cooled reactors becomes positive at a certain fuel burn-up level and this phenomenon presented new problems to the inherent safety aspects of the reactors of this type.

It is important, therefore, to clarify the transient characteristics of these reactors with positive temperature coefficient of reactivity, from the viewpoints of both reactor safety and control.

Three reactors of this type, the Calder Hall Reactor, JAPCO Reactor (a natural uranium gas-cooled reactor proposed to the Japan Atomic Power Co. by G. E. C. of Britain with an electrical output of 150 MW) and Hunterstone Reactor, each referred to as R-I, R-II and R-III, respectively, have been investigated so far, by means of a PACE analog computer, varying many parameters such as reactivity, positive temperature coefficient, inlet coolant temperature, coolant flow rate, etc., over a wide range.

At the beginning, R-I was chosen and analysed based on the simplest model as a first step of our study.

Secondly R-II was investigated, in which the design incorporates a graphite sleeve around each fuel element to provide a thermal insulation layer between the sleeve and graphite moderator so as to reduce temperature change in moderator. However, decisive conclusion has not yet been obtained on the effect of sleeves, and further investigation is required in this respect.

The third reactor investigated was R-III. In the last two cases, more comprehensive models were applied to the reactor side, however, a heat exchanger was still simulated in the simplest way and the turbine side was neglected.

To further investigate dynamic characteristics of the over-all plant of this type, study is under way simulating the reactor, heat exchanger and the turbine plant in practical detail.

Most of the results obtained in our study show rather good agreement with those obtained on R-I and R-III, presented in 2nd Geneva Conference Reports[1),2)].

Along with this study the degree of accuracy of an analog computation was checked by means of a digital computer for one special case and the pretty good agreement was obtained in both computations, as described in Appendix 5.

This result convinced us that computation error of analog computer analysis is almost negligible for our purposes, and extensive use was made of the analog computer for studies thereafter.

Most of the parameters of R-I and R-III necessary for calculations have been obtained from Reference 3), 4), those of R-II having been given by the Japan Atomic Power Co.

However, some of the parameters, which are not available have been estimated from others available, which are indicated in Appendix 2.

2. The Calder Hall Reactor (R-I)

The purposes of investigating the dynamic characteristics of the prototype reactor were to obtain basic knowledge in the field of reactor dynamic analysis and to proceed to the studies of the advanced reactors of this type.

It was for this reason that the simplest model was considered in this study.

2. 1. Method of Analysis

2. 1. 1. Major Assumptions

1) The reactor is simulated by the unit cell, using a spatially averaged value for each parameter. The model of the unit cell for R-I is shown in **Fig. 2. 1.**

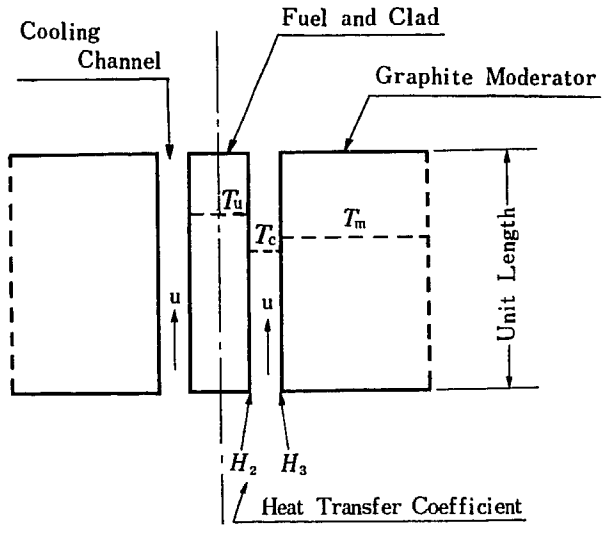

Fig. 2. 1. Model of unit cell for R-I.

2) A coolant loop outside the core is not considered. (The change in outlet temperature does not affect inlet temperature.)

3) Each parameter is represented by a value for the averaged temperature.

4) One delayed neutron group is considered.

5) Axial heat conduction in the solids is neglected.

6) Thermal resistance between the fuel and clad is neglected and heat capacity of the clad is added to the fuel.

7) Temperatures of the fuel, coolant and the graphite moderator are substantially uniform across any horizontal plane.

8) Total heat generation in the core is shared between the fuel rod and graphite block at a constant ratio.

9) Reactivity changes due to the accumulation of fission products are neglected.

10) Radiative heat transfer is neglected.

11) The mean temperatures along the channel are multiplied by the average temperature coefficients of reactivity to give a reactivity change.

2. 1. 2. Basic Equations

Nuclear characteristics are represented by the following two equations, assuming one delayed neutron group,

$$\frac{dn}{dt}=\frac{\rho-\beta}{l}n+\lambda C$$

$$\frac{dC}{dt}=\frac{\beta}{l}n-\lambda C \qquad (2.1)$$

Average power density Q is considered proportional to the average neutron density n, therefore,

$$\frac{dQ}{dt}=\frac{\rho-\beta}{l}Q+\lambda h$$
$$\frac{dh}{dt}=\frac{\beta}{l}Q-\lambda h \qquad (2.2)$$

Thermal equations are

$$C_u\frac{dT_u}{dt}=\mu_u Q+H_2(T_c-T_u)$$
$$C_c\frac{dT_c}{dt}=H_2(T_u-T_c)+H_3(T_m-T_c)-\frac{uC_c}{L}(T_{out}-T_{in})$$
$$C_m\frac{dT_m}{dt}=\mu_m Q+H_3(T_c-T_m)$$
$$T_c=\frac{1}{2}(T_{out}+T_{in}) \qquad (2.3)$$

Nuclear and thermal characteristics of a reactor are correlated through the effect of temperature on reactivity and this effect is divided into two parts: one is due to fuel temperature and the other to moderator temperature. Designating fuel temperature coefficient α_u and moderator coefficient α_m, total reactivity ρ is given by

$$\rho=\rho_{ex}+\alpha_u\Delta T_u+\alpha_m\Delta T_m \qquad (2.4)$$

where ρ_{ex} represents equivalent reactivity of the external disturbance.

Considering the deviation of each variable from the steady state value, and rearranging the above equations, they give

$$\frac{d\Delta Q}{dt}=\frac{\rho}{l}(Q_0+\Delta Q)-\frac{\beta}{l}\Delta Q+\lambda\Delta h$$
$$\frac{d\Delta h}{dt}=\frac{\beta}{l}\Delta Q-\lambda\Delta h$$
$$C_u\frac{d\Delta T_u}{dt}=\mu_u\Delta Q+H_2(\Delta T_c-\Delta T_u)$$
$$C_c\frac{d\Delta T_c}{dt}=H_2(\Delta T_u-\Delta T_c)+H_3(\Delta T_m-\Delta T_c)-\frac{2uC_c}{L}(\Delta T_c-\Delta T_{in})$$
$$C_m\frac{d\Delta T_m}{dt}=\mu_m\Delta Q+H_3(\Delta T_c-\Delta T_m)$$
$$\Delta T_c=\frac{\Delta T_{out}+\Delta T_{in}}{2} \qquad (2.5)$$

Although Eqs. (2.4), (2.5) are basic equations for analysis, a slight modification was applied to computation in a certain case.

2. 1. 3. Scope of Study

Changes of Q, T_u, T_c, T_m, ρ and h with time are recorded. Parameters are varied as follows:

1) α_m

Since value of α_m varies with fuel burn-up over a wide range and also satisfactory experimental data on α_m are not available at this moment, α_m was made variable within the range of $-5\sim+20\times10^{-5}/°C$.

2) ρ_{ex}

In order to investigate the transient characteristics caused by the step-wise reactivity insertion in the reactor operating at a steady state, ρ_{ex} was changed step-wise. The magnitude of the reactivity steps inserted covers from 9×10^{-5} (corresponding to about one inch movement of the

center control rod of R-I) to 9×10^{-3} (exceeding prompt criticality).

2) β

It is expected that the effective value of β decreases as plutonium builds up in the reactor with higher fuel burn-up. Therefore, this effect on the transient phenomena was investigated, varying value of β between 0.3% and 0.73%.

4) T_{in}

T_{in} was changed both step-wise and linear-wise in order to simulate the sudden change in inlet coolant temperature due to, for example, a heat exchanger failure. The change was made in the range of $-20°C\sim+50°C$ for the step-wise case and $0.02\sim0.1°C$/sec for the linear-wise case.

5) u

Anticipating the drastic change in coolant flow rate due to a blower failure or duct failure, transient response was studied to the step-wise changes in u. Substantial modifications were made to the equations shown in 2.1.2 for this study. Heat transfer coefficient is assumed to be proportional to $u^{0.8}$. u was chosen 90%, 50%, 5% of the rated flow.

2.2 Results

Only representative curves are illustrated in **Figs. 2.2.** through **2.5.**

1) Response to the step change in ρ_{ex} for R-I (**Fig. 2.2**)

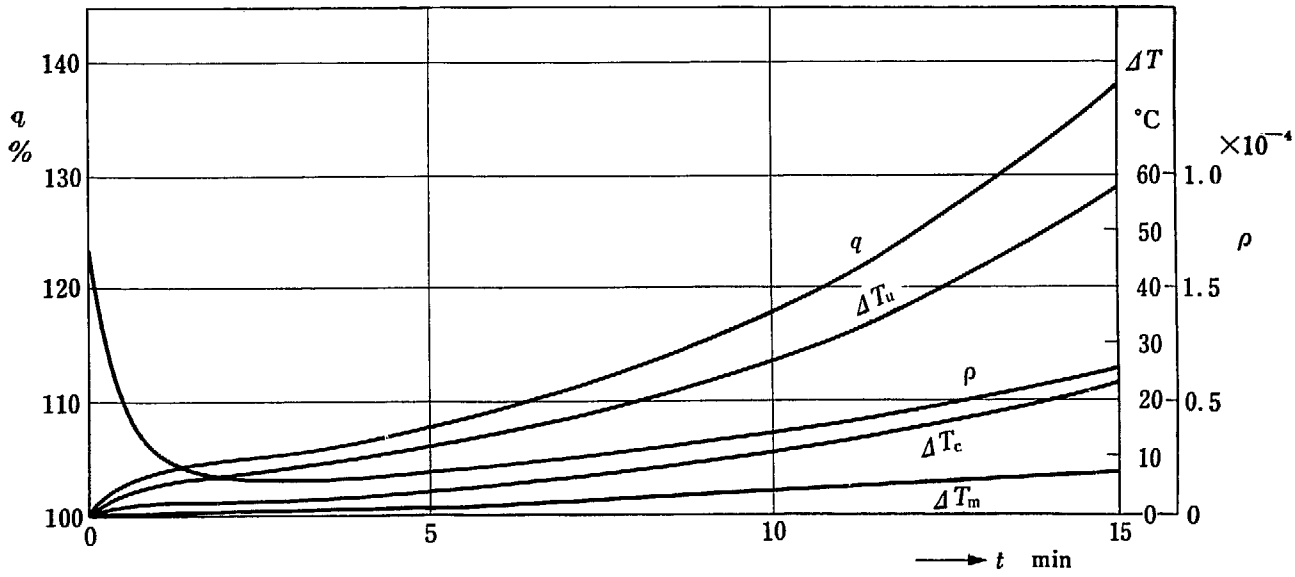

Fig. 2.2. Response to step change in ρ_{ex} for R-I. $\rho_{ex}=1.2\times10^{-4}$, $\alpha_m=15\times10^{-5}$/C°

Step-wise increase in ρ tends to cause a prompt increase in q, therefore, increase in T_u which in turn decreases ρ due to the negative α_u. In the meantime, however, T_m goes up slowly and ρ begins to rise due to the positive temperature coefficient of the moderator. It can be seen that transient behavior of this kind is based on the fact that initially the effect of shorter time constant of T_u is predominant and later on, longer time constant of T_m has primary effect on the response.

2) Response of q to various step changes in ΔT_{in} (**Figs. 2.3, 2.4**)

For the step-wise increase in T_{in}, T_u increases due to the higher coolant temperature and q decreases due to the negative α_u.

However, as T_m increases in the meanwhile, the effect of positive α_m becomes predominant

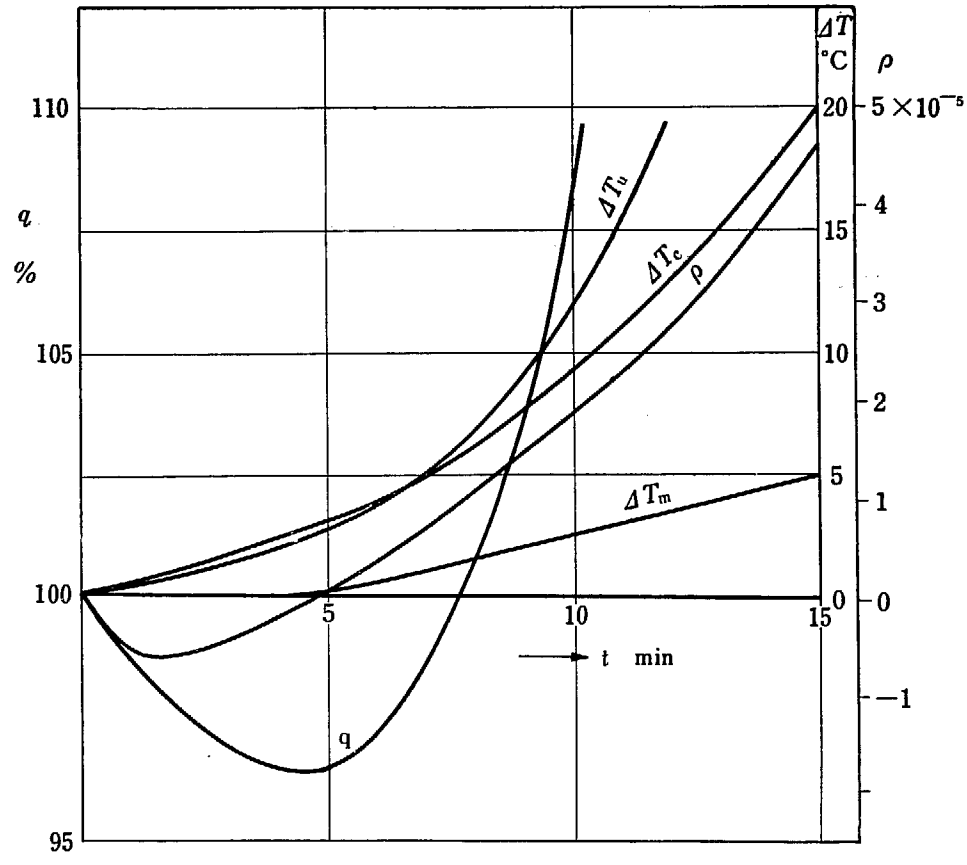

Fig. 2. 3. Response to ramp change in ΔT_{in} for R-I. 0.02°C/sec, $\alpha_m = 12.5 \times 10^{-5}$/°C

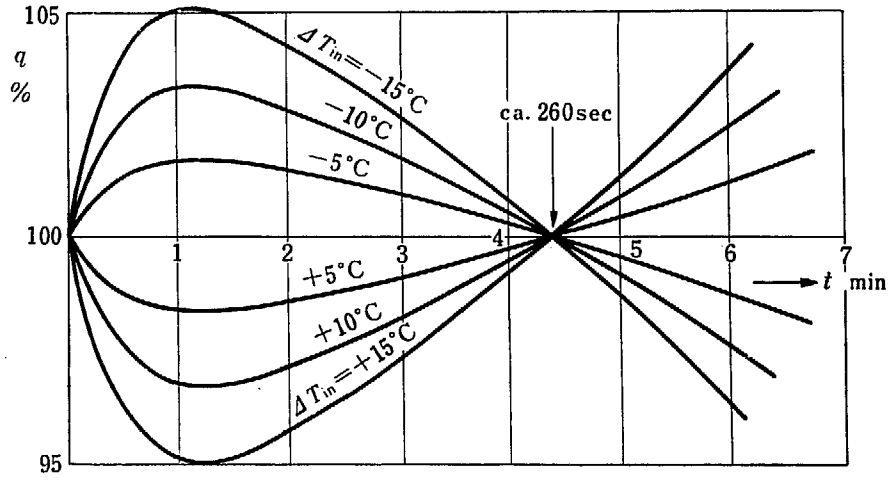

Fig. 2. 4. Response of q to various step change in ΔT_{in}. $\alpha_m = 12.5 \times 10^{-5}$/°C

and it causes steady increases in ρ and q. For the step-wise decrease in T_{in}, transient tendency is quite reverse. The most interesting features to be observed here is that the transient curves of q become equal to zero again about 4.5 minutes after the initiation of transient regardless of the magnitude of the step-wise T_{in}. The same tendency is also observed for the ramp-wise change in T_{in}. This feature can be explained as described in Appedix 6.

3) Response to the step change in Δu for R-I (**Fig. 2. 5**)

Step-wise decrease in u gives rise to sudden increase in T_u and q decreases for the first couple

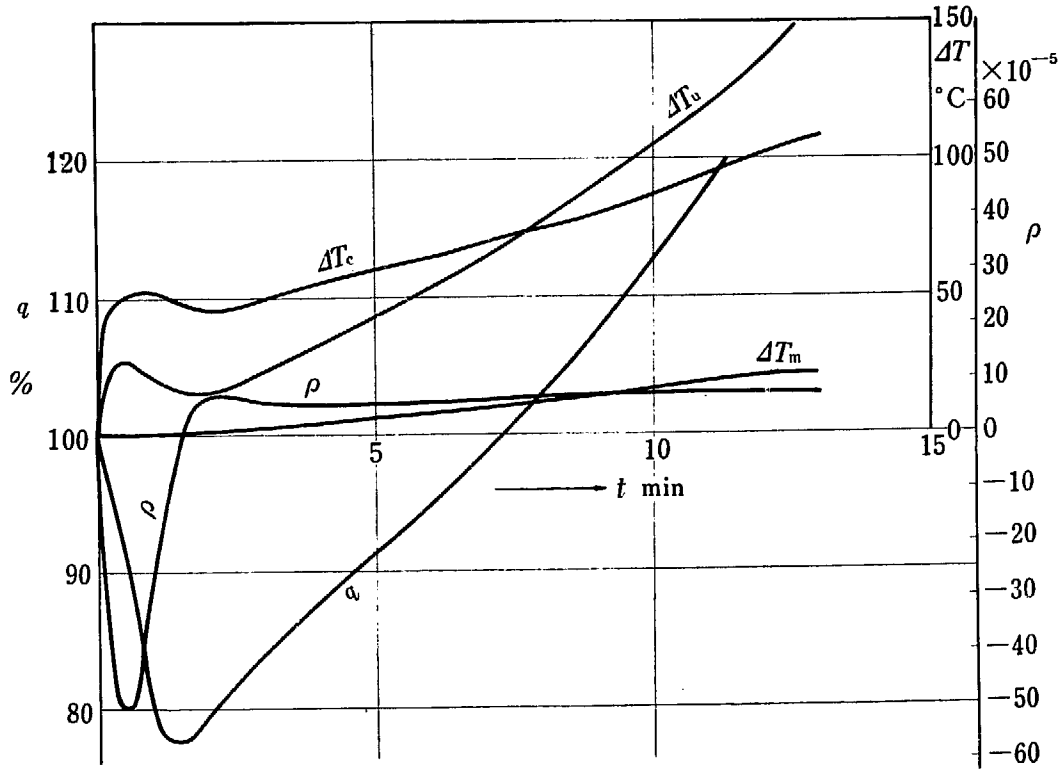

Fig. 2. 5. Response to step change in Δu for R-I. $\Delta u = -0.5u_0$, $\alpha_m = 12.5 \times 10^{-5}$/°C

of minutes due to the negative α_u, which balances the initial increase in T_u. Subsequently, both q and T_u begin to go up steadily due to positive α_m as T_m increases.

3. The JAPCO Reactor (R-II)

The primary purpose of this research is to investigate the dynamic characteristics of the gas-cooled reactors in general and to prove the safety features or to establish countermeasures against a power excursion for the JAPCO Reactor, even in case it operates with positive temperature coefficients of reactivity.

To solve these problems an extensive study was done on R-II and this was followed by the study on R-III for comparison.

The basic behavior of these reactors was clarified and some interesting results were obtained in comparing the designs of these two reactors.

3. 1. Method of Analysis

3. 1. 1. Major Assumptions[5)]

1) In order to represent the whole core by the unit cell, a statistically weighted value for the entire core was applied to each parameter. The model of the unit cell for R-II is shown in **Fig. 3. 1.**

2) Each parameter is represented by a value for averaged temperature.

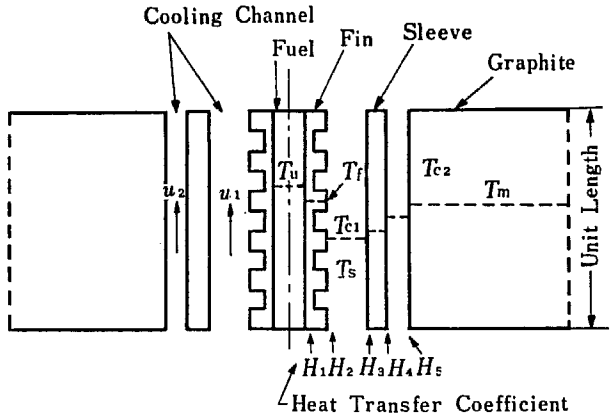

Fig. 3. 1. Model of unit cell for R-II.

3) One delayed neutron group is considered.

4) Axial heat conduction in the solids is neglected.

5) Temperatures of the clad, coolant, sleeve and the moderator are substantially uniform across any horizontal plane.

6) Total heat generation in the core is shared among the fuel rod, sleeve and the moderator at a constant ratio.

7) Reactivity change due to the accumulation of fission products is neglected.

8) The radiative heat transfer is proportional to the difference between the fourth powers of the mean temperatures.

9) Axial temperature distributions retain their steady state shape during transient.

10) The heat generation over the length of the fuel plus two extrapolation distances is of a cosine form and zero beyond the ends of the fuel.

11) The statistically weighted mean temperatures along the channel, $\bar{T}$, are multiplied by the average temperature coefficients of reactivity to give reactivity changes.

The axial statistically weighted mean values are determined by multiplying each term by the (flux shape factor)^2, i. e. $\cos^2\frac{\pi}{L_1}\left(x-\frac{L}{2}\right)$, and integrating along the length of the channel.

Thus, for temperature T, the statistically weighted mean value, $\bar{T}$, is given by

$$\bar{T}\int_0^L \cos^2\frac{\pi}{L_1}\left(x-\frac{L}{2}\right)dx=\int_0^L T\cos^2\frac{\pi}{L_1}\left(x-\frac{L}{2}\right)dx$$

12) Heat transfer through the boundary of the unit cell is zero.

13) The coolant mass flow between the sleeve and moderator is equal to one percent mass flow.

3. 1. 2. Basic Equations

In the thermal calculation, a unit cell of unit lenghth as shown in **Fig. 3. 1** was chosen.

At a distance x from the bottom of the channel, equations of heat balance for the unit cell of unit length are given as follows:

$$C_u(x,t)\frac{\partial T_u(x,t)}{\partial t}=\rho_u Q(x,t)-H_1(x,t)\left[T_u(x,t)-T_f(x,t)\right]$$

$$C_f(x,t)\frac{\partial T_f(x,t)}{\partial t}=H_1(x,t)\left[T_u(x,t)-T_f(x,t)\right]-H_2(x,t)\left[T_f(x,t)-T_{c1}(x,t)\right]$$
$$-R_1\left[T_f(x,t)^4-T_s(x,t)^4\right]$$

$$C_1(x,t)\left[\frac{\partial T_{c1}(x,t)}{\partial t}+u_1(x,t)\frac{\partial T_{c1}(x,t)}{\partial x}\right]=H_2(x,t)\left[T_f(x,t)-T_{c1}(x,t)\right]$$
$$-H_3(x,t)\left[T_{c1}(x,t)-T_s(x,t)\right]$$
$$C_s(x,t)\frac{\partial T_s(x,t)}{\partial t}=\mu_s Q(x,t)+H_3(x,t)\left[T_{c1}(x,t)-T_s(x,t)\right]+R_1\left[T_f(x,t)^4-T_s(x,t)^4\right]$$
$$-H_4(x,t)\left[T_s(x,t)-T_{c2}(x,t)\right]-R_2\left[T_s(x,t)^4-T_m(x,t)^4\right]$$
$$C_2(x,t)\left[\frac{\partial T_{c2}(x,t)}{\partial t}+u_2(x,t)\frac{\partial T_{c2}(x,t)}{\partial x}\right]=H_4(x,t)\left[T_s(x,t)-T_{c2}(x,t)\right]$$
$$-H_5(x,t)\left[T_{c2}(x,t)-T_m(x,t)\right]$$
$$C_m(x,t)\frac{\partial T_m(x,t)}{\partial t}=\mu_m Q(x,t)+H_5(x,t)\left[T_{c2}(x,t)-T_m(x,t)\right]+R_2\left[T_s(x,t)^4-T_m(x,t)^4\right] \quad (3.1)$$

Averaging the above equations along the channel, equations for statistically weighted mean temperatures are obtained.

$$C_u\frac{d\bar{T}_u}{dt}=\mu_u fQ-H_1(\bar{T}_u-\bar{T}_f)$$
$$C_f\frac{d\bar{T}_f}{dt}=H_1(\bar{T}_u-\bar{T}_f)-H_2(\bar{T}_f-\bar{T}_{c1})-R_1(\bar{T}_f^4-\bar{T}_s^4)$$
$$C_1\left[\frac{d\bar{T}_{c1}}{dt}+u_1 f\frac{2(\bar{T}_{c1}-T_{in})}{L}\right]=H_2(\bar{T}_f-\bar{T}_{c1})-H_3(\bar{T}_{c1}-\bar{T}_s)$$
$$C_s\frac{d\bar{T}_s}{dt}=\mu_s fQ+H_3(\bar{T}_{c1}-\bar{T}_s)+R_1(\bar{T}_f^4-\bar{T}_s^4)-H_4(\bar{T}_s-\bar{T}_{c2})-R_2(\bar{T}_s^4-\bar{T}_m^4)$$
$$C_2\left[\frac{d\bar{T}_{c2}}{dt}+u_2 f\frac{2(\bar{T}_{c2}-T_{in})}{L}\right]=H_4(\bar{T}_s-\bar{T}_{c2})-H_5(\bar{T}_{c2}-\bar{T}_m)$$
$$C_m\frac{d\bar{T}_m}{dt}=\mu_m fQ+H_5(\bar{T}_{c2}-\bar{T}_m)+R_2(\bar{T}_s^4-\bar{T}_m^4) \quad (3.2)$$

In addition, assuming that the temperature distribution of the clad along the channel is given and that the maximum clad temperature is attained at the distance x_m from the bottom of the channel, the maximum clad temperature is calculated from the equations of heat balance at that point.

$$C_{um}\frac{dT_{um}}{dt}=\mu_u Q_m-H_{1m}(T_{um}-T_{fm})$$
$$C_{fm}\frac{dT_{fm}}{dt}=H_{1m}(T_{um}-T_{fm})-H_{2m}(T_{fm}-T_{c1m})-R_1(T_{fm}^4-T_{sm}^4) \quad (3.3)$$

In the last term of the second eqution above, T_{sm} is approximated by $\bar{T}_s$ for simplifying the computation, and T_{c1m} is given as follows based on the assumption 9) above.

$$\frac{T_{c1m}-T_{in}}{\bar{T}_{c1}-T_{in}}=k \quad (3.4)$$

These equations are modified for use with a deviation of each variable. Terms of radiative heat transfer are linearized neglecting higher order terms of $\Delta\bar{T}$ in expansion of $(\bar{T}+\Delta\bar{T})^4$.

$$C_u\frac{d\Delta\bar{T}_u}{dt}=\mu_u fQ_0\Delta q-H_1(\Delta\bar{T}_u-\Delta\bar{T}_f)$$
$$C_f\frac{d\Delta\bar{T}_f}{dt}=H_1(\Delta\bar{T}_u-\Delta\bar{T}_f)-H_2(\Delta\bar{T}_f-\Delta\bar{T}_{c1})-R_1(4\bar{T}_{f0}^3\Delta\bar{T}_f-4\bar{T}_{s0}^4\Delta\bar{T}_s)$$
$$C_1\frac{d\Delta\bar{T}_{c1}}{dt}=H_2(\Delta T_f-\Delta\bar{T}_{c1})-H_3(\Delta\bar{T}_{c1}-\Delta\bar{T}_s)-\frac{2C_1u_1}{L}f(\Delta\bar{T}_{c1}-\Delta T_{in})$$
$$C_s\frac{d\Delta\bar{T}_s}{dt}=\mu_s fQ_0\Delta q+H_3(\Delta\bar{T}_{c1}-\Delta\bar{T}_s)+R_1(4\bar{T}_{f0}^3\Delta\bar{T}_f-4\bar{T}_{s0}^3\Delta\bar{T}_s)$$

$$-H_4(\Delta\bar{T}_s-\Delta\bar{T}_{c2})-R_2(4\bar{T}_{s0}^3\Delta\bar{T}_s-4\bar{T}_{m0}^3\Delta\bar{T}_m)$$

$$C_2\frac{d\Delta\bar{T}_{c2}}{dt}=H_4(\Delta\bar{T}_s-\Delta\bar{T}_{c2})-H_5(\Delta\bar{T}_{c2}-\Delta\bar{T}_m)-\frac{2C_2u_2}{L}f(\Delta\bar{T}_{c2}-\Delta T_{in})$$

$$C_m\frac{d\Delta\bar{T}_m}{dt}=\mu_m fQ_0\Delta q+H_5(\Delta\bar{T}_{c2}-\Delta\bar{T}_m)+R_2(4\bar{T}_{s0}^3\Delta\bar{T}_s-4\bar{T}_{m0}^3\Delta\bar{T}_m)$$

$$C_{um}\frac{d\Delta T_{um}}{dt}=\mu_u Q_{m0}\Delta q-H_{1m}(\Delta T_{um}-\Delta T_{fm})$$

$$C_{fm}\frac{d\Delta T_{fm}}{dt}=H_{1m}(\Delta T_{um}-\Delta T_{fm})-H_{2m}\{\Delta T_{fm}-k\Delta\bar{T}_{c1}+(k-1)\Delta T_{in}\}$$

$$-R_1(4T_{fm0}^3\Delta T_{fm}-4\bar{T}_{s0}^3\Delta\bar{T}_s) \tag{3.5}$$

Heat generation is given by the following equations of neutron kinetics.

$$\frac{dQ}{dt}=\frac{\rho-\beta}{l}Q+\lambda h$$

$$\frac{dh}{dt}=\frac{\beta}{l}Q-\lambda h \tag{3.6}$$

These are also modified for use with deviations.

$$\frac{d\Delta q}{dt}=\frac{\rho}{l}(1+\Delta q)-\frac{\beta}{l}\Delta q+\lambda\Delta r$$

$$\frac{d\Delta r}{dt}=\frac{\beta}{l}\Delta q-\lambda\Delta r \tag{3.7}$$

Nuclear and thermal behaviors of a reactor are correlated through the temperature coefficients of reactivity.

$$\rho=\rho_{ex}+\alpha_u\Delta\bar{T}_u+\alpha_s\Delta\bar{T}_s+\alpha_m\Delta\bar{T}_m \tag{3.8}$$

In the evaluation of the dynamic response of the reactor with a wide range change in coolant flow rate, heat transfer coefficients H_2, H_3, H_4 and H_5 are assumed to be proportional to $u^{0.8}$ therefore, Eqs. (3.5) must be modified as follows:

$$C_u\frac{d\Delta\bar{T}_u}{dt}=\mu_u fQ_0\Delta q-H_1(\Delta\bar{T}_u-\Delta\bar{T}_f)$$

$$C_f\frac{d\Delta\bar{T}_f}{dt}=H_1(\Delta\bar{T}_u-\Delta\bar{T}_f)-H_{20}(\bar{T}_{f0}-\bar{T}_{c10})(\xi^{0.8}-1)-H_{20}(\Delta\bar{T}_f-\Delta\bar{T}_{c1})\xi^{0.8}$$

$$-R_1(4\bar{T}_{f0}^3\Delta\bar{T}_f-4\bar{T}_{f0}^3\Delta\bar{T}_s)$$

$$C_1\frac{d\Delta\bar{T}_{c1}}{dt}=H_{20}(\bar{T}_{f0}-\bar{T}_{c10})\xi^{0.8}-H_{30}(\bar{T}_{c10}-\bar{T}_{s0})\xi^{0.8}-\frac{2u_{10}C_1}{L}f(\bar{T}_{c10}-T_{in0})\xi$$

$$+H_{20}(\Delta\bar{T}_f-\Delta\bar{T}_{c1})\times\xi^{0.8}-H_{30}(\Delta\bar{T}_{c1}-\Delta\bar{T}_s)\times\xi^{0.8}-\frac{2u_{10}C_1}{L}f(\Delta\bar{T}_{c1}-\Delta T_{in})\xi$$

$$C_s\frac{d\Delta\bar{T}_s}{dt}=\mu_s fQ_0\Delta q+H_{30}(\bar{T}_{c10}-\bar{T}_{s0})(\xi^{0.8}-1)-H_{40}(\bar{T}_{s0}-\bar{T}_{c20})(\xi^{0.8}-1)$$

$$+R_1(4\bar{T}_{f0}^3\Delta\bar{T}_f-4\bar{T}_{s0}^3\Delta\bar{T}_s)-R_2(4\bar{T}_{s0}^3\Delta\bar{T}_s-4\bar{T}_{m0}^3\Delta\bar{T}_m)$$

$$+H_{30}(\Delta\bar{T}_{c1}-\Delta\bar{T}_s)\xi^{0.8}-H_{40}(\Delta\bar{T}_s-\Delta\bar{T}_{c2})\times\xi^{0.8}$$

$$C_2\frac{d\Delta\bar{T}_{c2}}{dt}=H_{40}(\bar{T}_{s0}-\bar{T}_{c20})\xi^{0.8}-H_{50}(\bar{T}_{c20}-\bar{T}_{m0})\xi^{0.8}-\frac{2u_{20}C_2}{L}f(\bar{T}_{c20}-T_{in0})\xi$$

$$+H_{40}(\Delta\bar{T}_s-\Delta\bar{T}_{c2})\times\xi^{0.8}-H_{50}(\Delta\bar{T}_{c2}-\Delta\bar{T}_m)\times\xi^{0.8}-\frac{2u_{20}C_2}{L}f(\Delta\bar{T}_{c2}-\Delta T_{in})\xi$$

$$C_m\frac{d\Delta\bar{T}_m}{dt}=\mu_m fQ_0\Delta q+H_{50}(\bar{T}_{c20}-\bar{T}_{m0})(\xi^{0.8}-1)+R_2(4\bar{T}_{s0}^3\Delta\bar{T}_s-4\bar{T}_{m0}^3\Delta\bar{T}_m)$$

$$+H_{50}(\Delta\bar{T}_{c2}-\Delta\bar{T}_m)\times\xi^{0.8}$$

$$C_{um}\frac{d\Delta T_{um}}{dt}=\mu_u Q_{m0}\Delta q-H_{1m}(\Delta T_{um}-\Delta T_{fm})$$

$$C_{fm}\frac{d\Delta T_{fm}}{dt}=H_1(\Delta T_{um}-\Delta T_{fm})-H_{20}\{T_{fm0}-k\bar{T}_{c10}+(k-1)T_{in0}\}(\xi^{0.8}-1)$$
$$-R_1(4T_{fm0}{}^3\Delta T_{fm}-4\bar{T}_{s0}{}^3\Delta\bar{T}_s)-H_{20}\{\Delta T_{fm}-k\Delta\bar{T}_{c1}+(k-1)\Delta T_{in}\}\times\xi^{0.8} \quad (3.9)$$

3. 1. 3. Scope of study

1) α_m

The moderator temperature coefficient of reactivity is -5×10^{-5}/°C for the new fuel, and becomes positive and as large as $+15\times10^{-5}$/°C as plutonium builds up in the fuel[6),11)]. Therefore, these two extreme values are applied to α_m in this study.

2) α_s α_s is chosen as $1.8\times\alpha_m\frac{V_s}{V_s+V_m}$.

3) ρ_{ex} Step-wise and ramp-wise reactivity increases are applied as a disturbance.
step-wise 1.2×10^{-4}
ramp-wise 2.0×10^{-6}/sec* for 60 sec

4) T_{in} Ramp-wise inlet temperature rise, 0.02°C/sec for 60 sec, is applied.

5) u Ramp-wise flow rate decrease, −2%/sec for 30 sec, is applied.

3. 2. Results

Representative results are shown in **Figs. 3. 2.** through **3. 5.** In general, tendencies of transient characteristics for R-II are quite similar to those obtained for R-I, however, it can be understood very easily that R-II gives better transient characteristics for R-II compared to R-I. Although better transient characteristics for R-II are considered due to the effect of the sleeve, the detailed

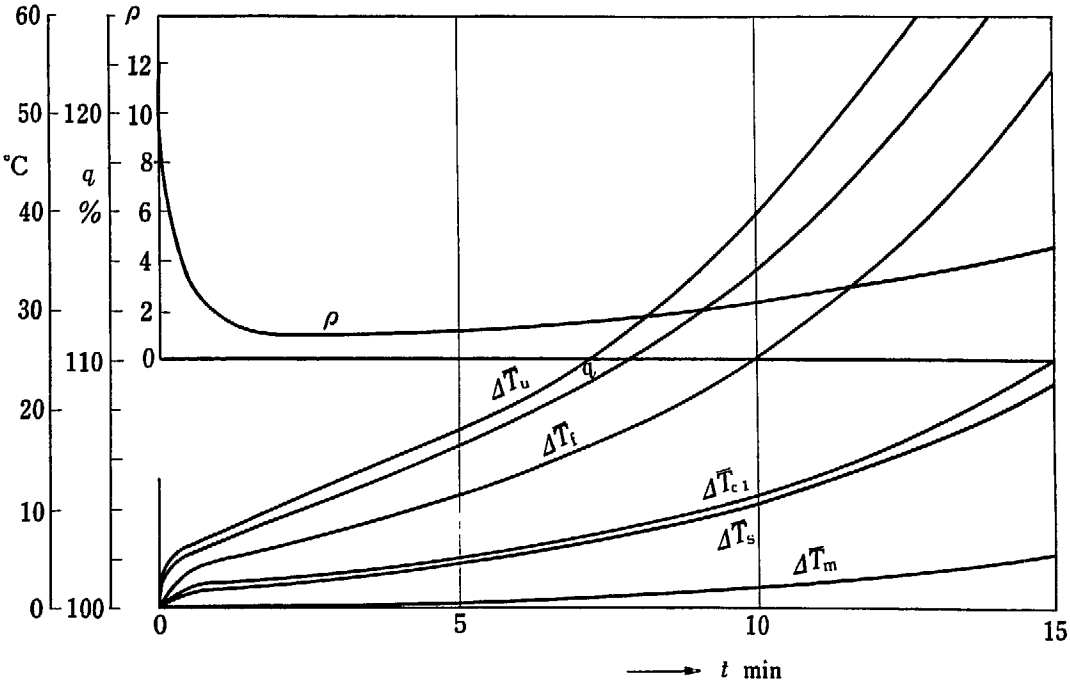

Fig. 3. 2. Response to step change in ρ_{ex} for R-II. $\rho=1.2\times10^{-4}$, $\alpha_m=15\times10^{-5}$/°C

* (2.0×10^{-6}/sec is the rate of withdrawal of control rods for R-I, not for R-II)

analyses are given in Chapt. 4.

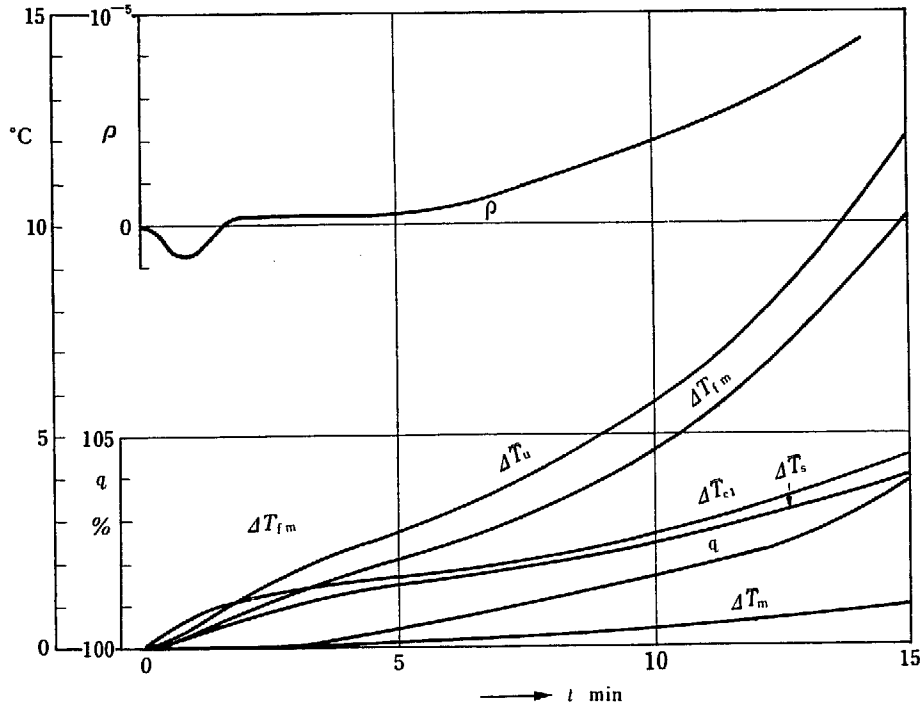

Fig. 3. 3. Response to ramp change in ΔT_{in} for R-II. 0.02°C/sec×60sec. $\alpha_m = 15 \times 10^{-5}$/°C

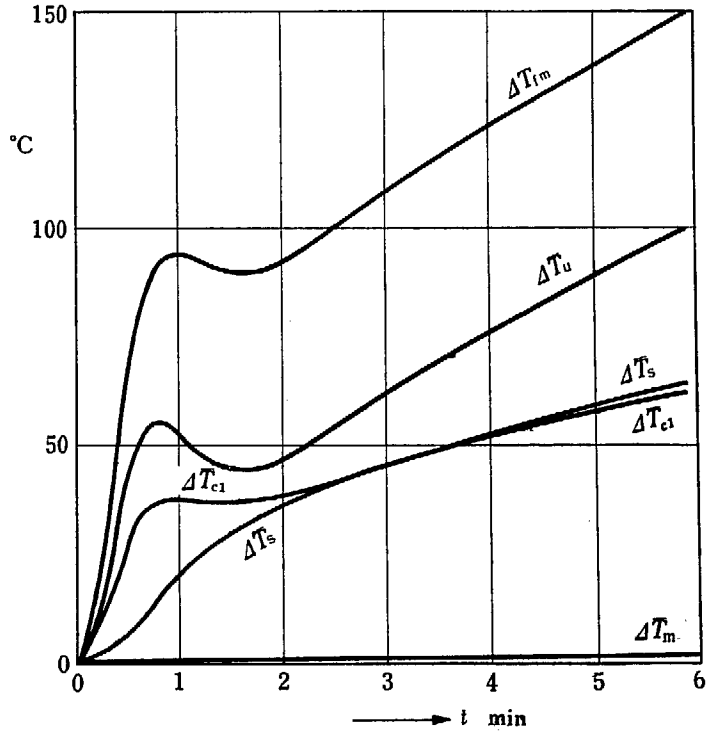

Fig. 3. 4. Response of ΔT to Ramp Change in Δu for R-II. −2%/sec×30sec. $\alpha = 15 \times 10^{-5}$/°C

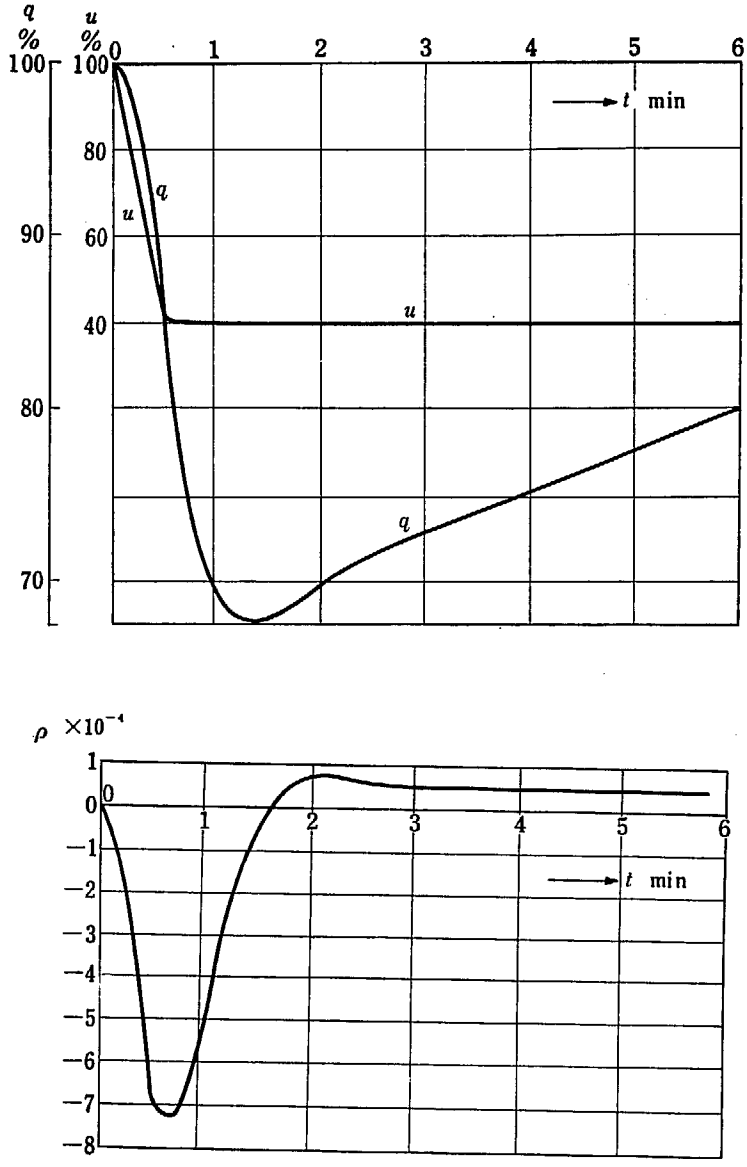

Fig. 3. 5. Response of q and ρ to Ramp Change in Δu for R-II. $-2\%/\text{sec} \times 30\text{sec}$, $\alpha_m = 15 \times 10^{-5}/°C$

4. The Hunterstone Reactor (R-III)

4. 1. Method of Analysis

4. 1. 1. Major Assumptions

The same assumptions as R-II are applied,

4. 1. 2. Basic Equations

Basic equations are almost same as Eqs. (3. 1) through (3. 9) for R-II. However, the simply weighted mean temperatures, T, are used here instead of the statistically weighted mean temperature, $\bar{T}$. Therefore, factor f is introduced into Eq. (3. 8), since $\Delta\bar{T}=f\Delta T$ holds, assuming a cosine distribution of ΔT along the channel. It is noted that $\bar{T}$ is shown in the figures for R-II, while T for R-III, therefore $\bar{T}$ should be divided by f for a comparison purpose.

4. 1. 3. Scope of Study

1) β and λ

The values of β and λ are changed in three ways.

Case	β	λ	$\Sigma_{a49}/\Sigma_{a25}$
I	0.0064	0.0768	0
II	0.005	0.075	1/2
III	0.004	0.07	1/1

As for Σ_{a25} and Σ_{a49} as a function of burnup of fuel, refer to 11).

2) α_m

Three values, -5, 0 and 15×10^{-5}/°C are applied to α_m.

3) α_s

In most cases the sleeve temperature coefficient, α_s, is given by,

$$\alpha_s=1.8\ \alpha_m\frac{V_s}{V_s+V_m}.$$

However, the factor 1. 15 in the place of 1. 8 is also applied in some cases for comparison.

4) H

Because of the uncertainly in calculation of the heat transfer coefficients H_1, H_2, H_3, H_4 and H_5, these values are also varied in the range of $\pm30\%$ of the calculated values.

5) The effect of sleeves

In order to clarify the effect of sleeves on the dynamic characteristics of the reactor, comparison is made on two models, one with sleeves and the other without sleeves. For this purpose, the following fictitious model is considered.

i) The gap between the sleeve and moderator is filled with graphite,

ii) the heat capacity of the moderator of this model is equal to that of the moderator plus the sleeve for the model with sleeves, and

iii) the moderator temperature coefficient is equal to the sum of α_m and α_s for the model with sleeves.

6) ρ_{ex}

Step-wise reactivities, $+1.2\times10^{-4}$ and $+3\times10^{-4}$, are added as a disturbance. (The rate of withdrawal of the control rods is roughly equal to 3×10^{-5}/sec.)

7) T_{in}

T_{in} is changed as follows:

Step-wise 12°C,

Ramp-wise 0. 2°C/sec × 60 sec
0. 1 〃 × 60 〃
0. 02 〃 × 60 〃
−0. 2 〃 × 60 〃
−0. 1 〃 × 60 〃

8) The effect of heat exchangers

A heat exchanger is simulated in the simplest way.

$$\Delta T_{in}(t) = \mu T_{out}(t-20), \quad \text{where} \quad \mu = 0 \sim 1. \tag{4.1}$$

Twenty seconds represents the time required for the coolant recirculation from the outlet to the inlet of the reactor through the heat exchanger, and $\mu=0$ stands for an extreme case where T_{in} can be maintained at a constant value regardless of ΔT_{out}.

The responses to step change in ρ_{ex} are obtained for different values of μ.

9) u

The coolant flow rate is varied as follows:

Ramp-wise $-1\%/\text{sec} \times 60$ sec
-2 〃 $\times 30$ 〃
-2 〃 $\times 15$ 〃
-4 〃 $\times 7.5$ 〃

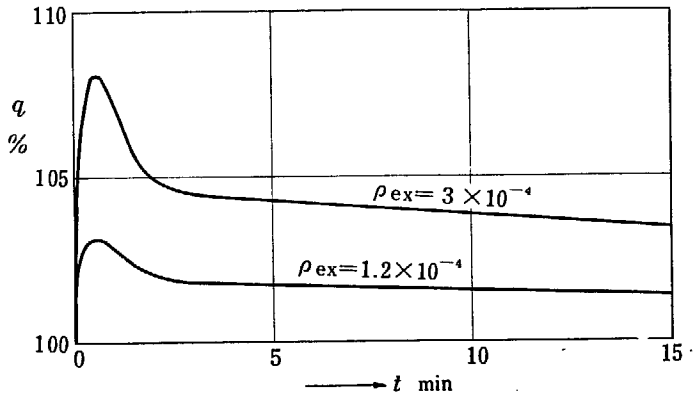

Fig. 4. 1. a. Response of q to step change in ρ_{ex} for R-III. $\rho_{ex}=3\times10^{-4}$, 1.2×10^{-4}, $\alpha_m=-5\times10^{-5}/°C$

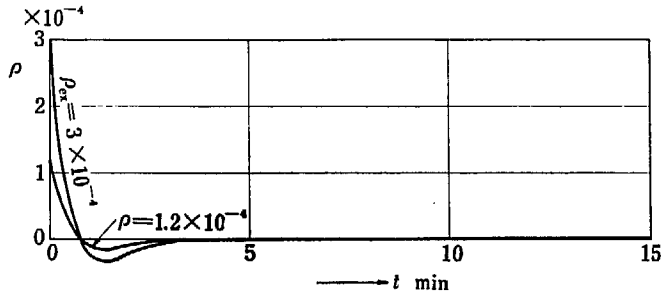

Fig. 4. 1. b. Response of ρ to step change in ρ_{ex} for R-III. $\rho_{ex}=3\times10^{-4}$, 1.2×10^{-4}, $\alpha_m=-5\times10^{-5}/°C$

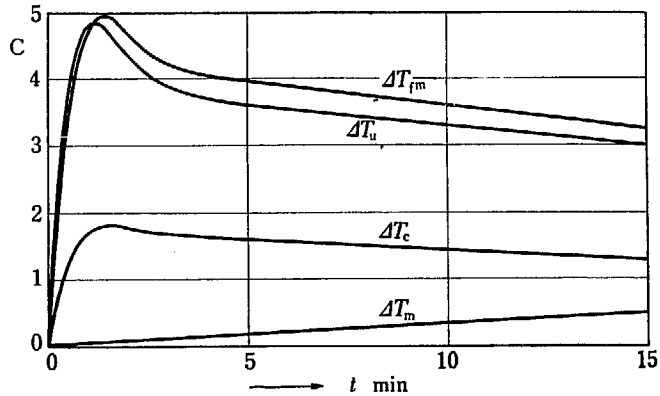

Fig. 4. 1. c. Response of ΔT to step change in ρ_{ex} for R-III. $\rho_{ex}=1.2\times10^{-4}$, $\alpha_m=-5\times10^{-5}/°C$

4. 2. Results

Rather comprehensive results are shown in **Figs. 4. 1** through **4. 18.**

1) Response of R-III with $\alpha_m<0$ to the step change in ρ_{ex}. (**Figs. 4. 1. a., 4. 1. b., 4. 1. c.**)

In the case of $\alpha_m<0$ and $\alpha_m=0$, the reactor is self-regulating for external disturbance in ρ. Strictly speaking, even for $0<\alpha_m<\alpha_{mc}$, the reactor is still self-regulating, as described in 5. 3. For $\alpha_m<0$, temperatures other than T_m are slowly decreasing even after 15 minutes, while only T_m which has longer time constant is still slightly increasing. T_u decreases by the amount just compensating for the reduction in ρ due to the increase of T_m.

2) Response of R-III with $\alpha_m>0$ to the step change in ρ_{ex}.

Since $\alpha_m>\alpha_{mc}$ in this case, the system is not self-regulating. Detailed responses are given in **Figs. 4. 5, 4. 6,** and **4. 7.**

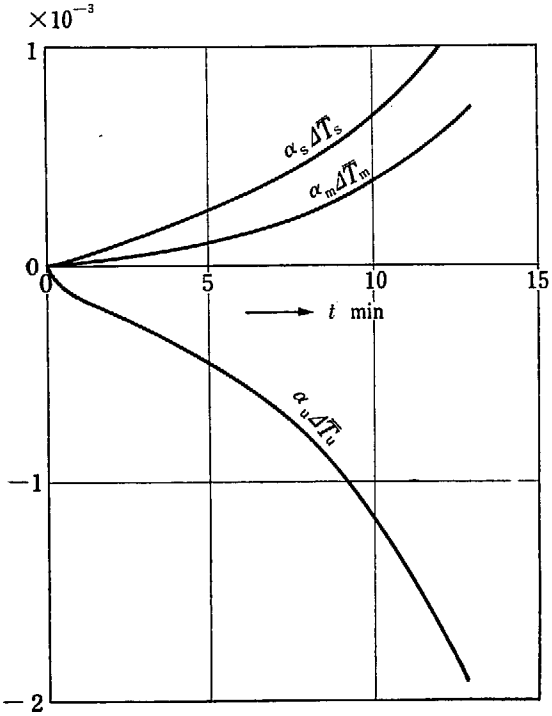

Fig. 4. 2. Response of $\alpha_u\Delta T_u$, $\alpha_s\Delta T_s$, $\alpha_m\Delta T_m$ to step change in ρ_{ex} for R-III.
$\rho_{ex}=1.2\times10^{-4}$, $\alpha_m=15\times10^{-5}$/°C $a=1.8$

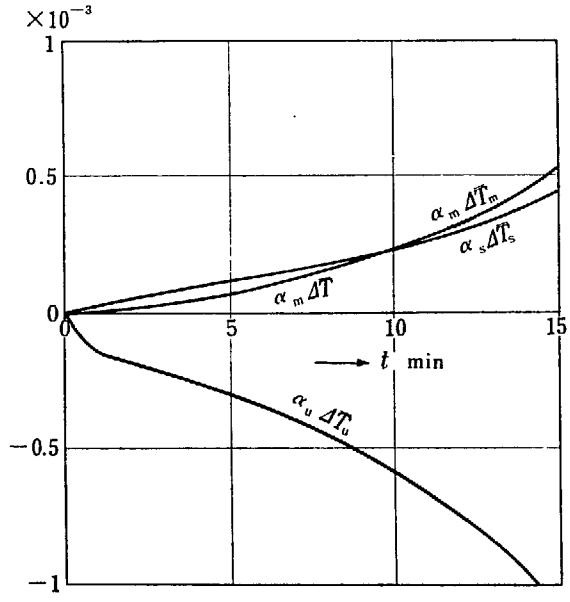

Fig. 4. 3. Response of $\alpha_u\Delta T_u$, $\alpha_s\Delta T_s$, $\alpha_m\Delta T_m$ to step change in ρ_{ex} for R-III.
$\rho_{ex}=1.2\times10^{-4}$, $\alpha_m=15\times10$/°C, $a=1.15$

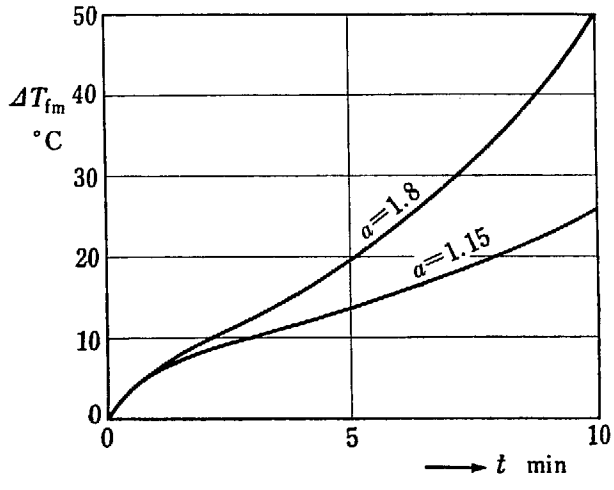

Fig. 4. 4. Response of ΔT_{fm} to step change in ρ_{ex} for R-III.
$\rho_{ex}=1.2\times10^{-4}$, $a=1.8$, 1.15

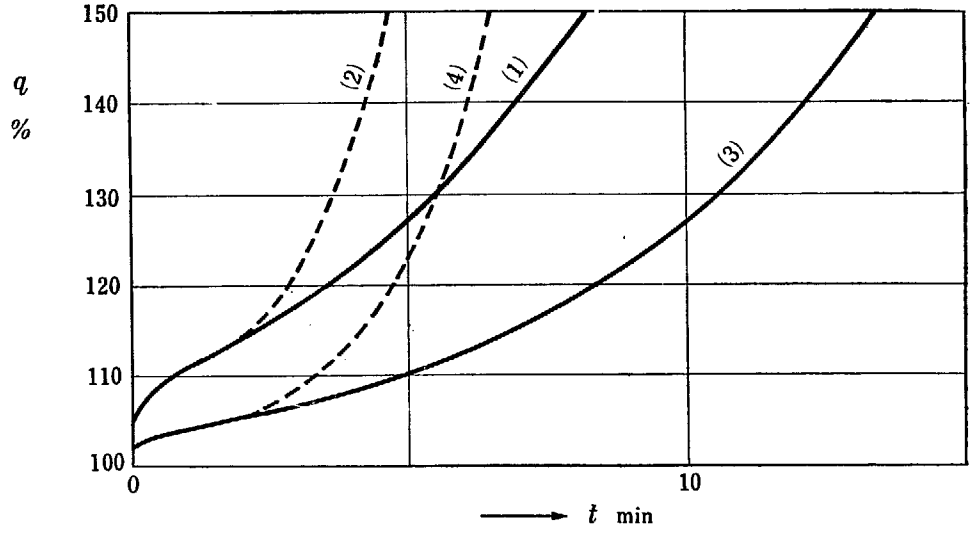

Fig. 4. 5. Response of q to step change in ρ_{ex} for R-III with and without sleeve.
$\rho_{ex}=3\times10^{-4}$, 1.2×10^{-4}, $\alpha_m=15\times10^{-5}$/°C
(1) $\rho_{ex}=3\times10^{-4}$ with sleeve (2) $\rho_{ex}=3\times10^{-4}$ without sleeve
(3) $\rho_{ex}=1.2\times10^{-4}$ with sleeve (4) $\rho_{ex}=1.2\times10^{-4}$ without sleeve

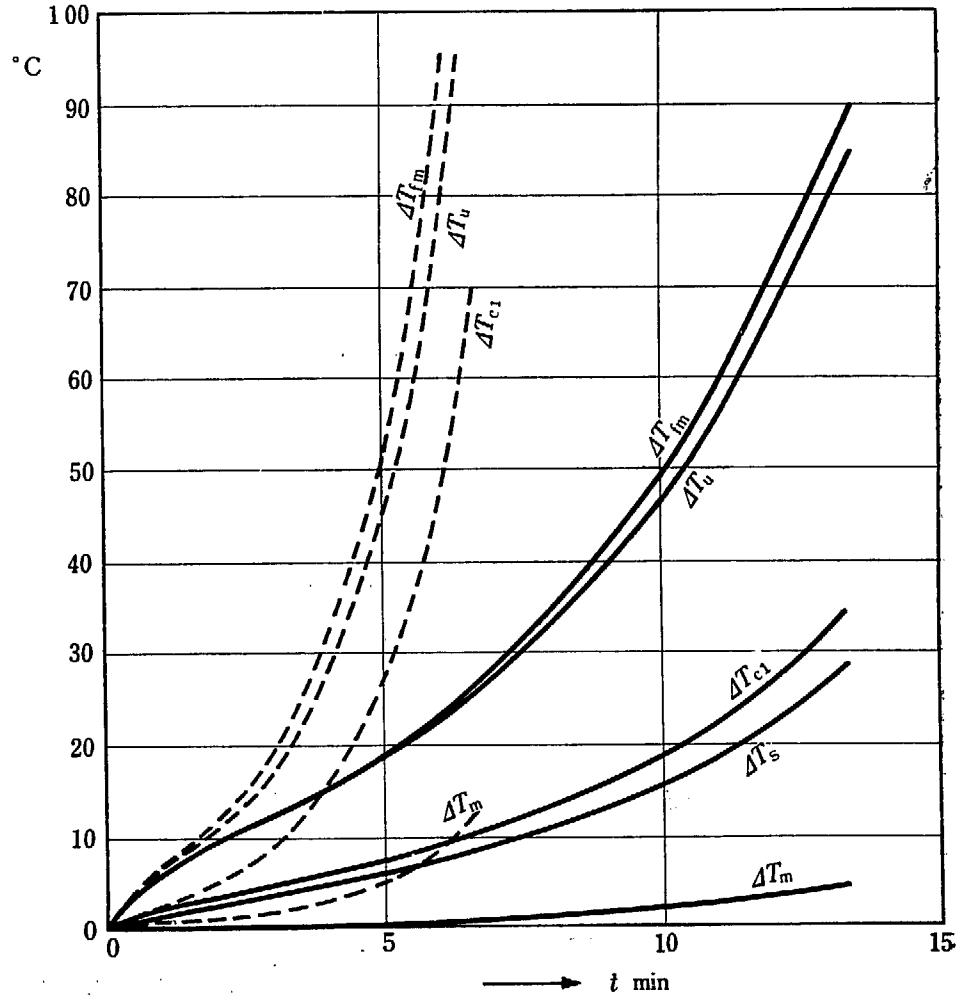

Fig. 4. 6. Response of ΔT to step change in ρ_{ex} for R-III with and without sleeve.
$\rho_{ex}=1.2\times10^{-4}$, $\alpha_m=15\times10^{-5}$/°C
---- without sleeve —— with sleeve

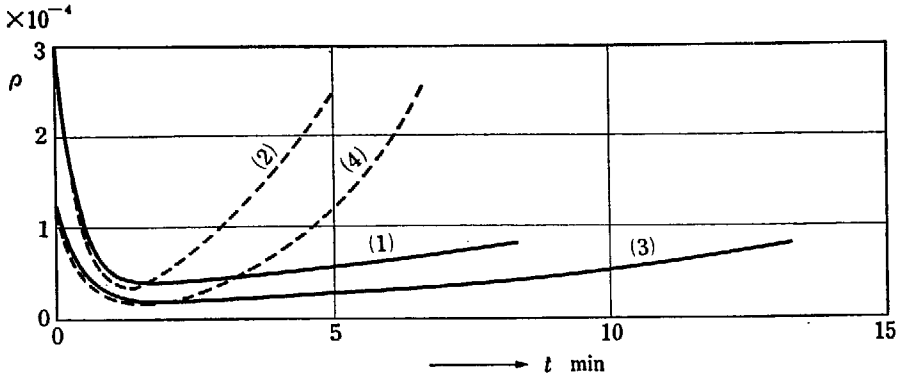

Fig. 4. 7. Response of ρ to step change in ρ_{ex} for R-III with and without sleeve. $\rho_{ex}=3\times10^{-4}$, 1.2×10^{-4}, $\alpha_m=15\times10^{-5}$/°C

(1) $\rho_{ex}=3\times10^{-4}$ with sleeve (2) $\rho_{ex}=3\times10^{-4}$ without sleeve
(3) $\rho_{ex}=1.2\times10^{-4}$ with sleeve (4) $\rho_{ex}=1.2\times10^{-4}$ without sleeve

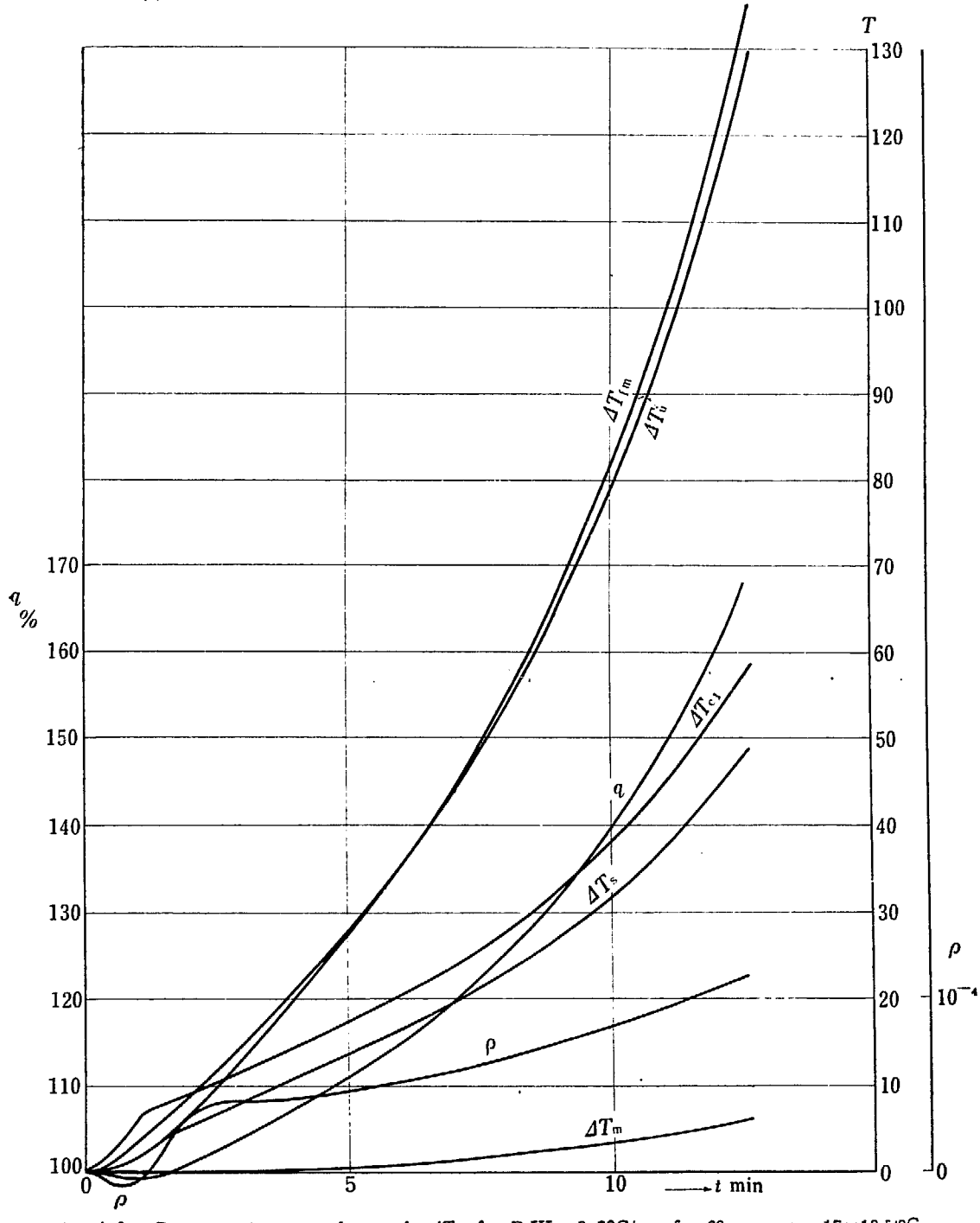

Fig. 4. 8. Response to ramp change in ΔT_{in} for R-III. 0.2°C/sec for 60 sec. $\alpha_m=15\times10^{-5}$/°C

3) Comparison of the responses of R-III with different values of a. (**Figs. 4. 2, 4. 3, 4.4.**)

Comparison is given for two values of a, i. e., $a=1.8$ and $a=1.15$. Considerable difference is observed in the two corresponding transient curves of $\alpha_s \Delta \bar{T}_s$ and ΔT_{fm}.

4) Response to the step change in ρ_{ex} for R-III with and without sleeves. (**Figs. 4. 5., 4. 6., 4. 7.**)

Comparison is made between the two models of R-III, one with sleeves and the other without sleeves (the fictitious model mentioned in 4. 1. 3). A sizable difference is obtained and the model with sleeves gives a much better transient behavior. For the model without sleeves this fact is primarily attributed to larger heat transfer coefficient between the coolant and moderator, in other words, a smaller time constant of moderator.

5) Response of R-III to the ramp change in ΔT_{in} (**Figs. 4. 8., 4. 9.**)

For $\alpha_m>0$, q falls down at first, then goes up afterwards, as was the case with R-I and R-II. This reverse reaction against positive disturbance is a typical characteristic of the reactors with positive α_m.

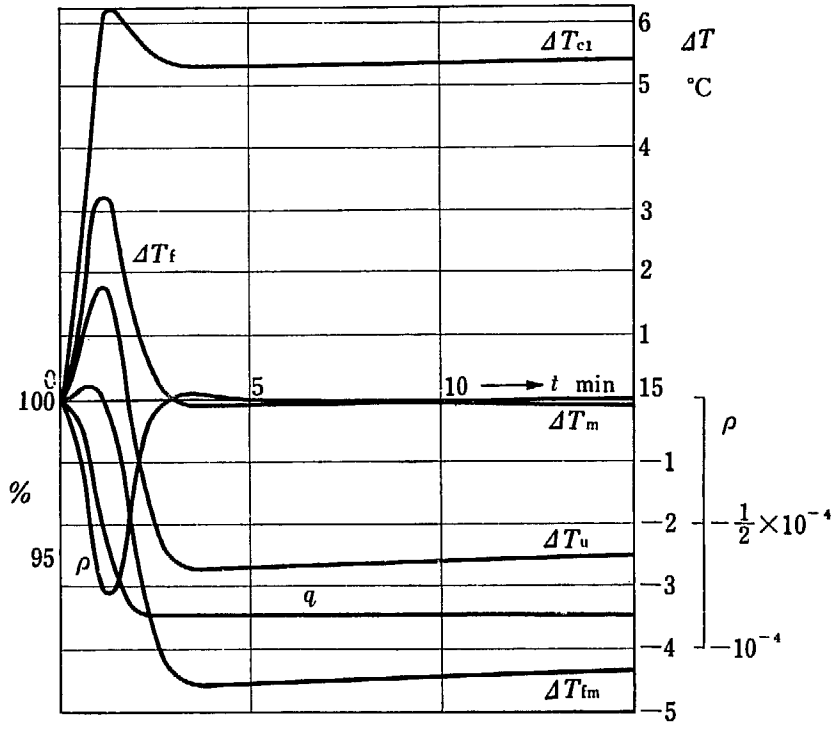

Fig. 4. 9. Response to ramp change in ΔT_{in} for R-III. 0.2°C/sec×60sec. $\alpha_m=-5\times10^{-5}$/°C

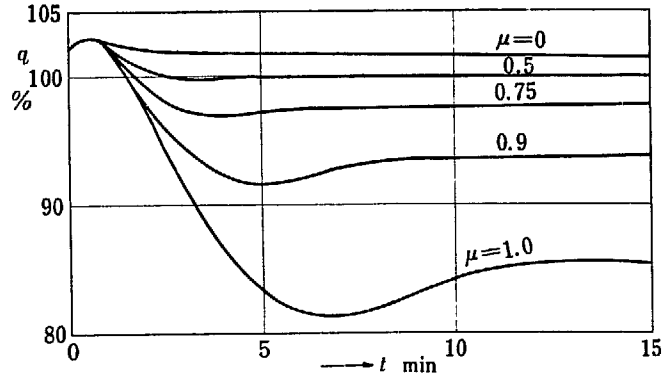

Fig. 4. 10. Response of q to step change in ρ_{ex} for R-III with simplified model of heat exchanger. $\rho_{ex}=1.2\times10^{-4}$, $\alpha_m=-5\times10^{-5}$/°C, $\Delta T_{in}=\mu\Delta T_{out}(t-20)$

T_{out}, However, does not show a reverse reaction. Therefore, the output of a reactor with positive α_m can be controlled without difficulty by detecting a change in T_{out}. For $\alpha_m < 0$, a reactor is again self-regulating.

6) Response to the step change in ρ_{ex} for R-III with a simplified model of heat exchanger. (**Figs. 4. 10., 4. 11., 4. 12.**)

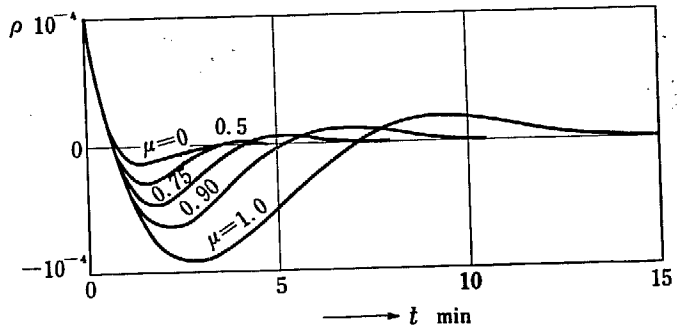

Fig. 4. 11. Response of q to step change in ρ_{ex} for R-III with simplified model of heat exchanger.
$\rho_{ex}=1.2\times10^{-4}$, $\alpha_m=-5\times10^{-5}/°C$, $\Delta T_{in}=\mu\Delta T_{out}(t-20)$

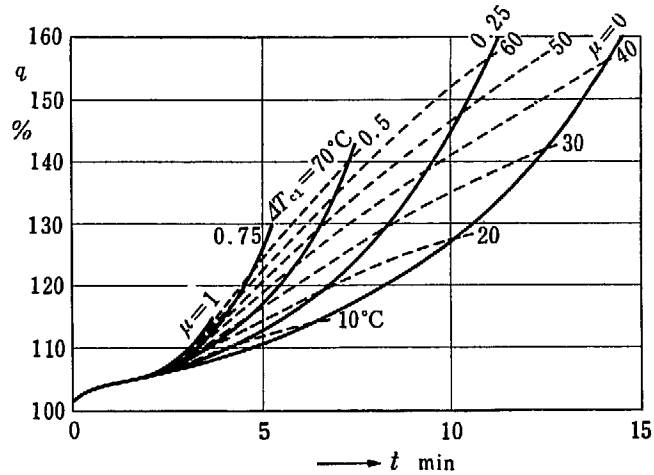

Fig. 4. 12. Response of q to step change in ρ_{ex} for R-III with simplified model of heat exchanger.
$\rho_{ex}=1.2\times10^{-4}$, $\alpha_m=15\times10^{-5}/°C$, $\Delta T_{in}=\mu\Delta T_{out}(t-20)$

For $\alpha_m>0$, the larger the value of μ, the greater the increases in q and ΔT. This is especially remarkable for ΔT_{c1}.

For $\alpha_m<0$, q also increasese initially, however, it settles down to a certain constant power level due to self-regulation. The larger the value of μ, the lower the settled-down power level. This is qualitatively explained as follows: The reactor output can be represented by integrating ρ over the transient period, therefore, the greater the negative portion of ρ during the transient, the lower the settled-down power level.

7) Response of R-III to the ramp change in u (**Figs. 4. 13., 4. 14., 4. 15., 4. 16., 4. 17., 4. 18.**)

As u falls down, ρ becomes negative initially due to negative α_u and short time constant of fuel, then it begins to rise due to the positive α_s and α_m.

For $\alpha_m<0$, the system is again self-regulating and q settles down to a certain level after some transient period. The same qualitative explanation as stated above can be given to the different settled-down power level due to a different change in u.

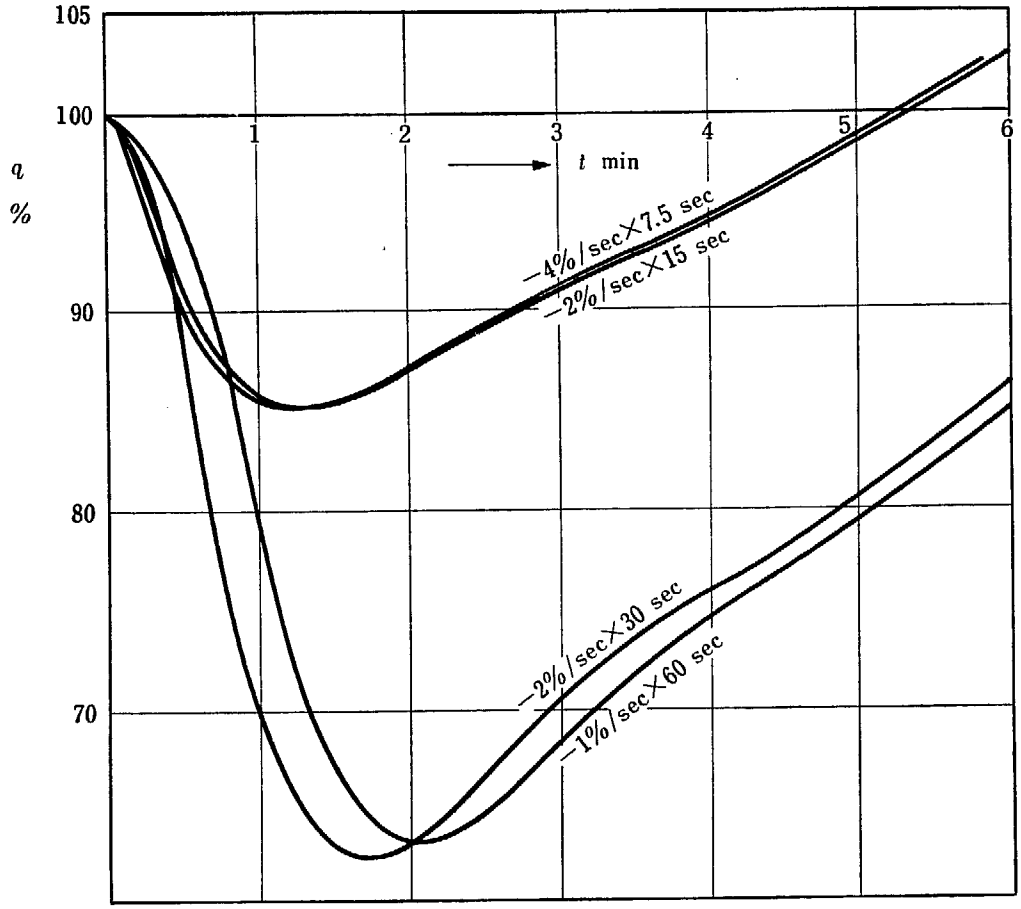

Fig. 4. 13. Responses of q to various ramp changes in Δu for R-III. $\alpha_m = 15 \times 10^{-5}/°C$

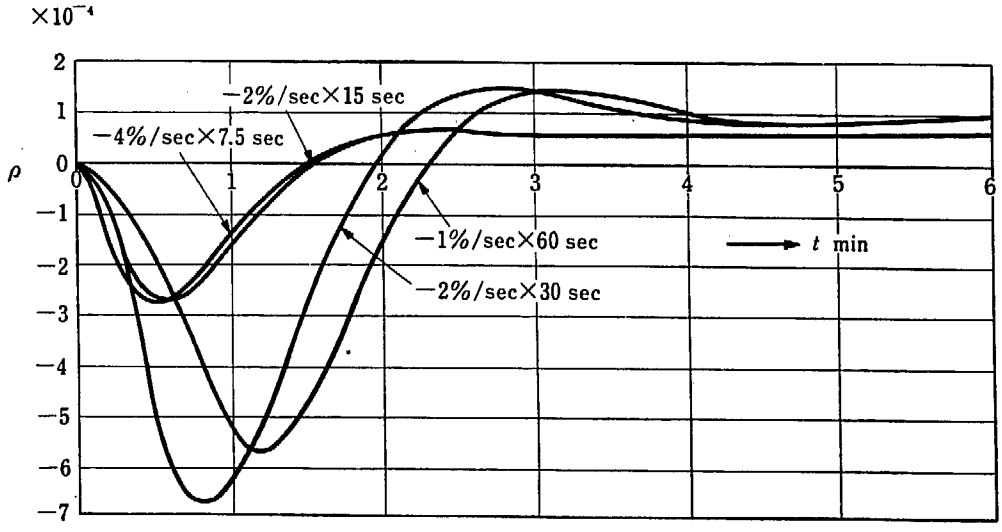

Fig. 4. 14. Responses of ρ to various ramp changes in Δu for R-III. $\alpha_m = 15 \times 10^{-5}/°C$

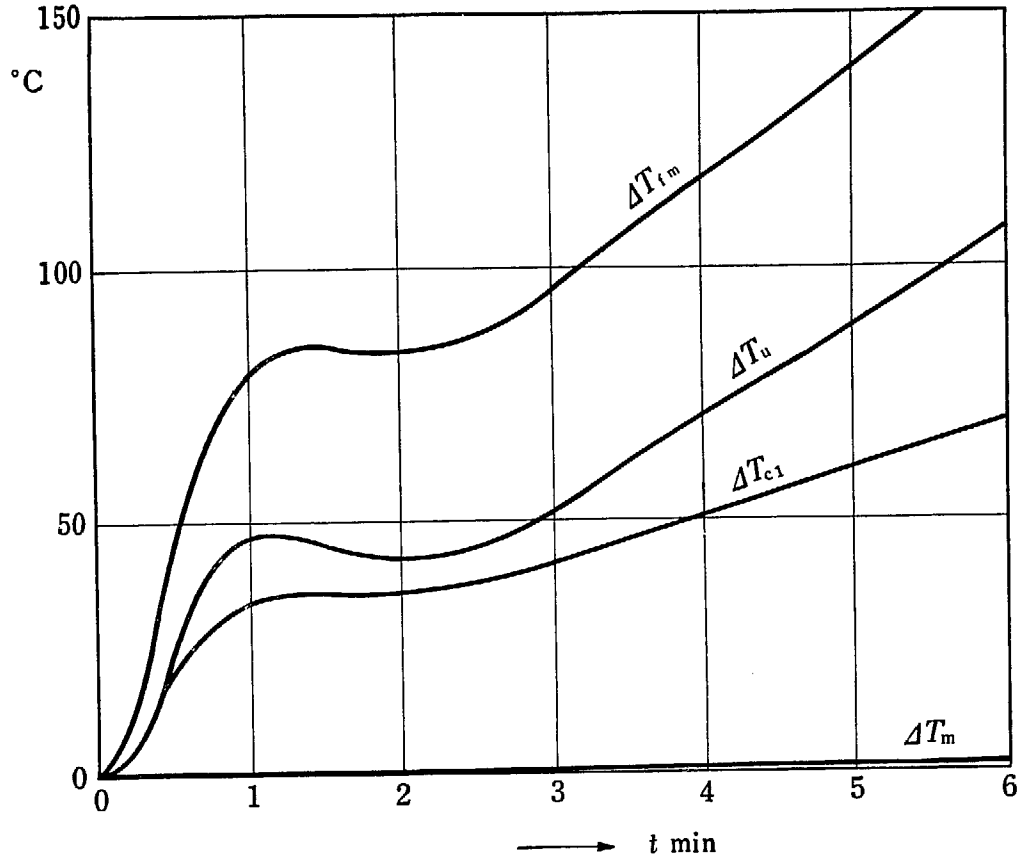

Fig. 4. 15. Response of ΔT to ramp change in Δu for R-III.
$\Delta u = -2\%/\text{sec} \times 30$ sec. $\alpha_m = 15 \times 10^{-5}/°C$

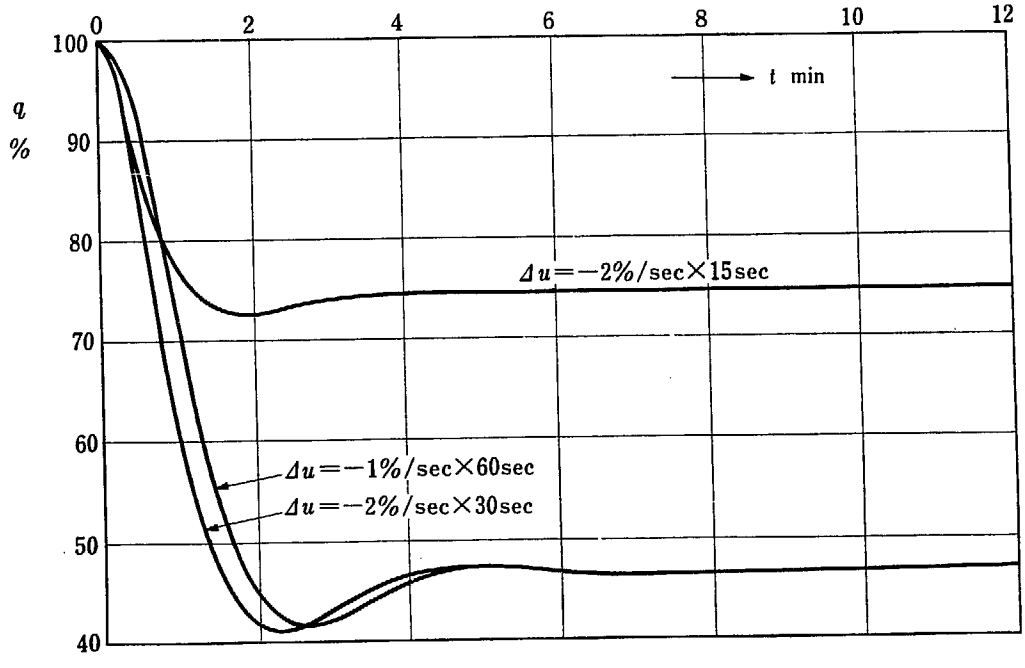

Fig. 4. 16. Response of q to various ramp change in Δu for R-III.
$\alpha_m = -5 \times 10^{-5}/°C$

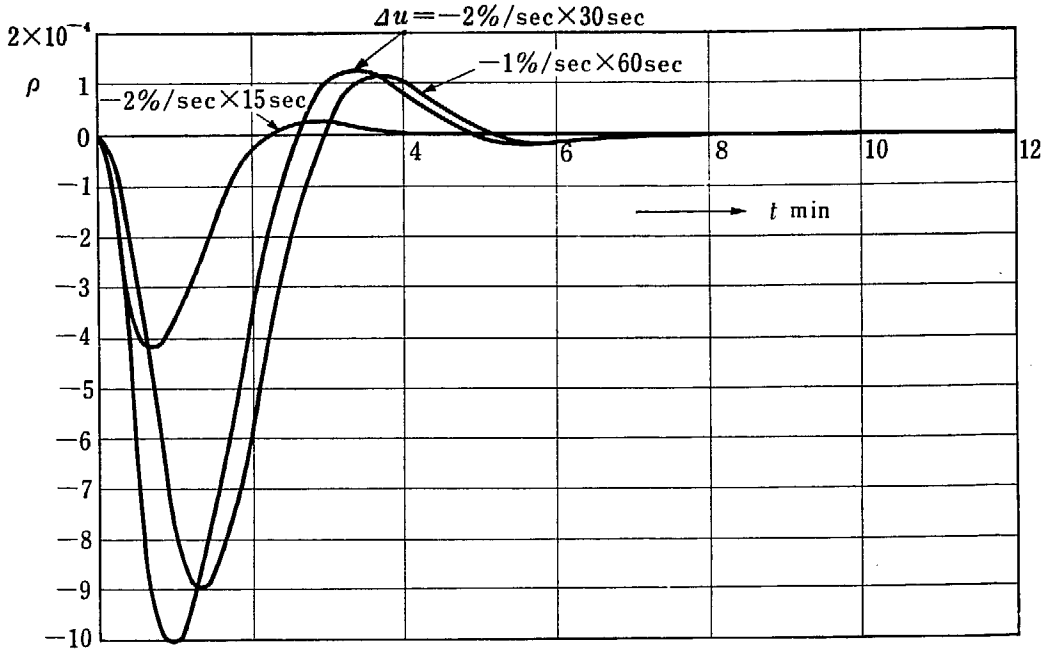

Fig. 4. 17. Response of ρ to various ramp change in Δu for R-III. $\alpha_m = -5\times10^{-5}/°C$

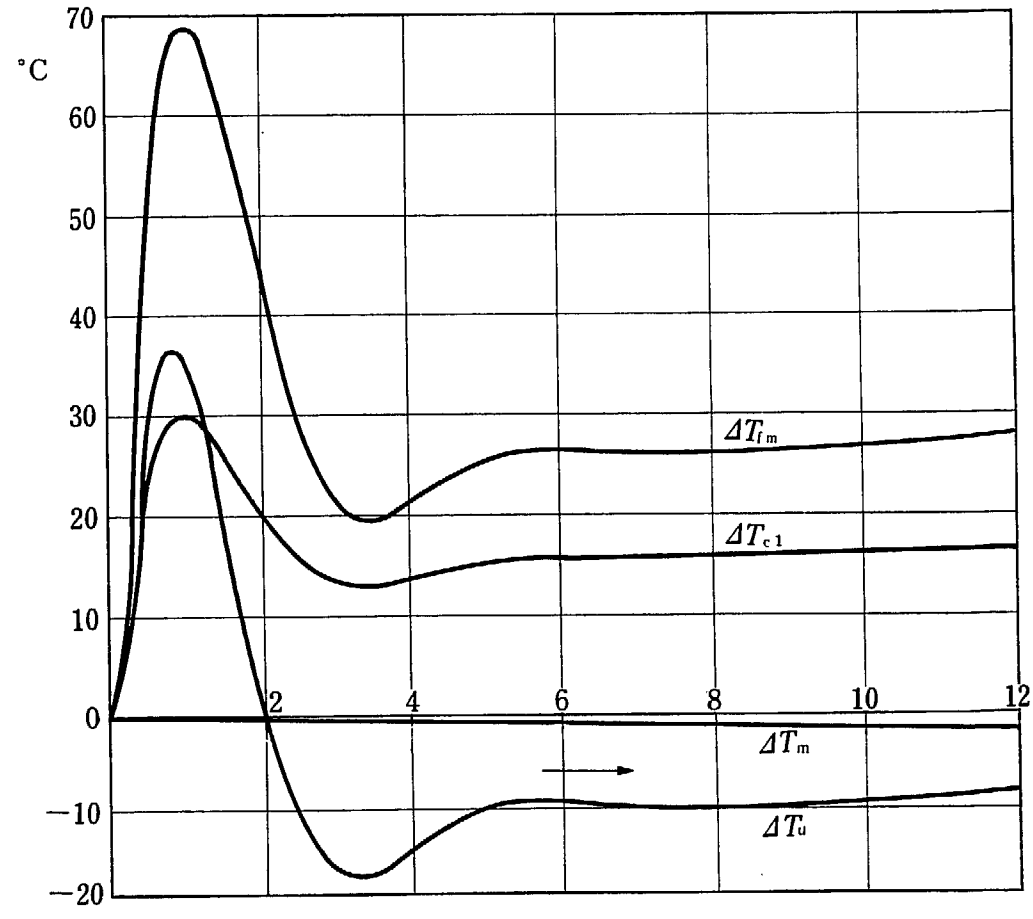

Fig. 4. 18. Response of ΔT to ramp change in Δu for R-III.
$\Delta u = -2\%$ /sec×30 sec. $\alpha_m = -5\times10^{-5}/°C$

5. Analysis of Results

Dynamic responses of a reactor subjected to change in reactivity, coolant inlet temperature and coolant flow rate have been obtained in the previous chapters, where a number of solutions by an analog computer have been shown. However, analyses of these results are of great importance, since characteristic features of a gas cooled reactor with positive temperature coefficient can be easily derived.

In this chapter comparison of the three reactors is firstly made, showing typical responses obtained. Secondly a preliminary description of the approach is given by which dynamic responses of a reactor are correlated to design parameters. This approach is now proceeding in our research group and will need further study. Detailed descriptions of this approach will appear in later reports.

Thirdly a critical value of positive temperature coefficient of moderator will be discussed, below which a reactor is still self-regulating.

5. 1. Comparison of the Three Types of Reactors

Typical responses of the three types of reactors are shown in **Fig. 5. 1. 1** through **Fig. 5. 1. 10.**

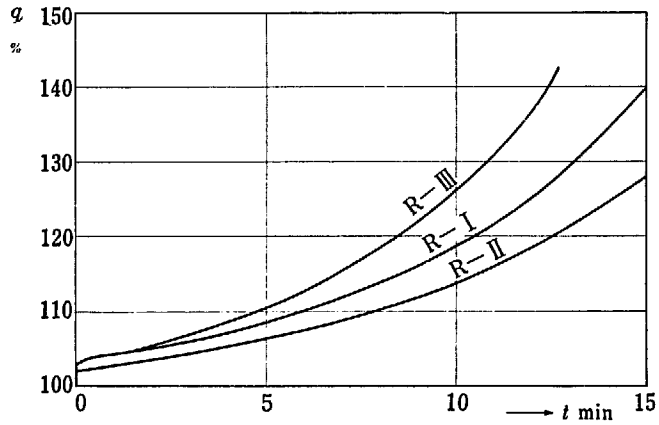

Fig. 5. 1. 1. Response of q to step change in ρ_{ex}. $\rho_{ex}=1.2\times10^{-4}$, $\alpha_m=15\times10^{-5}$/°C

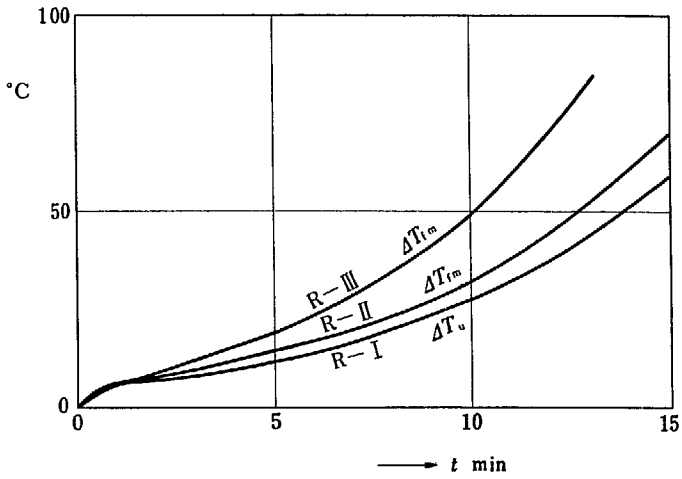

Fig. 5. 1. 2. Response of ΔT_{fm}, ΔT_u to step change in ρ_{ex}. $\rho_{ex}=1.2\times10^{-4}$, $\alpha_m=15\times10^{-5}$/°C

Corresponding responses under an identical condition are shown in one figure, in the case of R-I where α_m and disturbances are slightly different from others as indicated in each figure.

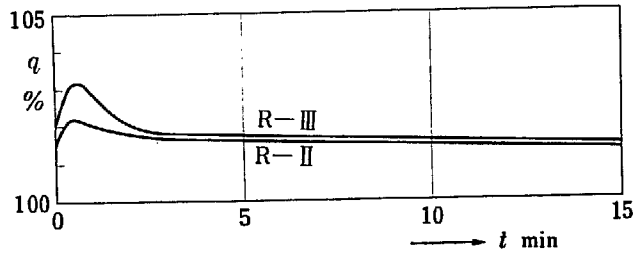

Fig. 5. 1. 3. Response of q to step change in ρ_{ex}. $\rho_{ex}=1.2\times10^{-4}$, $\alpha_m=-5\times10^{-5}$/°C

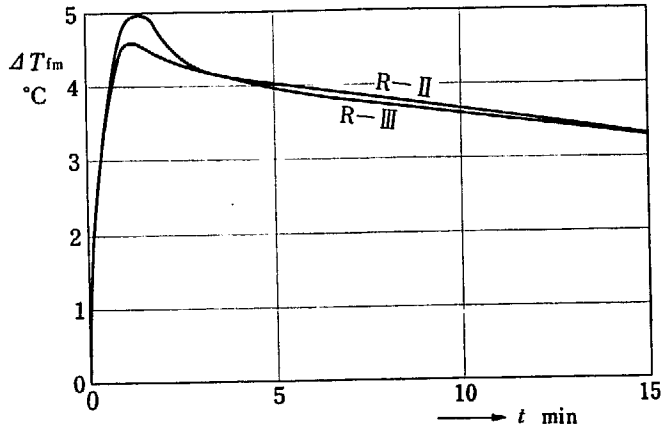

Fig. 5. 1. 4. Response of ΔT_{fm} to step change in ρ_{ex}. $\rho_{ex}=1.2\times10^{-4}$, $\alpha_m=-5\times10^{-5}$/°C

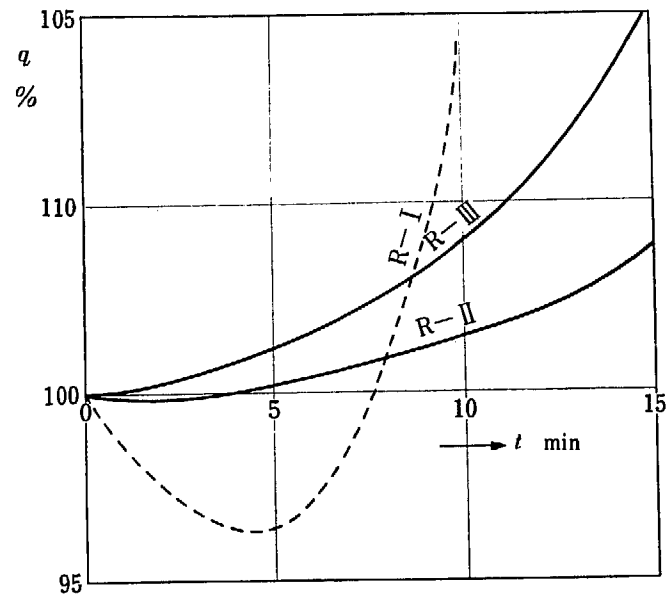

Fig. 5. 1. 5. Response of q to ramp change in ΔT_{in}.
R-I: 0.02°C/sec, $\alpha_m=12.5\times10^{-5}$/°C
R-II: 0.02°C/sec×60 sec, $\alpha_m=15\times10^{-5}$/°C
R-III: 〃 〃 〃

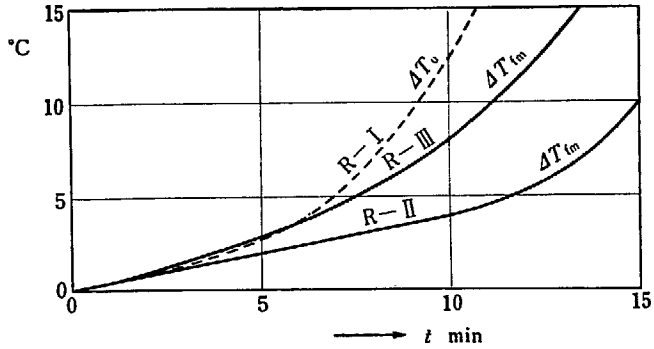

Fig. 5. 1. 6. Response of ΔT_{fm}, ΔT_u to ramp chang in T_{in}.
R-I: 0.02°C/sec, $\alpha_m = 12.5 \times 10^{-5}$/°C
R-II: 0.02°C/sec×60 sec, $\alpha_m = 15 \times 10^{-5}$/°C
R-III: 〃 〃 〃

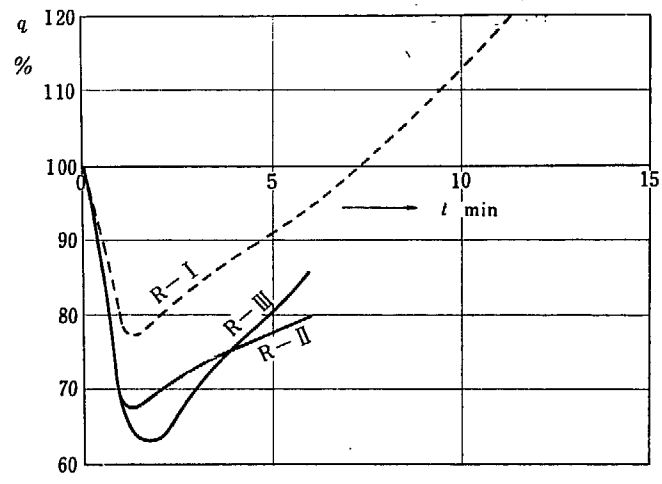

Fig. 5. 1. 7. Response of q to change in u.
R-I: step change $-0.5u_0$, $\alpha_m = 12.5 \times 10^{-5}$/°C
R-II: ramp change $-2\%u_0$/sec×30 sec
R-III: 〃 〃
$\alpha_m = 15 \times 10^{-5}$/°C

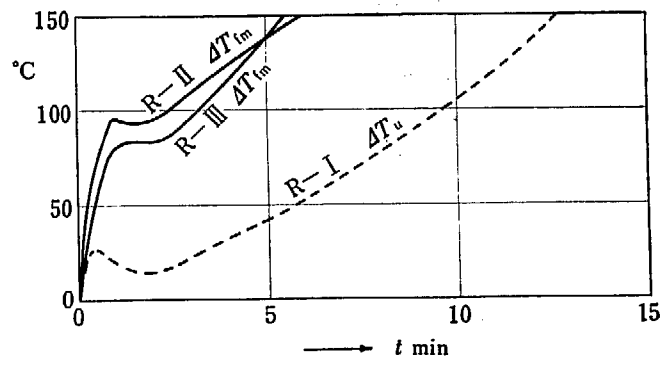

Fig. 5. 1. 8. Response of ΔT_{fm}, ΔT_u to change in u.
R-I: step change $-0.5u_0$, $\alpha_m = 12.5 \times 10^{-5}$/°C
R-II: ramp change −2% sec×30 sec
R-III: 〃 〃
$\alpha_m = 15 \times 10^{-5}$/°C

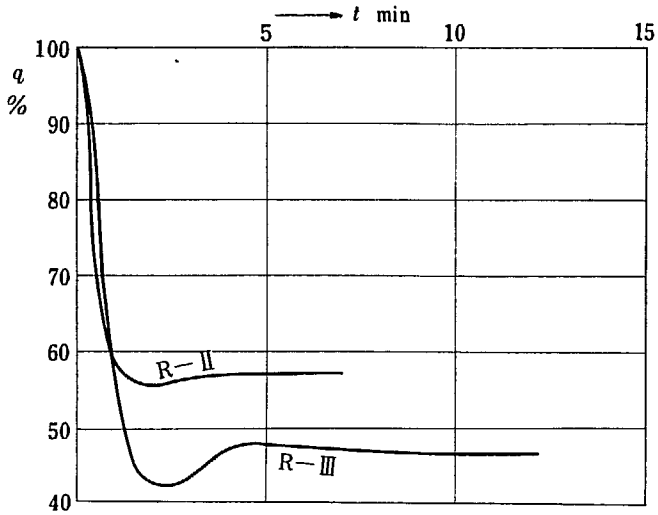

Fig. 5. 1. 9. Response of q to ramp change in u.
R-II: $-2\%/\text{sec} \times 30$ sec, $\alpha_m = -5 \times 10^{-5}/°C$
R-III: 〃 〃

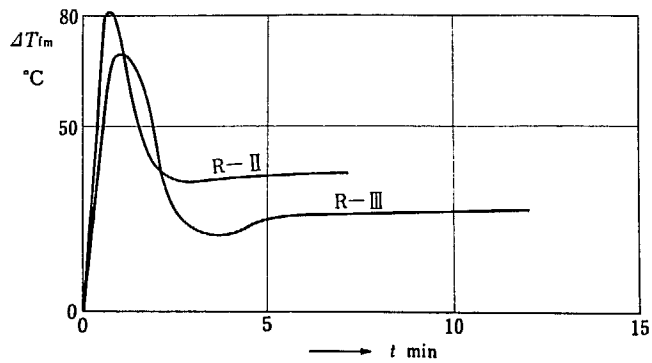

Fig. 5. 1. 10. Response of ΔT_{fm} to ramp change in u.
R-II: $-2\%/\text{sec}$ for 30 sec, $\alpha_m = -5 \times 10^{-5}/°C$
R-III: 〃 〃

It should be noted that R-II and R-III have graphite sleeves around the fuel rods, while R-I has not. Accordingly responses of R-I are quite different from those of others. It is observed that R-II has better characteristics, in other words, smaller excursions, than R-III, in almost all cases throughout the figures.

Transient response is obviously dependent on thermal system parameters, that is, heat transfer coefficient and heat capacity, Appendix 2, TABLE 4 shows some of the design parameters of a thermal system and power densities. It is noted that R-II has larger values of heat transfer coefficient, heat capacities, and coolant flow rate as well as power density compared to those of R-III.

It can be seen from the computer solutions obtained that transients in q die out in about one to two minutes and then after 5 minutes q continues to increase for $\alpha_m > 0$, while for $\alpha_m < 0$ it settles down to a certain constant value. However, this is not the case with the response to the change in u, where transients in q do not die out until about 5 minutes passes.

It is of interest to see the periods after 5 minutes for characteristic responses, which will be shown below. The period τ here is defined as

$$\frac{1}{\tau} = \frac{1}{q} \frac{dq}{dt}.$$

Table 5. 1. 1. q, τ and ΔT_u after 5 minutes for R-I.

Conditions	q	τ	ΔT_u	Refer to
$\rho_{ex}=1.2\times10^{-4}$, $\alpha_m=15\times10^{-5}$/°C	108.5%	72 min	12°C	Fig. 2.2
$\Delta u=-0.5u_0$, $\alpha_m=12.5\times10^{-5}$/°C	91	24	42	Fig. 2.5

Table 5. 1. 2. q, τ and ΔT_{fm} after 5 minutes for R-II with $\alpha_m=15\times10^{-5}$/°C

Conditions	q	τ	ΔT_{fm}	Refer to
$\rho_{ex}=1.2\times10^{-4}$	106.5%	107 min	14°C	Fig. 3.2
$\Delta T_{in}=0.02$°C/sec×60 sec	100.5	670	2.3	Fig. 3.3
$\Delta u=-2$%/sec×30 sec	78	31	137	Figs. 3.4, 3.5

Table 5. 1. 3. q, τ and ΔT_{fm} after 5 minutes for R-III with $\alpha_m=15\times10^{-5}$/°C

Conditions	q	τ	ΔT_{fm}	Refer to
$\rho_{ex}=3.0\times10^{-4}$	127%	23 min	50°C	Figs. 4.5, 4.6
$\rho_{ex}=1.2\times10^{-4}$	110	56	19	
$\rho_{ex}=3.0\times10^{-4}$, without sleeve	160	5.4	140	
$\rho_{ex}=1.2\times10^{-4}$, without sleeve	123	10.2	54	
$\Delta T_{in}=0.2$°C/sec×60 sec	111	28	27	Fig. 4.8
$\Delta T_{in}=0.75\,\Delta T_{out}(t-20)$	125	8.3	76	Fig. 4.12
$\Delta u=-2$%/sec×30 sec	79	15.8	139	Figs. 4.13, 4.15

5. 2. Virtual Time Constant Analysis

In the previous section is given the comparison of typical transient behaviors of the three reactors. And it was found that difference in design parameters affects the dynamic behavior of the system considerably. This fact was ascertained by use of a simplified model of the system, where reactor thermal system was represented by transfer functions of single time constant.

A reactor thermal system includes heat productions in fuel, graphite sleeves and moderators as well as heat transfers from these to the coolant gas. A more detailed block diagram of this is shown in **Fig. 5. 2. 1.**

In this figure, six time constants represent each part of the core unit cell, i. e. fuel, clad, a graphite sleeve, a coolant gas inside and outside the sleeve and graphite moderator. These are actual time constants, which are determined by heat capacities, heat transfer coefficients and so on as shown by **Fig. 5. 2. 1.** But change in temperature of any material is not determined only by the time constant representing the material. For example, ΔT_u is influenced by the change in ΔT_f, which in turn is affected by ΔT_{c1} and so forth. Thus the complete transfer functions from reactor power Q to ΔT_u and other temperatures such as ΔT_s and ΔT_m are quite complicated functions of complex frequency, s. If these functions can be approximated with single virtual time constants, $\hat{\theta}_u$, $\hat{\theta}_s$ and $\hat{\theta}_m$, respectively, the whole system will be something like the one shown in **Fig. 5. 2. 2.** The model is so much simplified that the comparison between different reactors is now easier.

The outline of the treatment is described in the case of R-I, for which equations are much simpler. The same approach is applicable for the other cases, but the equations are more complicated.

The reactor heat transfer equations (2. 5) can be rewritten as follows:

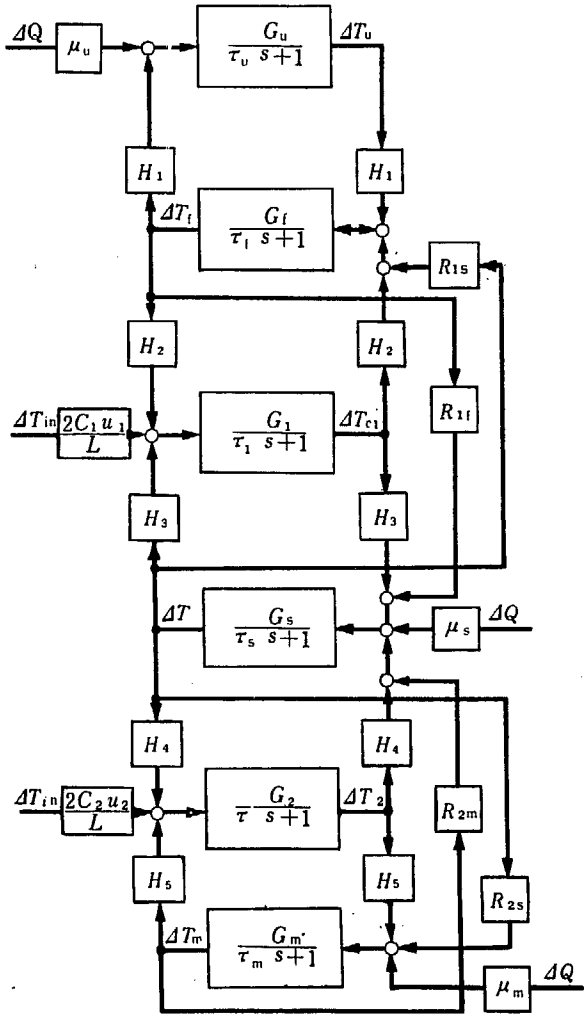

$$\tau_u = \frac{C_u}{H_1} \qquad G_u = \frac{1}{H_1}$$

$$\tau_f = \frac{C_f}{H_1+H_2+R_{1f}} \qquad G_f = \frac{1}{H_1+H_2+R_{1f}}$$

$$\tau_1 = \frac{C_1}{H_2+H_3+\frac{2C_1u_1}{L}} \qquad G_1 = \frac{1}{H_2+H_3+\frac{2C_1u_1}{L}}$$

$$\tau_s = \frac{C_s}{H_4+H_3+R_{1s}+R_{2s}} \qquad G_s = \frac{1}{H_4+H_3+R_{1s}+R_{2s}}$$

$$\tau_2 = \frac{C_2}{H_4+H_5+\frac{2C_2u_2}{L}} \qquad G_2 = \frac{1}{H_4+H_5+\frac{2C_2u_2}{L}}$$

$$\tau_m = \frac{C_m}{H_5+R_{2m}} \qquad G_m = \frac{1}{H_5+R_{2m}}$$

Fig. 5. 2. 1. Block diagram for reactor thermal system. (As for numerical values of constants, refer to Appendix 2, Table 6)

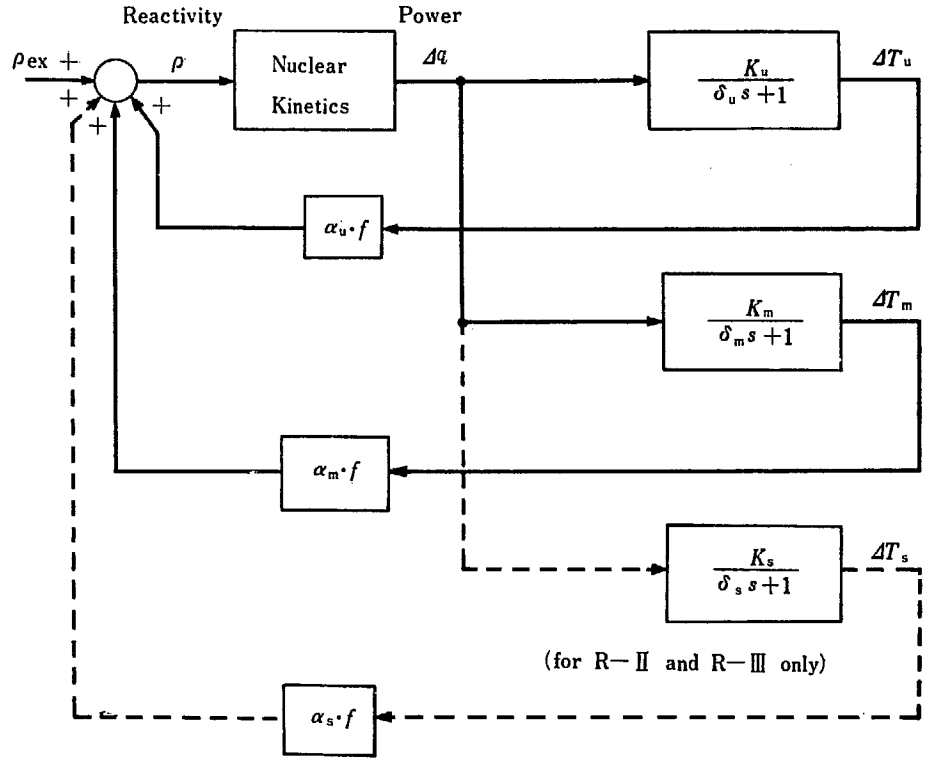

Fig. 5. 2. 2. Block diagram of simplified Model with thermal system represented by single time constant. (As for numerical values of constants, refer to AppendiyTable. 7)

$$\begin{pmatrix} \tau_u s+1 & -1 & 0 \\ -K_1 & \tau_c s+1 & -K_2 \\ 0 & -1 & \tau_m s+1 \end{pmatrix} \begin{pmatrix} \Delta T_u \\ \Delta T_s \\ \Delta T_m \end{pmatrix} = \begin{pmatrix} \nu_u \\ 0 \\ \nu_m \end{pmatrix} \Delta Q \tag{5.2.1}$$

where

$$\tau_u = \frac{C_u}{H_2} \qquad \tau_c = \frac{C_c}{H_2+H_3+\frac{2C_c u}{L}} \qquad \tau_m = \frac{C_m}{H_3}$$

$$\nu_u = \frac{\mu_u}{H_2} \qquad \nu_m = \frac{\mu_m}{H_3}$$

$$K_1 = \frac{H_2}{H_2+H_3+\frac{2C_c u}{L}} \qquad K_2 = \frac{H_3}{H_2+H_3+\frac{2C_c u}{L}}$$

The heat capacity of the coolant gas is small compared to those of fuel and moderator, so the time constant τ_c can be neglected.

Then the transfer functions from ΔQ to ΔT_u and to ΔT_m are easily obtained from Eq. (5. 2. 1) as follows:

$$\Delta T_u = \frac{\nu_u \tau_m s+\nu_u(1-K_2)+\nu_m K_2}{\tau_u \tau_m s^2+\{(1-K_2)\tau_u+(1-K_1)\tau_m\}s+(1-K_1-K_2)} \Delta Q \tag{5.2.2}$$

and

$$\Delta T_m = \frac{\nu_m \tau_u s+\nu_m(1-K_1)+\nu_u K_1}{\tau_u \tau_m s^2+\{(1-K_2)\tau_u+(1-K_1)\tau_m\}s+(1-K_1-K_2)} \Delta Q \tag{5.2.3}$$

These equations can be written as a sum of partial fractions.

$$\Delta T_u = \left\{ \frac{K_{uA}}{\delta_u s+1} + \frac{K_{uB}}{\delta_m s+1} \right\} \Delta Q \tag{5.2.4}$$

$$\Delta T_m = \left\{ \frac{K_{mA}}{\delta_u s+1} + \frac{K_{mB}}{\delta_m s+1} \right\} \Delta Q \tag{5.2.5}$$

where, $\delta_u = -1/s_1$ and $\delta_m = -1/s_2$; and s_1 and s_2 are the roots of

$$\tau_u \tau_m s^2 + \{(1-K_2)\tau_u + (1-K_1)\tau_m\} s + (1-K_1-K_2) = 0 \tag{5.2.6}$$

The roots are easily found to be

$$s_1 = \frac{-1}{2\tau_u\tau_m} \{(1-K_2)\tau_u + (1-K_1)\tau_m + \sqrt{\{(1-K_2)\tau_u + (1-K_1)\tau_m\}^2 - 4\tau_u\tau_m(1-K_1-K_2)}\} \tag{5.2.7}$$

$$s_2 = \frac{-1}{2\tau_u\tau_m} \{(1-K_2)\tau_u + (1-K_1)\tau_m - \sqrt{\{(1-K_2)\tau_u + (1-K_1)\tau_m\}^2 - 4\tau_u\tau_m(1-K_1-K_2)}\} \tag{5.2.8}$$

The gain constant K_{uA} and so forth are obtained as follows:

$$K_{uA} = \frac{\nu_u\tau_m s_1 + \nu_u(1-K_2) + \nu_m K_2}{\tau_u\tau_m s_1 (s_2 - s_1)} \tag{5.2.9}$$

$$K_{uB} = \frac{\nu_u\tau_m s_2 + \nu_u(1-K_2) + \nu_m K_2}{\tau_u\tau_m s_2 (s_1 - s_2)} \tag{5.2.10}$$

$$K_{mA} = \frac{\nu_m\tau_u s_1 + \nu_m(1-K_1) + \nu_u K_1}{\tau_u\tau_m s_1 (s_2 - s_1)} \tag{5.2.11}$$

$$K_{mB} = \frac{\nu_m\tau_u s_2 + \nu_m(1-K_1) + \nu_u K_1}{\tau_u\tau_m s_2 (s_1 - s_2)} \tag{5.2.12}$$

The major part of heat is produced in fuel, which implies $\nu_u > \nu_m$ and time constant of the moderator is much larger than that of fuel, or $\tau_m \gg \tau_u$. With these two conditions it is easily shown that

$$K_{uA} \gg K_{uB}, \quad K_{mB} \gg K_{mA}. \tag{5.2.13}$$

Thus Eqs. (5.2.4) and (5.2.5) can be further simplified and the single time constant model for the reactor thermal system is obtained.

$$\Delta T_u = \frac{K_{uA}}{\delta_u s+1} \Delta Q \tag{5.2.14}$$

$$\Delta T_m = \frac{K_{mB}}{\delta_m s+1} \Delta Q \tag{5.2.15}$$

Here the single time constant model was obtained by simply neglecting the term of smaller gain constant in Eqs. (5.2.4) and (5.2.5). However, a much better model would be obtained by slightly modifying the procedure, in which the transfer function of two time constants such as Eqs. (5.2.4) and (5.2.5) would be approximated by that of an appropriate single time constant.

The simplified model of the whole system is shown in **Fig. 5.2.2**, where δ_u and δ_m are the "virtual time constants" of the reactor thermal system. Their numerical values are shown in Appendix 2, TABLE 7.

The virtual time constants for R-II and R-III, including δ_s for ΔT_s are also shown in Appendix 2, TABLE 7. The reactor thermal system model was replaced by these single time constants, and transient responses for step reactivity change were obtained. The results, shown in **Figs. 5.2.3** and **5.2.4**, were compared with the actual responses in **Figs. 3.2** and **4.5** through **4.7** and the approximation was found to be satisfactory.

The transients were further examined changing the values of virtual time constants, δ's and gain constants, K's.

The effect of changing virtual time constants is shown in **Fig. 5.2.5** From this figure it may be concluded that:

a) Larger δ_u makes power increase more rapid, because larger δ_u means a slower of the fuel temperature and henceforth slower build up of the negative reactivity. On the contrary

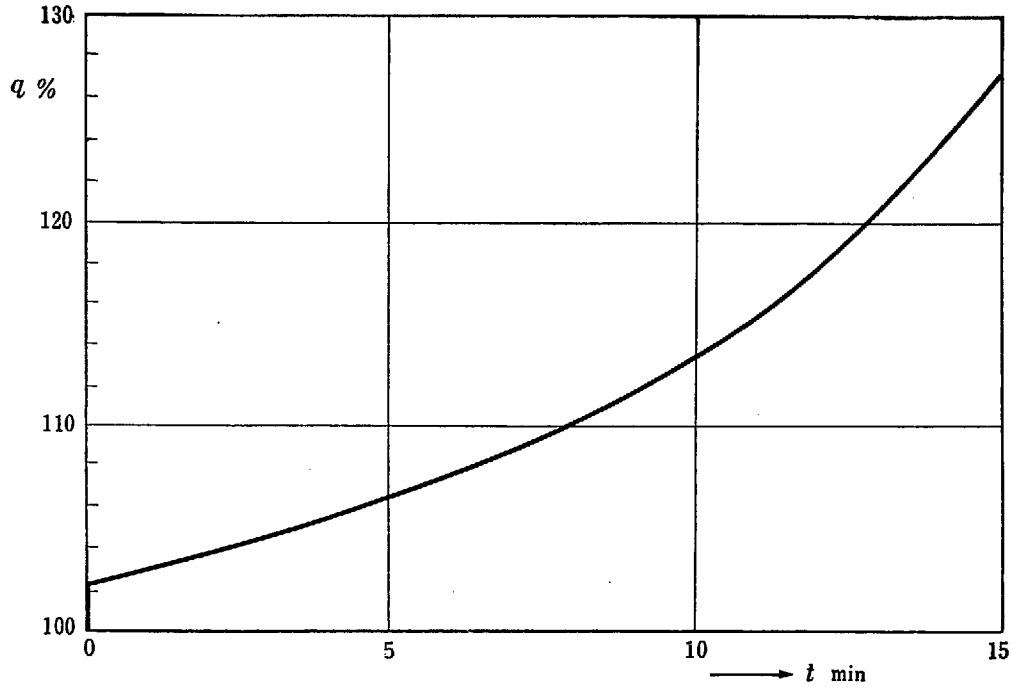

Fig. 5. 2. 3. (a) Response to step change in ρ_{ex} for R-II using simplified model of Fig. 5. 2. 2. $\rho_{ex}=1.2\times10^{-4}$, $\alpha_m=15\times10^{-5}/°C$

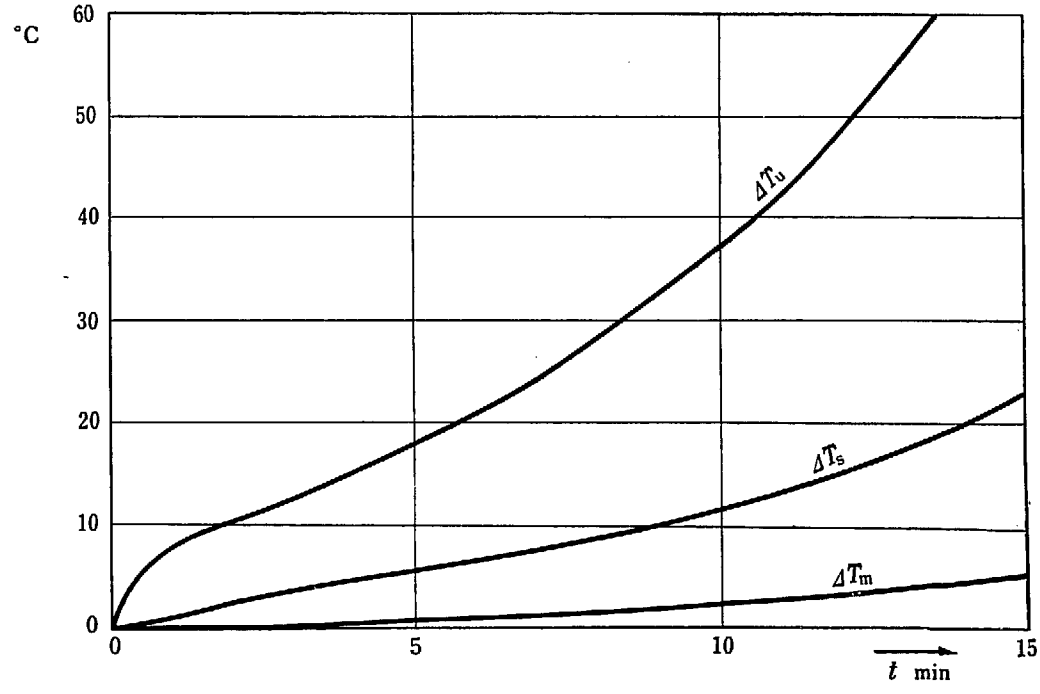

Fig. 5. 2. 3. (b) Response to step change in ρ_{ex} for R-II using simplified model of Fig. 5. 2. 2. $\rho_{ex}=1.2\times10^{-4}$, $\alpha_m=15\times10^{-5}/°C$

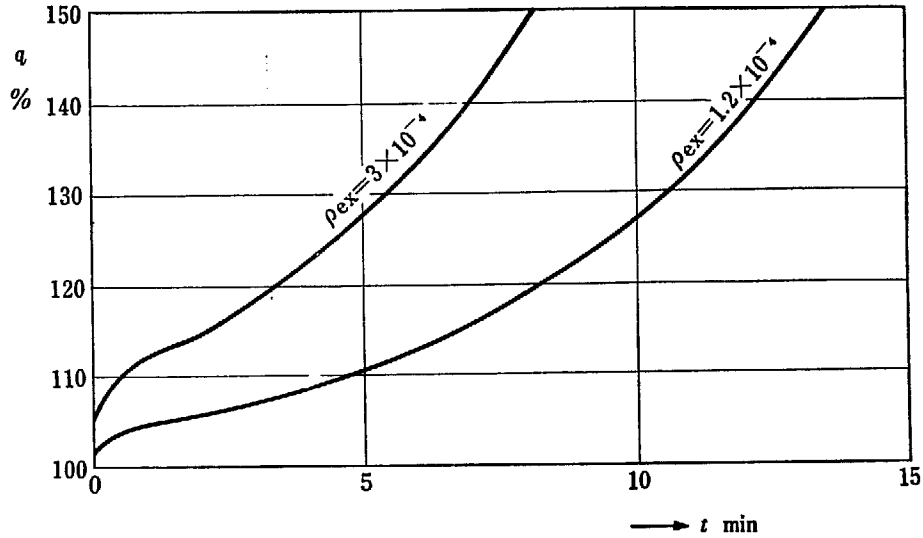

Fig. 5. 2. 4. (a) Response to step change in ρ_{ex} for R-III using simplified model of Fig. 5. 2. 2. $\rho_{ex}=1.2\times10^{-4}$ and 3×10^{-4}, $\alpha_m=15\times10^{-5}/°C$

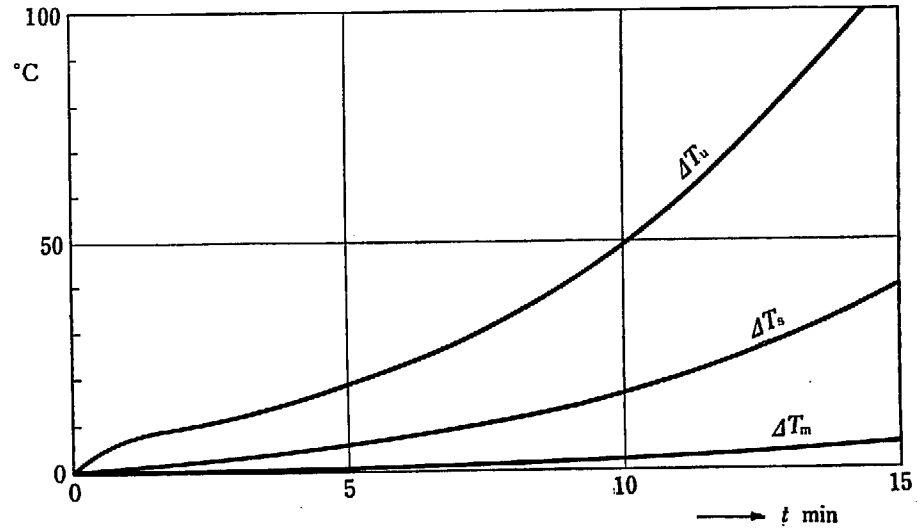

Fig. 5. 2. 4. (b) Response to step change in ρ_{ex} for R-III using simplified model of Fig. 5. 2. 2. $\rho_{ex}=1.2\times10^{-4}$, $\alpha_m=15\times10^{-5}/°C$

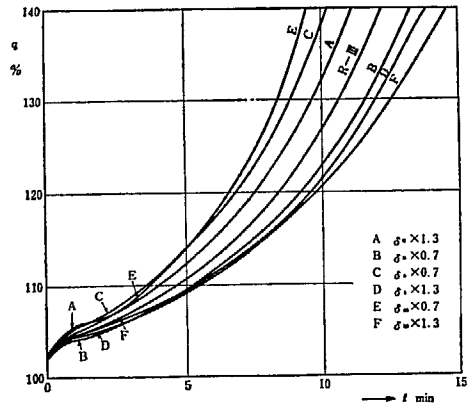

Fig. 5. 2. 5. Effect of change in δ's upon power excursion.
$\rho_{ex}=1.2\times10^{-4}$, $\alpha_m=15\times10^{-5}/°C$

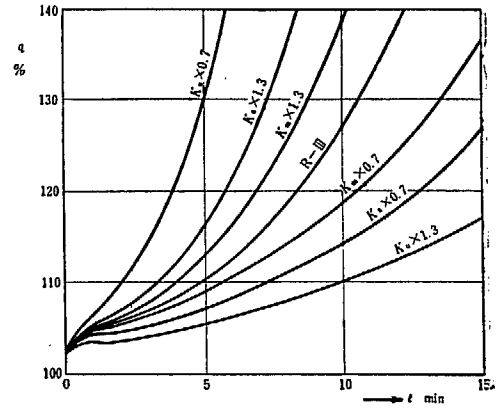

Fig. 5. 2. 6. Effect of change in K's upon power excursion.
$\rho_{ex}=1.2\times10^{-4}$, $\alpha_m=15\times10^{-5}/°C$

larger δ_s or δ_m makes power increase less rapid.

b) After several minutes the effect of changing δ_m is larger than that of δ_s, which in turn is larger than that of δ_u, if the virtual time constants are changed at a constant ratio ($\times 1.3$ and $\times 0.7$ in this case).

The effect of changing gain constants is shown in **Fig. 5. 2. 6.** The following conclusions are obtained from this figure.

c) Smaller K_u makes power increase more rapid, while smaller K_s or K_m makes a power excursion smaller.

d) The effect of changing K_u is larger than that of changing K_s and K_m. The situation is quite different from the case of changing virtual time constants.

Now that the effects of δ's and K's upon transient behavior are known, the transient responses of R-II and R-III are compared in **Fig. 5. 2. 7.** The power excursion is larger for R-III than for R-II as indicated in the figure. When δ_u and K_u of fuel are replaced by those of R-II, the response of R-III becomes curve A in the figure. This is consistent with the conclusion a) obtained from **Fig. 5. 2. 5,** because δ_u is smaller for R-II than for R-III. When δ_s, K_s and a_v of the sleeve are replaced by those of R-II, the response becomes Curve B. This may seem to contradict the conclusion a), because a sleeve time constant is smaller for R-II and smaller δ_s must result in the larger power excursion. However, the volume ratio of sleeve to moderator is larger for R-III $\left(\frac{V_s}{V_s+V_m}=0.13 \text{ for R-III and } 0.1 \text{ for R-II}\right)$ and because it is assumed that temperature coefficient of the sleeve is proportional to the volume ratio, the same temperature change results in a larger positive reactivity in the case of R-III. This is ascertained by **Fig. 5. 2. 8,** in which response of R-III is compared to response of a fictitious reactor, which has a smaller volume ratio of 0.1 and is in other respects same as R-III. The effect of the change in δ_m is also shown in **Fig. 5. 2. 7** (Curve C), and the result is again consistent with the conclusion a).

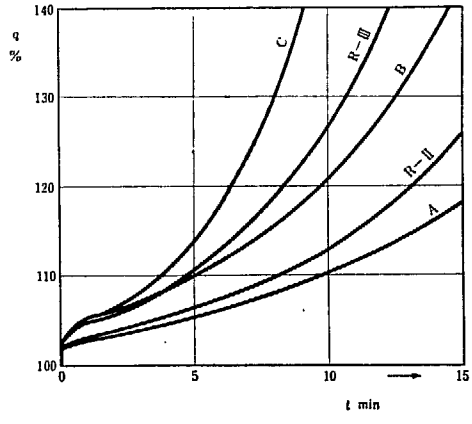

Fig. 5. 2. 7. Comparison of power excursion of R-II and R-III.
$\rho_{ex}=1.2\times10^{-4}$, $\alpha_m=15\times10^{-5}$/°C

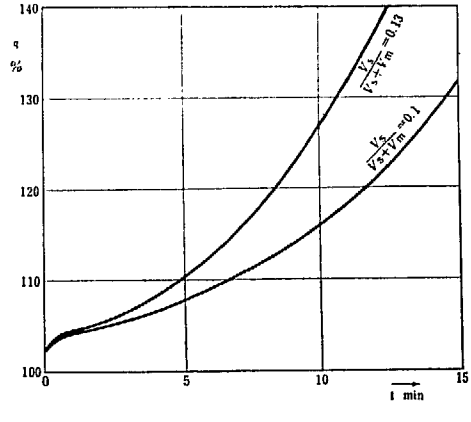

Fig. 5. 2. 8. Effect of sleeve volume upon power excursion.
$\rho_{ex}=1.2\times10^{-4}$, $\alpha_m=15\times10^{-5}$/°C

Thus the following conclusions are obtained.

(1) δ_u is larger for R-III, which is one of the principal causes of the more rapid power increase in R-III.

(2) δ_s is also larger for R-III, which must make the power increase somewhat smaller.

(3) However, the volume ratio is larger for R-III, which makes the effect of the sleeve temperature rise more severe and which is the other cause of the more rapid power increase in R-III.

(4) ∂_m is larger for R-III, which makes the power increase somewhat smaller.
and then,

(5) to realise a better transient behavior——a smaller power excursion——, the reactor thermal system must be designed so as to have small ∂_u and the volume of the sleeve must be made as small as possible.

It is interesting then, to correlate ∂_u, ∂_s and ∂_m with design parameters, for this implies the possibility of anticipation of a transient behavior of some newly designed reactors without tedious calculations. The correlations are already found for R-I in Eqs. (5. 2. 7) through (5. 2. 12), but the situation is much more complicated for R-II and R-III and the formulas are not completed yet. The virtual time constants used in the above analysis were obtained from analog computer results.

5. 3. Critical Value of Positive Temperature Coefficient of Moderator.

It is self-evident that a reactor is absolutely stable and self-regulating, so far as both α_u and α_m are negative. However, a reactor with positive temperature coefficient of moderator is either stable or unstable, depending upon the magnitude of α_m. The threshould of α_m exists below which a reactor is still self-regulating and it is hereafter referred to as the critical value of positive temperature coefficient α_{mc}, which will be discussed below.

A schematic diagram of a reactor with temperature feedback loops is shown in **Fig. 5. 3. 1.**

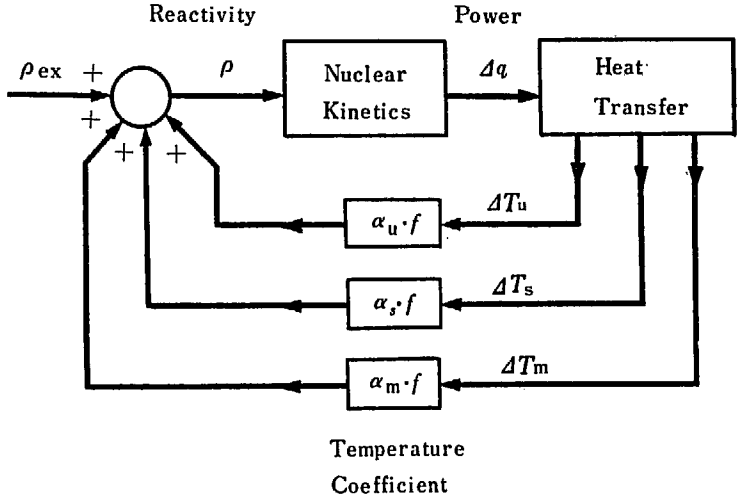

Fig. 5. 3. 1. Block diagram with temperature feedback (for R-II, R-III)

Supposing that an equilibrium steady state exists with constant ρ_{ex} introduced, then Δq, ΔT_u, ΔT_s and ΔT_m should be constant and $\rho=0$.

As far as a small change in temperature is concerned, the radiation terms may be linearized as in Eqs. (3. 5). Then, it is easily seen that Δq, ΔT_u, ΔT_s and ΔT_m have a constant ratio with each other at an equilibrium state. Of interest among them are a_s and a_m, which are defined as below. (Hereafter, superscript* is attached to indicate the values at equilibrium)

$$a_s=\Delta T_s^*/\Delta T_u^*$$
$$a_m=\Delta T_m^*/\Delta T_u^* \qquad (5.3.1)$$

Another equilibrium condition, $\rho=0$, gives,

$$\rho_{ex}+\alpha_u f\Delta T_u^*+\alpha_s f\Delta T_s^*+\alpha_m f\Delta T_m^*=0. \qquad (5.3.2)$$

Substituting Eq. (5. 3. 1), into Eq. (5. 3. 2), it gives

$$\rho_{ex}+\{\alpha_u+(a_v a_s+a_m)\alpha_m\}f\Delta T_u^*=0, \qquad (5.3.3)$$

where $a_v=\alpha_s/\alpha_m$ is constant for a particular reactor. From Eq. (5. 3. 3) it follows,

$$\Delta T_u^*=\frac{-\rho_{ex}}{\{\alpha_u+(a_v a_s+a_m)\alpha_m\}f}. \tag{5. 3. 4}$$

Since $\alpha_u<0$, $\alpha_m>0$ and also $a_v a_s+a_m>0$, denominator of Eq. (5. 3. 4) is negative, so long as α_m satisfies the following condition:

$$\alpha_m<\frac{-\alpha_u}{a_v a_s+a_m}. \tag{5. 3. 5}$$

In this case a finite value of ΔT_u^* exists and the system is stable and self-regulating. However, the absolute magnitude of the denominator becomes smaller as α_m increases, and vanishes when α_m is equal to critical value α_{mc}, where ΔT_u^* becomes infinite and the system is not self-regulating. Putting denominator of Eq. (5. 3. 4) equal to zero, α_{mc} is defined as follows:

$$\alpha_{mc}=\frac{-\alpha_u}{a_v a_s+a_m} \tag{5. 3. 6}$$

Under the condition $\alpha_m>\alpha_{mc}$, the system subjected to reactivity disturbances is diverging, unless other means is taken to reduce the reactivity.

And for reactors without sleeve Eq. (5. 3. 5) reduces to Eq. (5. 3. 7), putting $a_s=0$,

$$\alpha_m<\frac{-\alpha_u}{a_m}. \tag{5. 3. 7}$$

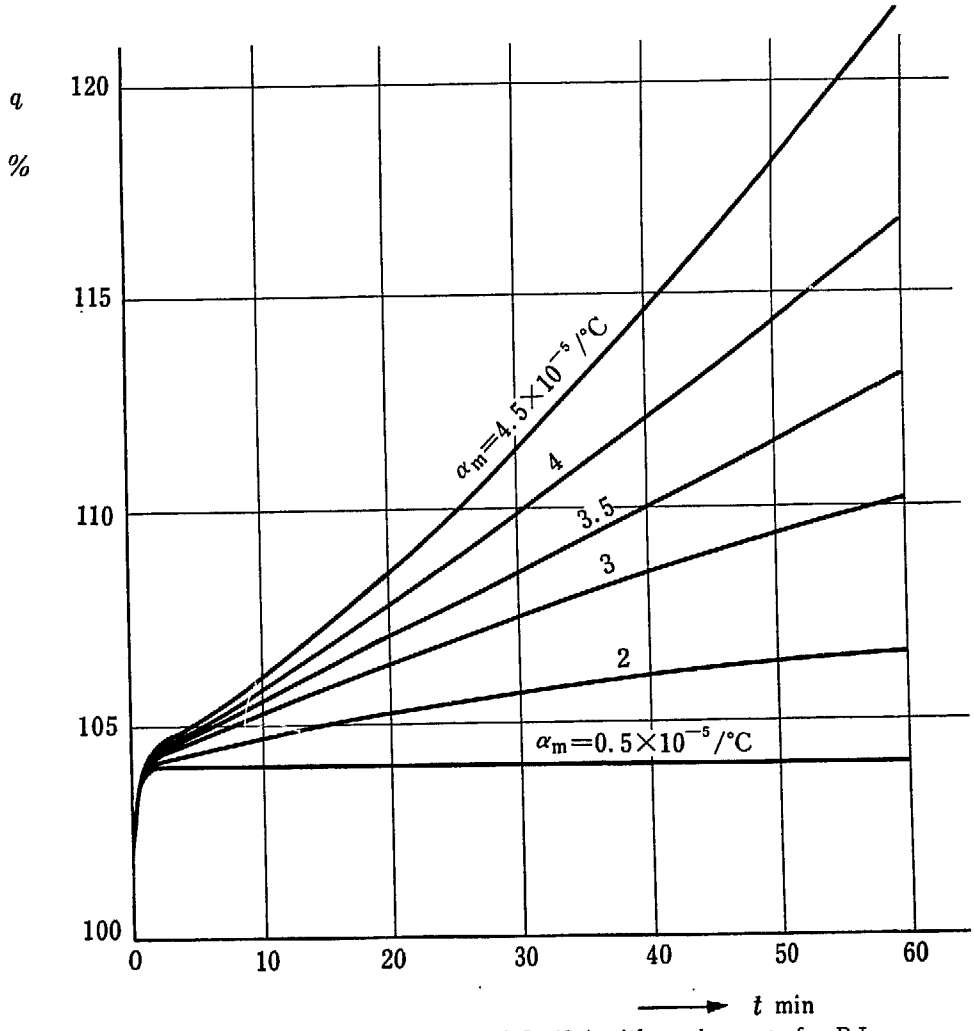

Fig. 5. 3. 2. Response of q to $\rho_{ex}=1.2\times10^{-4}$ with various α_m for R-I.

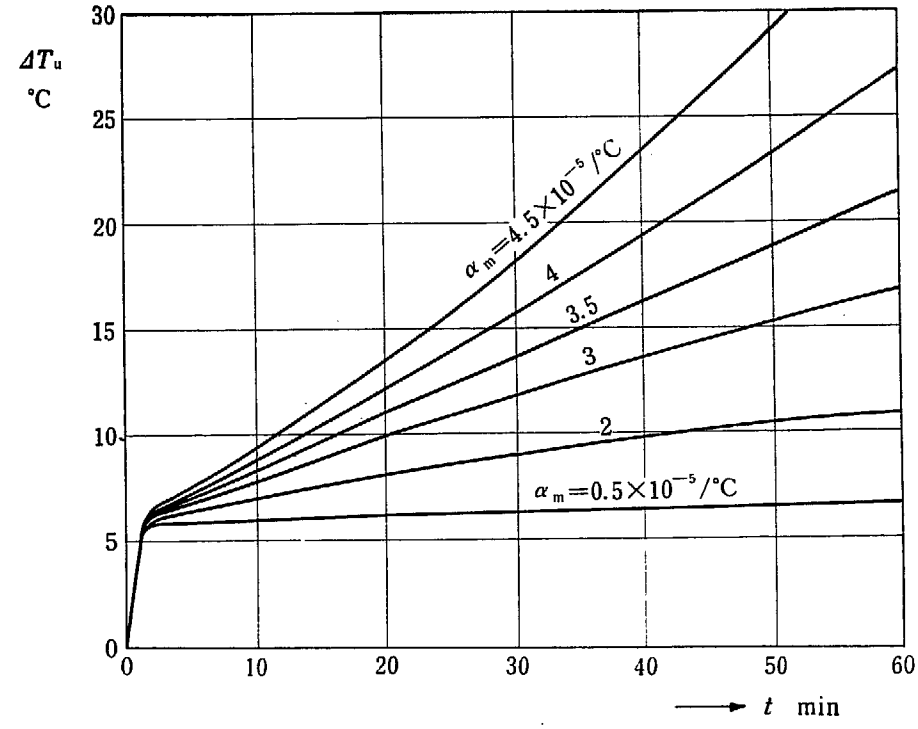

Fig. 5. 3. 3. Response of ΔT_u to $\rho_{ex}=1.2\times10^{-4}$ with various α_m for R-I.

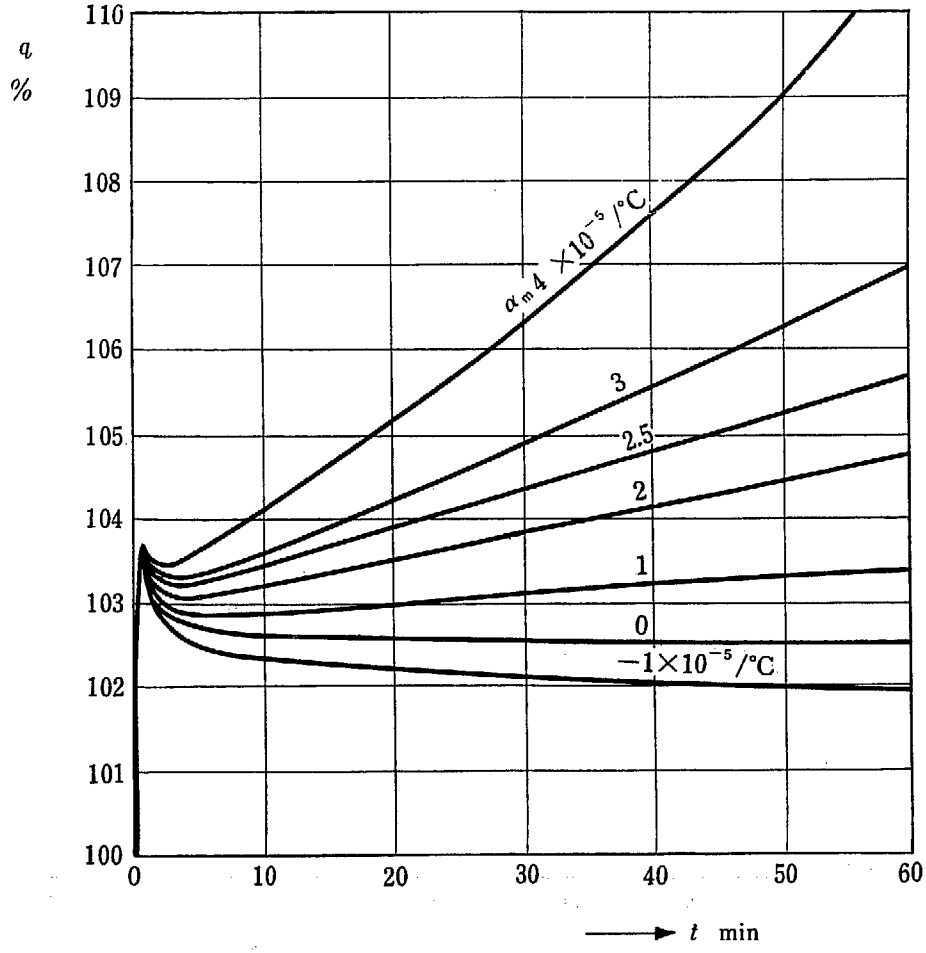

Fig. 5. 3. 4. Response of q to $\rho_{ex}=1.2\times10^{-4}$ with various α_m for R-III.

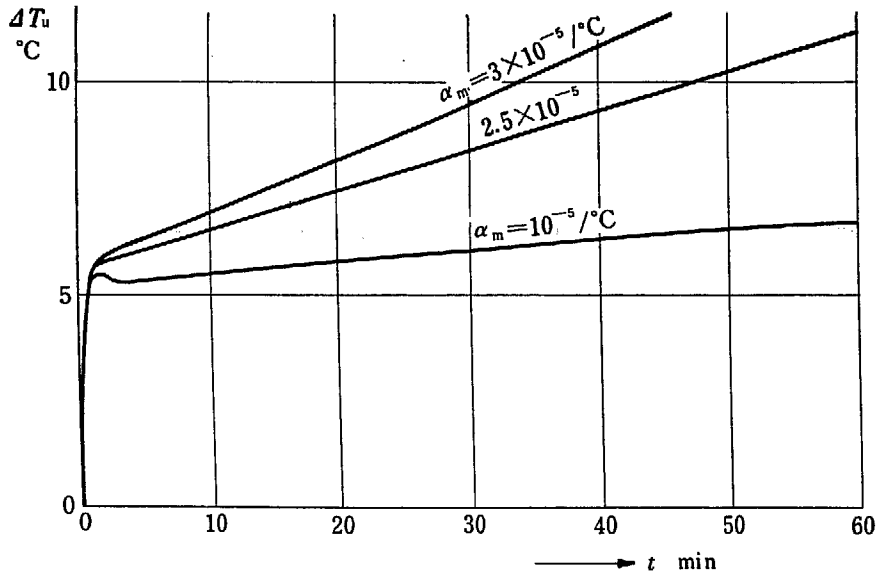

Fig. 5. 3. 5. Response of ΔT_u to $\rho_{ex}=1.2\times10^{-4}$ with various α_m for R-III.

Another approach, more rigorous treatment regarding α_{mc}, is given in Appendix 4. Appendix 2, TABLE 8 shows values of α_u, a_v, a_s and a_m for R-I, R-II and R-III. α_{mc} calculated from Eq. (5. 3. 6) using the above values is also given.

In order to examine this predicted value of α_{mc}, an analog computer solution has been obtained on R-I and R-III, and the results are shown in **Fig. 5. 3. 2** and **Fig. 5. 3. 3** on R-I, and in **Fig. 5. 3. 4** and **Fig. 5. 3. 5** on R-III. Critical value of α_m is not accurately obtained from these figures, since a long running time of a computer is needed until solution attains an equilibrium value due to a long time constant of moderator. However, criticality can be easily observed from these figures, that is, curves are convex with respect to abscissa in the case of $\alpha_m>\alpha_{mc}$., and concave, in the case of $\alpha_m<\alpha_{mc}$. From these observations computer solutions agree with a predicted value of α_{mc}. From the safety point of view it is desirable for α_{mc} to be as high as possible. It is noted that in Eq. (5. 3. 6) α_{mc} increases as a_s and a_m decrease, which are the functions of the heat transfer coefficients of the thermal system. This requirement will contradict other requirements on the thermal system. Thus engineering compromise should be made in designing reactors.

6. Conclusions.

Dynamic characteristics of the British type gas cooled reactors have been given so far for a Calder Hall type as well as for the advanced types. A great deal of information on the characteristic features of this type of reactors has been obtained. Important features among then are :

(1) Period of a power rise under the conditions considered in this report is longer than several minutes, 5 minutes after the introduction of disturbances.

(2) The effect of a sleeve on transient behaviors is favorable in many respects.

(3) A critical value of positive α_m exists, below which a reactor is still self-regulating. These values are of the order of 3×10^{-5}/°C. (for the details, refer to Appendix 2, TABLE 8).

(4) The virtual time constant approach treated in 5. 2 has given valuable information on correlations between dynamic response and thermal system parameters although a few of them have been done so far. Development of this approach is still under way.

From the viewpoints of reactor control and safety a great deal still remains to be done. It should be noted that the control systems and heat exchangers were not included in most cases.

Accordingly more complicated systems should be treated in order to include control systems and heat exchangers.

It should be also noted that a unit cell model for thermal system approximation is adopted. In order to examine the accuracy of this model, a multi-region model along the channel should be adopted.

For more information on other analog computer solutions than shown in this report and the setup of the computer, References 6), 7), 8) should be consulted.

Acknowledgements

The authors wish to express their deep appreciation to the Japan Atomic Power Company for their kind offering of many data necessary for computations. They also wish to thank Messrs. T. KUROYANAGI and M. AKIYAMA who not only prepared necessary data but also gave them many suggenstions for computations and Mr. M. ISHIZUKA, who gave them invaluable help in the preparation of this report.

Thanks are due to Mr. Y. SAWAGUCHI of the Japan Atomic Power Co. and Mr. K. ONO of the Central Research Institute of Electrical Power Industry, who made computations by use of an IBM 650 for comparison with the analog computation, and also due to the IBM staff in JAERI who gave an opportunity to use the IBM 650 for this purpose.

REFERENCES

1) R. J. SMITH: 2nd Geneva Conf., P/85 (1958)
2) G. BROW *et al.*: Ibid, P/267
3) R. V. MOORE: J. B. N. E. C. 2, 2: 61–82 (1957)
4) R. N. MILLAR: 2nd Geneva Conf. P/74 (1958)
5) T. J. O'NEILLE: 2nd Geneva Conf. P/21 (1958)
6) Analysis of problems in connection with the positive temperature coefficient of Advanced Calder Hall type reactor (Interim Report No. 2) JAERI, (1958) (in Japanese)
7) Progress Report No.4 of Control and Instrumentation Section, JAERI (1958) (in Japanese)
8) Progress Report No.6 of Control and Instrumentation Section, JAERI (1959) (in Japanese)
9) Influence of the positive temperature coefficient of gas cooled reactor upon thermal transient behavior, Data No. 1 of Mechanical Engineering Section JAERI (1958)(in Japanese)
10) T. KAGAYAMA: Journal of Japan Association of Automatic Control Engineers, 3. 5. 278 (1959) (Abstract in English).
11) K. INOUE, M. IIZUMI, K. NISHIMURA: Temperature Coefficient of Reactivity of Calder Hall Type Reactor, JAERI 1006-A (1959)

Appendix 1. Notation

a	coefficient of effectiveness of graphite sleeve to that of graphite moderator with respect to temperature coefficient	
$a_m = \Delta T_m^*/\Delta T_u^*$		
$a_s = \Delta T_s^*/\Delta T_u^*$		
$a_v = \frac{aV_s}{V_s+V_m}$		
C	heat capacity per unit length along channel	cal/cm°C
$f = \frac{5+\cos\frac{\pi L}{L_1}}{3\left(1+\frac{L_1}{\pi L}\sin\frac{\pi L}{L_1}\right)}$	[Refer to 5)]	
G	gain constant	°C sec cm/cal
h	variables proportional to concentration of delayed neutron precursor	cal/cm sec
H	heat transfer coefficient per unit length along channel (as for subscript, refer to **Fig. 3. 1**)	cal/cm sec°C
k	constant (Refer to Eq. 3. 4)	
K	virtual gain constant	°C
l	mean effective lifetime of a neutron	sec
L	fuel length	cm
L_1	effective extrapolated length of axial flux	cm
n	neutron density	$1/cm^3$
q	Q/Q_0	
Δq^*	(Refer to 5. 3)	
Q	power production per unit length along channel	cal/cm sec
r	h/Q_0	
R_1	heat transfer coefficient for radiation between clad and sleeve	cal/cm sec°K^4
R_2	heat transfer coefficient for radiation between sleeve and moderator	cal/cm sec°K^4
$R_{1f} = 4T_{f0}^3 \cdot R_1$		cal/cm sec°C
$R_{1s} = 4T_{s0}^3 R_1$		cal/cm sec°C
$R_{2s} = 4T_{s0}^3 R_2$		cal/cm sec°C
$R_{2m} = 4T_{m0}^3 R_2$		cal/cm sec°C
t	time	sec
T	mean temperature	°K
$T(x)$	temperature at a point x	°K
$\bar{T}$	statistically weighted mean value of temperature	°K
$\Delta T = T-T_0$		°C
ΔT^*	(Refer to 5. 3)	°C
u_1, u_2	coolant gas velocities inside and outside sleeve, respectively	cm/sec
V_m	volume of graphite moderator in unit cell	cm^3
V_s	volume of graphite sleeve in unit cell	cm^3
x	distance from lower end of channel	cm
x_m	a point where temperature of clad is maximum	cm
α_m	temperature coefficient of graphite moderator	1/°C
α_{mc}	critical value of positive temperature coefficient	1/°C
α_s	temperature coefficient of graphite sleeve	1/°C
α_u	temperature coefficient of fuel	1/°C

β fraction of delayed neutron
δ virtual time constant sec
λ decay constant of delayed neutron precursor 1/sec
μ attenuation of temperature within heat exchanger. (Refer to Eq. 4. 1)
μ_u, μ_s, μ_m proportions of power generated in fuel, sleeve and main moderator, respectively $(\mu_u+\mu_s+\mu_m=1)$
$\xi = (u-u_0)/u_0$
ρ reactivity
ρ_{ex} externally applied reactivity
τ time constant sec

Subscript
u stands for fuel
f " clad
c_1 " gas inside sleeve
s " sleeve
c_2 " gas outside sleeve
m " main moderator
in " inlet gas
out " outlet gas
o " equilibrium value

Second Subscript
m stands for values at a point where temperature of clad is maximum

Appendix 2. Tables of Parameters

TABLE 1. Dimensions of Reactor

Item	Unit	R-I	R-II	R-II (Rev.)	R-III
Fuel Diameter	cm	—	4.06, O.D. 2.37, I.D.		2.92
Fin Root Diameter	"	2.92	4.47		3.58
Fin Tip Diameter	"	5.40	6.65		6.05
Sleeve I.D.	"	—	10.41		10.16
Sleeve O.D.	"	—	12.70		12.65
Moderator I.D.	"	10.16	13.72		13.67
Unit Cell O.D.	"	22.94	25.80		23.65
Nominal Core Diameter	"	942	1168		1353
" Height	"	638	655		699
Fuel Length	"	610	657		608
Number of Unit Cell	—	1696	2056		3288
Reactor Thermal Output	MW	176	595		535

TABLE 2. Temperature at Normal Operation
(Values in parentheses are estimated from given parameters)

Item		Unit	R-I	R-II	R-II (Rev.)	R-III
Coolant Inlet Temp.	T_{in}	°C	140	191		204
" Outlet Temp.	T_{out}	"	334	402		391
Max Clad Surface Temp.		"	408	454		454
Coolant Temp. inside Sleeve	T_{c1o}	"	237	(289)	(291)	(298)
Fuel Temperature	T_{uo}	"	326	(464)	(446)	(412)
Clad "	T_{fo}	"	—	(376)	(376)	(374)
Sleeve "	T_{so}	"	—	(304)	(310)	(309)
Coolant Temp. outside Sleeve	T_{c2o}	"	—	(346)	(384)	(328)
Moderator Temp.	T_{mo}	"	250	(427)	(459)	(376)

TABLE 3. Material Constants

Item	Unit	R-I	R-II	R-II (Rev.)	R-III
Specific Heat					
U	cal/g°C	0.03224	0.0399	0.039	0.0368
Magnox	〃	—	0.2834	0.287	0.2845
CO_2 inside sleeve	〃	0.245	0.2536	0.2536	0.254
outside side	〃	—	0.2536	0.259	0.257
Graphite sleeve	〃	—	0.323	0.322	0.324
Moderator	〃	0.2914	0.365	0.358	0.350
Specific Gravity					
U	g/cm³	18.7	18 9	—	18.9
Magnox	〃	—	—	—	1.685
CO_2 inside Sleeve	〃	6.89×10^{-3}	11.47×10^{-3}	11.47×10^{-3}	10.5×10^{-3}
outside Sleeve	〃	—	11.47×10^{-3}	11.49×10^{-3}	10.17×10^{-3}
Graphite Sleeve	〃	—	1.75	1.75	1.73
Moderator	〃	1.73	1.75	1.75	1.73
Viscosity of CO_2 inside Sleeve	g/cm sec	2.48×10^{-4}	2.68×10^{-4}	2.54×10^{-4}	2.56×10^{-4}
outside Sleeve	〃	—	〃	2.67×10^{-4}	2.604×10^{-4}
Thermal Conductivity					
U	cal/cm/sec°C	—	0.081	0.071	0.081
CO_2 inside Sleeve	〃	7.5×10^{-5}	9.36×10^{-5}	9.36×10^{-5}	8.27×10^{-5}
outside Sleeve	〃	—	〃	10.11×10^{-5}	8.68×10^{-5}

TABLE 4. Parameters for Heat Transfer and Coolant flow

Item		Unit	R-I	R-II	R-II (Rev.)	R-III
Power Density	Q_0	cal/sec cm	40.6	142.5		55.5
Heat Capacity						
U	C_u	cal/cm°C	4.03	6.43	5.363	4.75
Clad	C_f	〃	—	4.63	3.914	4.78
CO_2 inside Sleeve	C_1	〃	0.0982	0.147	0.147	0.139
outside Sleeve	C_2	〃	—	0.0616	0.06299	0.0555
Graphite Sleeve	C_s	〃	—	23.7	23.33	25.06
Moderator	C_m	〃	167.5	239	234.7	178.6
Heat Production Ratio						
in Fuel	μ_u	—	0.95	0.93	0.92	0.93
in Sleeve	μ_s	—	—	0.008	0.0082	0.01
in Moderator	μ_m	—	0.05	0.062	0.0718	0.06
Heat Transfer Rate						
h_1		cal/cm²sec°C	—	0.143	0.155	0.149
h_2		〃	0.025	0.0719	0.0868	0.035
h_3		〃	0.005	0.0183	0.019	0.012
h_4		〃	—	1.22×10^{-3}	1.00×10^{-3}	5.7×10^{-4}
h_5		〃	—	〃	1.28×10^{-3}	〃
Heat Transfer Coefficient						
H_1		cal/cm sec°C	—	1.82	1.894	1.37
H_2		〃	0.424	1.502	1.517	0.665
H_3		〃	0.160	0.598	0.6229	0.384
H_4		〃	—	0.0485	0.0399	0.0228
H_5		〃	—	0.0525	0.05517	0.0246
Radiative Heat transfer Coefficient						
R_1		cal/cm sec°K⁴	—	1.766×10^{-11}	2.704×10^{-11}	1.617×10^{-11}
R_2		〃	—	3.56×10^{-11}	3.562×10^{-11}	3.46×10^{-11}
Gas Flow Rate per Channel		kg/sec	0.605	1.81	1.81	0.814

Item	Unit	R-I	R-II	R-II (Rev.)	R-III
Gas Velocity inside Sleeve u_1	cm/s	1511	3125	3153	1470
outside Sleeve u_2	〃	—	74.6	32.9	37
Reynolds Number (inside sleeve)	—	2×10^5	5×10^5	5.3×10^5	2.5×10^5
Stanton Number (inside sleeve)	—	9.8×10^{-3}	7.91×10^{-3}	9.46×10^{-3}	8.7×10^{-3}
Prandtl Number	—	0.81	0.724	0.724	0.73
Gas Pressure	kg/cm²	7	13.4		11.5

TABLE 5. Nuclear Constants

Item		Unit	R-I	R-II	R-II (Rev.)	R-III
Delayed Neutron Fraction	β	—	0.0073	0.0064	0.00539	0.0064
Decay Constant	λ	sec^{-1}	0.0787	0.0768	0.0769	0.0768
Neutron Lifetime	l	sec	10^{-3}	10^{-3}	1.4×10^{-3}	10^{-3}
Fuel Temp. Coef.	α_u	1/°C	-2×10^{-5}	-2×10^{-5}	-2.1×10^{-5}	-2×10^{-5}
Sleeve 〃	α_s	〃	—	*	2.75×10^{-5}	*
Moderator 〃	α_m	〃	*	*	10.8×10^{-5}	*

* Described in Chapt. 2 through 4.

TABLE 6. Parameters in Fig. 5.2.1.

Item	Unit	R-I	R-II	R-II (Rev.)	R-III
τ_u	sec	9.50	3.53	2.83	3.47
τ_f	〃	—	1.40	1.14	2.35
τ_1	〃	0.0918	0.0420	0.0415	0.0852
τ_s	〃	—	35.2	32.8	57.7
τ_2	〃	—	0.536	0.621	1.04
τ_m	〃	1050	2260	2120	2860
G_u	°C sec cm/cal	2.36	0.55	0.528	0.73
G_f	〃	—	0.303	0.29	0.492
G_1	〃	0.935	0.286	0.282	0.613
G_s	〃	—	1.48	1.41	2.30
G_2	〃	—	8.70	9.86	18.8
G_m	〃	6.25	9.45	9.26	16.0
$2u_1C_1/L$	cal/sec cm°C	0.486	1.40	1.41	0.583
$2u_2C_1/L$	—	—	0.0140	0.00631	0.00598

TABLE 7. Parameters in Fig. 5.2.2.

Item	Unit	R-I	R-II	R-II (Rev.)	R-III
δ_u	sec	15.6	15	15.5	35
δ_s	〃	—	72.5	73	140
δ_m	〃	1385	2600	2700	3300
K_u	°C	150	243	249	200
K_s	〃	—	83	99	86
K_m	〃	94	131	149	110

K_u, K_s and K_m should be equal to $\Delta T_u^*/\Delta q^*$, $\Delta T_s^*/\Delta q^*$ and $\Delta T_m/\Delta q^*$, respectively. However, $K's$ shown above are not exactly equal to the values shown in Table 9, since small partial fractions are ignored in the single time constant model.

TABLE 8. Parameters Concerning α_{mc}.

Item	Unit	R-I	R-II	R-II (Rev.)	R-III
α_u	1/°C	-2×10^{-5}	-2×10^{-5}	-2.1×10^{-5}	-2×10^{-5}
a_v	—	—	0.18	0.254	0.236
a_s	—	—	0.408	0.484	0.514
a_m	—	0.544	0.680	0.797	0.697
α_{mc}	1/°C	3.7×10^{-5}	2.7×10^{-5}	2.3×10^{-5}	2.4×10^{-5}

TABLE 9. The Ratio of ΔT^* to Δq^*

Item	Unit	R-I	R-II	R-II (Rev.)	R-III
$\Delta T_u^*/\Delta q^*$	°C	172	245	256	208
$\Delta T_f^*/\Delta q^*$	〃	—	171	187	171
$\Delta T_{c1}^*/\Delta q^*$	〃	82	83	104	95
$\Delta T_s^*/\Delta q^*$	〃	—	100	124	107
$\Delta T_{c2}^*/\Delta q^*$	〃	—	116	160	113
$\Delta T_m^*/\Delta q^*$	〃	94	167	204	145

Most of values in TABLE 4 through 9 are estimated from given parameters.

Appendix 3. Equations for Computation

Substituting design values to parameters in Eqs. (2.4), (2.5), (3.5), (3.7), (3.8) and (3.9), equations for analog computation are obtained as follows:

(1) For R-I, from Eqs. (2.4), (2.5)

$$\rho=\rho_{ex}-2\times10^{-5}\,\Delta T_u+\alpha_m\Delta T_m$$

$$\frac{d\Delta Q}{dt}=10^3\rho(Q_0+\Delta Q)-7.3\Delta Q+0.079\Delta h$$

$$\frac{d\Delta h}{dt}=7.3\Delta Q-0.079\Delta h$$

$$\frac{d\Delta T_u}{dt}=0.236\Delta Q+0.105(\Delta T_c-\Delta T_u)$$

$$\frac{d\Delta T_c}{dt}=4.3\Delta T_u-11\Delta T_c+1.6\Delta T_m+5.0\Delta T_{in}$$

$$\frac{d\Delta T_m}{dt}=0.0003\Delta Q+0.00095(\Delta T_c-\Delta T_m) \qquad \text{(A. 3. 1)}$$

(2) For R-II, from Eqs. (3.5), (3.7) and (3.8)

$$\rho=\rho_{ex}-2.0\times10^{-5}\Delta\bar{T}_u+0.18\alpha_m\Delta\bar{T}_s+\alpha_m\Delta\bar{T}_m$$

$$\frac{d\Delta q}{dt}=10^3\rho(1+\Delta q)-6.4\Delta q+0.0768\Delta r$$

$$\frac{d\Delta r}{dt}=6.4\Delta q-0.0768\Delta r$$

$$\frac{d\Delta\bar{T}_u}{dt}=25\Delta q-0.28\Delta\bar{T}_u+0.28\Delta\bar{T}_f$$

$$\frac{d\Delta\bar{T}_f}{dt}=0.393\Delta\bar{T}_u-0.724\Delta\bar{T}_f+0.324\Delta\bar{T}_{c1}+0.003\Delta\bar{T}_s$$

$$\frac{d\Delta\bar{T}_{c1}}{dt}=10.2\Delta\bar{T}_f-25.8\Delta\bar{T}_{c1}+4.07\Delta\bar{T}_s+11.5\Delta T_{in}$$

$$\frac{d\Delta\bar{T}_s}{dt}=0.058\Delta q-0.029\Delta\bar{T}_s+0.025\bar{T}_{c1}+0.002\Delta\bar{T}_{c2}+0.0009\Delta\bar{T}_f+0.0023\Delta\bar{T}_m$$

$$\frac{d\Delta\bar{T}_{c2}}{dt}=0.79\Delta\bar{T}_s-1.9\Delta\bar{T}_{c2}+0.85\Delta\bar{T}_m+0.28\Delta T_{in}$$

$$\frac{d\Delta\bar{T}_m}{dt}=0.045\Delta q-4.5\times10^{-4}\Delta\bar{T}_m+2.2\times10^{-4}\Delta\bar{T}_{c2}+1.2\times10^{-4}\Delta\bar{T}_s$$

$$\frac{d\Delta\bar{T}_{fm}}{dt}=0.393\Delta T_{um}-0.724\Delta T_{fm}+0.53\Delta\bar{T}_{c1}-0.21\Delta T_{in}+0.003\Delta T_s$$

$$\frac{d\Delta T_{um}}{dt}=23\Delta q-0.28\Delta T_{um}+0.28\Delta T_{fm} \qquad \text{(A. 3. 2)}$$

and from Eqs. (3. 9)

$$\frac{d\Delta\bar{T}_u}{dt}=25\Delta q-0.28\Delta\bar{T}_u+0.28\Delta\bar{T}_f$$

$$\frac{d\Delta\bar{T}_f}{dt}=0.393\Delta\bar{T}_u-0.40\Delta\bar{T}_f+0.003\Delta\bar{T}_s+34.3(1-\xi^{0.8})+0.324(\Delta\bar{T}_{c1}-\Delta\bar{T}_f)\xi^{0.8}$$

$$\frac{d\Delta\bar{T}_{c1}}{dt}=(10.2\Delta\bar{T}_f-14.3\Delta\bar{T}_{c1}+4.07\Delta\bar{T}_s)\times\xi^{0.8}-11.5\Delta\bar{T}_{c1}\times\xi+1160(\xi^{0.8}-\xi)$$

$$\frac{d\Delta\bar{T}_s}{dt}=0.058\Delta q+0.0009\Delta\bar{T}_f-0.00177\Delta\bar{T}_s+0.0023\Delta\bar{T}_m$$
$$+(0.0252\Delta\bar{T}_{c1}-0.0272\Delta\bar{T}_s+0.002\Delta\bar{T}_{c2})\times\xi^{0.8}+0.36(1-\xi^{0.8})$$

$$\frac{d\Delta\bar{T}_{c2}}{dt}=(0.79\Delta\bar{T}_s-1.64\Delta\bar{T}_{c2}+0.85\Delta\bar{T}_m)\times\xi^{0.8}-0.275\Delta\bar{T}_{c2}\times\xi+43.9(\xi^{0.8}-\xi)$$

$$\frac{d\Delta\bar{T}_m}{dt}=0.045\Delta q+1.2\times10^{-4}\Delta\bar{T}_s-2.3\times10^{-4}\Delta\bar{T}_m$$
$$+2.2\times10^{-4}(\Delta\bar{T}_{c2}-\Delta\bar{T}_m)\times\xi^{0.8}+0.021(1-\xi^{0.8})$$

$$\frac{d\Delta\bar{T}_{um}}{dt}=23\Delta q-0.28\Delta T_{um}+0.28\Delta T_{fm}$$

$$\frac{d\Delta T_{fm}}{dt}=0.393\Delta T_{um}-0.40\Delta T_{fm}+0.003\Delta\bar{T}_s+0.324(1.65\Delta\bar{T}_{c1}-\Delta T_{fm})\times\xi^{0.8}+31(1-\xi^{0.8})$$

(A. 3. 3)

(3) For R-III, from Eqs. (3. 5), (3. 7), (3. 8)

$$\rho=\rho_{ex}-2.4\times10^{-5}\Delta T_u+0.283\alpha_m\Delta T_s+1.2\alpha_m\Delta T_m$$

$$\frac{d\,\Delta q}{dt}=10^3\rho q-6.4\Delta q+0.0768\Delta r$$

$$\frac{d\,\Delta r}{dt}=6.4\Delta q-0.0768\Delta r$$

$$\frac{d\Delta T_u}{dt}=10.87\Delta q-0.288\Delta T_u+0.288\Delta T_f$$

$$\frac{d\Delta T_f}{dt}=0.287\Delta T_u-0.429\Delta T_f+0.139\Delta T_{c1}+0.00267\Delta T_s$$

$$\frac{d\Delta T_{c1}}{dt}=4.78\Delta T_f-11.7\Delta T_{c1}+2.76\Delta T_s+4.16\Delta T_{in}$$

$$\frac{d\Delta T_s}{dt}=0.022\Delta q+0.0153\Delta T_{c1}-0.0178\Delta T_s+0.00091\Delta T_{c2}+0.0007\Delta T_f+0.00151\Delta T_m$$

$$\frac{d\Delta T_{c2}}{dt}=0.411\Delta T_s-0.959\Delta T_{c2}+0.443\Delta T_m+0.105\Delta T_{in}$$

$$\frac{d\Delta T_m}{dt}=0.0186\Delta q+1.38\times10^{-4}\Delta T_{c2}-3.5\times10^{-4}\Delta T_m+1.52\times10^{-4}\Delta T_s$$

$$\frac{d\Delta T_{um}}{dt}=11.1\Delta q-0.263\Delta T_{um}+0.263\Delta T_{fm}$$

$$\frac{d\Delta T_{fm}}{dt}=0.275\Delta T_{um}-0.416\Delta T_{fm}+0.221\Delta T_{c1}+0.00256\Delta T_s-0.0844\Delta T_{in} \qquad \text{(A. 3. 4)}$$

and from Eqs. (3. 9)

$$\frac{d\Delta T_u}{dt}=10.9\Delta q-0.288\Delta T_u+0.288\Delta T_f$$

$$\frac{d\Delta T_f}{dt}=0.287\Delta T_u-0.290\Delta T_f+0.00267\Delta T_s+10.6(1-\xi^{0.8})+0.139(\Delta T_{c1}-\Delta T_f)\times\xi^{0.8}$$

$$\frac{d\Delta T_{c1}}{dt}=(4.78\Delta T_f-7.55\Delta T_{c1}+2.76\Delta T_s)\times\xi^{0.8}-4.19\Delta T_{c1}\times\xi+394(\xi^{0.8}-\xi)$$

$$\frac{d\Delta T_s}{dt}=0.022\Delta q+0.0007\Delta T_f-0.00160\Delta T_s+0.00151\Delta T_m$$
$$+(0.0153\Delta T_{c1}-0.0162\Delta T_s+0.00091\Delta T_{c2})\times\xi^{0.8}+0.151(1-\xi^{0.8})$$

$$\frac{d\Delta T_{c2}}{dt}=(0.411\Delta T_s-0.854\Delta T_{c2}+0.443\Delta T_m)\times\xi^{0.8}-0.105\Delta T_{c2}\times\xi+13.4(\xi^{0.8}-\xi)$$

$$\frac{d\Delta T_m}{dt}=0.0186\Delta q+1.53\times10^{-4}\Delta T_s-2.12\times10^{-4}\Delta T_m+1.38\times10^{-4}(\Delta T_{c2}-\Delta T_m)\times\xi^{0.8}$$
$$+0.0066(1-\xi^{0.8})$$

$$\frac{d\Delta T_{um}}{dt}=11.1\Delta q-0.263\Delta T_{um}+0.263\Delta T_{fm}$$

$$\frac{d\Delta T_{fm}}{dt}=0.275\Delta T_{um}-0.28\Delta T_{fm}+0.00256\Delta T_s+(0.221\Delta T_{c1}-0.136\Delta T_{fm})\times\xi^{0.8}+12.3(1-\xi^{0.8})$$
(A. 3. 5)

Appendix 4. Stability Analysis of Reactor Including Temperature Coefficients of Reactivity

The system including reactor neutron kinetics, heat transfer and temperature coefficients of reactivity is shown in Fig. A. 4. 1.

The neutron kinetics is represented by a linearized transfer function, assuming small input in ρ.

$$\frac{\Delta Q(s)}{\rho(s)}=\frac{Q_0\tau_2(\tau_1 s+1)}{l\tau_1 s(\tau_2 s+1)} \qquad \text{(A. 4. 1)}$$

The transfer functions from ΔQ to ΔT_u and to ΔT_m are approximated by a single time constant as mentioned in 5. 2, considering reactor without sleeve for simplicity.

$$\frac{\Delta T_u(s)}{\Delta Q(s)}=\frac{K_u}{\delta_u s+1} \qquad \text{(A. 4. 2)}$$

$$\frac{\Delta T_m(s)}{\Delta Q(s)}=\frac{K_m}{\delta_m s+1} \qquad \text{(A. 4. 3)}$$

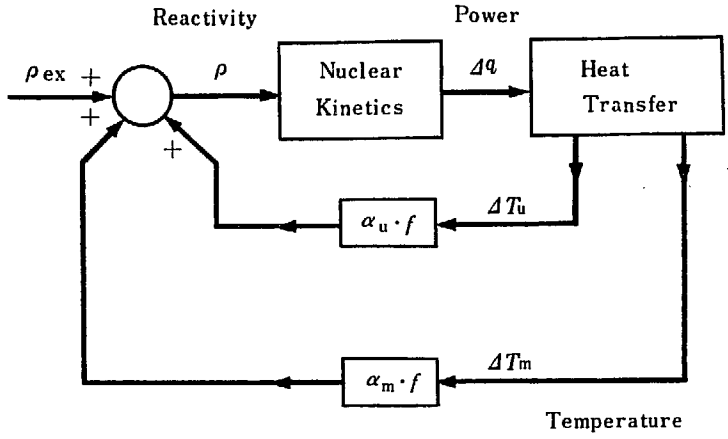

Fig. A. 4. 1. Block diagram with temperature feedback. (for R-I)

Then the overall transfer function from $\rho_{ex}(s)$ to $\Delta Q(s)$ equals

$$\frac{\Delta Q(s)}{\rho_{ex}(s)}=\frac{\bar{Q}_0\dfrac{\tau_1 s+1}{s(\tau_2 s+1)}}{1-\bar{Q}_0\dfrac{\tau_1 s+1}{s(\tau_2 s+1)}\left\{\dfrac{-U}{\delta_u s+1}+\dfrac{M}{\delta_m s+1}\right\}} \tag{A. 4. 4}$$

where $\bar{Q}_0=\dfrac{Q_0\tau_2}{l\tau_1}$

$U=-\alpha_u f K_u$

$M=\alpha_m f K_m$

The characteristic equation for stability analysis is obtained as follows

$$1-\bar{Q}_0\frac{\tau_1 s+1}{s(\tau_2 s+1)}\left\{\frac{-U}{\delta_u s+1}+\frac{M}{\delta_m s+1}\right\}=0 \tag{A. 4. 5}$$

which reduces to a fourth order algebraic equation

$$a_0 s^4+a_1 s^3+a_2 s^2+a_3 s+a_4=0 \tag{A. 4. 6}$$

where $a_0=\delta_u\delta_m\tau_2$

$a_1=\delta_u\delta_m+\tau_2\delta_u+\tau_2\delta_m$

$a_2=\delta_u+\delta_m+\bar{Q}_0\tau_1(U\delta_m-M\delta_u)$

$a_3=1+\bar{Q}_0\{(U\delta_m-M\delta_u)+\tau_1(U-M)\}$

$a_4=\bar{Q}_0(U-M)$

According to Hurwitz's criterion the necessary and sufficient conditions for stability are

(1) $a_0>0,\ a_1>0,\ a_2>0,\ a_3>0,\ a_4>0$ (A. 4. 7)

(2) $H_2=a_1a_2-a_0a_3>0$ (A. 4. 8)

(3) $H_3=a_1a_2a_3-a_0a_3^2-a_4a_1^2>0$ (A. 4. 9)

a_0 and a_1, are always positive. The necessary condition for $a_4>0$ is $U>M$. In practice the moderator has much larger time constant because of its large heat capacity, i. e. $\delta_u\ll\delta_m$. Then the conditions $a_2>0$ and $a_3>0$ are fulfilled.

The conditions (A. 4. 8) and (A. 4. 9) are also easily proved with the asscemptions $U>M$, $\delta_u\ll\delta_m$ and τ_2 much smaller than any of τ_1, δ_u and δ_m.

$$\frac{H_2}{\delta_u\delta_m}=(\delta_u+\delta_m-\tau_2)+U\bar{Q}_0\{\delta_m(\tau_1-\tau_2)-\tau_1\tau_2\}-M\bar{Q}_0\{\delta_u(\tau_1-\tau_2)-\tau_1\tau_2\}>0$$

$$\frac{H_3}{\delta_u\delta_m}=(\delta_u+\delta_m-\tau_2)+\bar{Q}_0\{\tau_1(\delta_m+\delta_u-2\tau_2)(U-M)+(U\delta_m-M\delta_u)(\tau_1-2\tau_2)$$

$$+(U\delta_m^2-M\delta_u^2)\}+\bar{Q}_0^2[(U\delta_m-M\delta_u)^2(\tau_1-\tau_2)+\tau_1(U-M)\{U(\tau_1\delta_m-2\tau_2\delta_m-\tau_1\tau_2)$$
$$-M(\tau_1\delta_u-2\tau_2\delta_u-\tau_1\tau_2)\}]>0$$

(Here approximation $a_1\fallingdotseq\delta_u\delta_m$ is adopted, since $\tau_2\delta_u+\tau_2\delta_m$ is much smaller than $\delta_u\delta_m$)

Thus the necessary and sufficient condition for stability is $U>M$. U is always positive since α_u is negative. If α_m is negative, i. e. M is negative, then naturally $U>M$. If α_m is positive the condition $U>M$ implies.

$$-\alpha_u K_u>\alpha_m K_m \tag{A. 4. 10}$$

or

$$\alpha_m>\frac{K_u}{K_m}(-\alpha_u) \tag{A. 4. 11}$$

Eq. (A. 4. 11) gives the critical value of positive α_m above which the reactor is unstable. It is remarkable that the critical α_m does not depend upon Q_0, thus a reactor stable at a certain power level is also stable at any other power level, so long as a small change in ρ is concerned and transfer function method is applicable.

It is easily shown that Eq. (A. 4. 11) is equivalent to Eq. (5. 3. 7) because ΔT_u^* and ΔT_m^* are proportional to the gain constant K_u and K_m respectively and so

$$a_m=\Delta T_m^*/\Delta T_u^*=K_m/K_u.$$

A more rigorous treatment than stated in 5. 3 gives here the same conclusion as obtained in 5. 3.

Appendix 5. Comparison of Digital and Analog Computation

In order to check the accuracy of analog computation, a portion of transient behaviors of R-II was computed by use of a digital computer IBM 650.

The differential equations A. 3. 2 were solved numerically by Runge-Kutta's method, time increment for each step being 0. 1 sec.

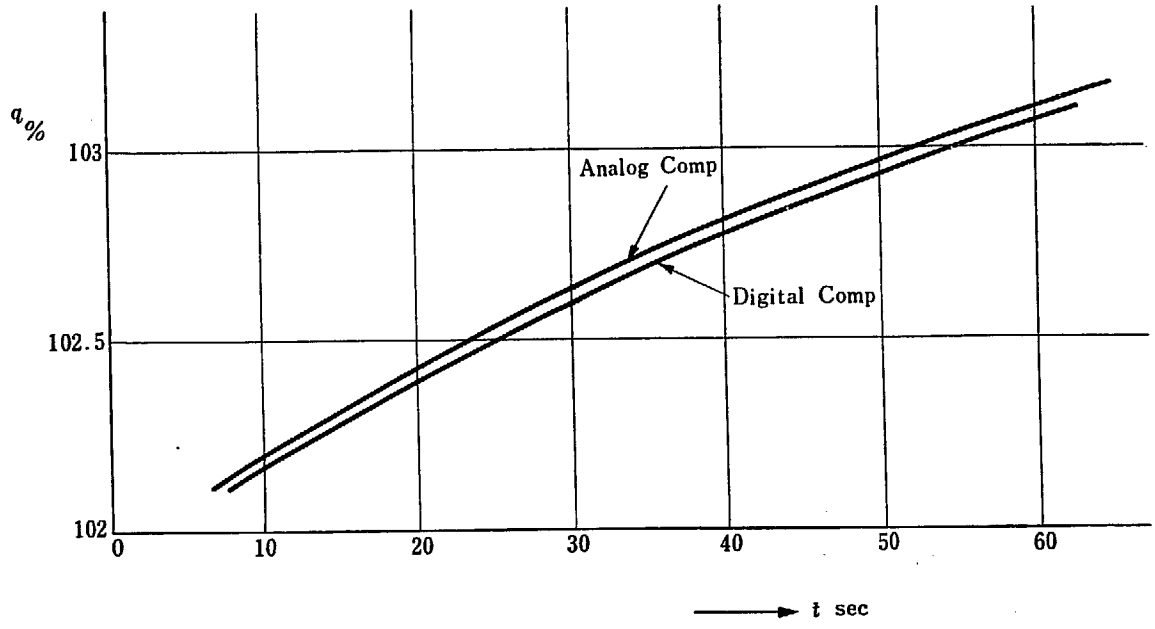

Fig. A. 5. 1. Comparison of solution obtained by digital and analog computation. (R-II)
Response of q to step change in $\rho_{ex}=1.2\times10^{-4}$, $\alpha_m=15\times10^{-5}$/°C

The results are shown in **Figs. A. 5. 1** and **A. 5. 2** and are compared with those obtained by analog computer. As far as the transient of short interval is concerned, the accuracy of analog computation is satisfactory. It is desirable to check the accuracy for longer interval, but digital calculation would consume tremendous computing time and in fact calculation of transient for more than one minute was impractical.

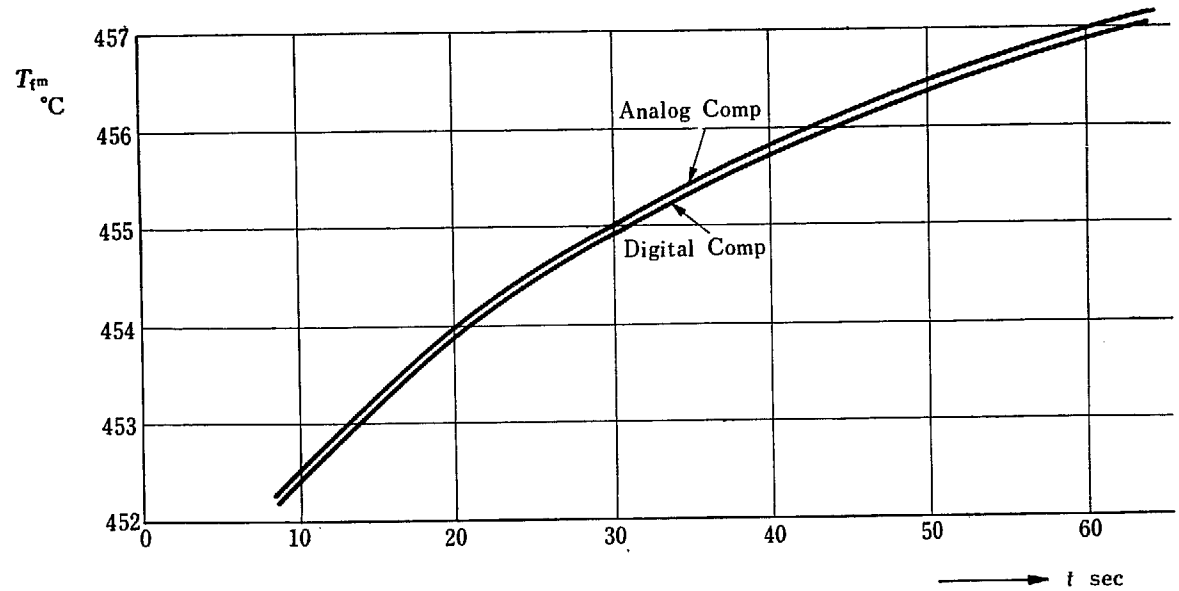

Fig. A. 5. 2. Comparison of solution obtained by digital and analog computation. (R-II)
Response of ΔT_{fm} to step change in $\rho_{ex}=1.2\times10^{-4}$, $\alpha_m=15\times10^{-5}$/°C

Appendix 6. Remarks on Response of q to Change in ΔT_{in}

Responses of q to change in ΔT_{in} have been observed to intersect abscissa at one point irrespective of magnitude of the disturbance ΔT_{in} as stated in 2. 2 (see also **Fig. 2. 4**). This fact is readily explained as follows.

It is assumed that neutron kinetics be represented by a linearized transfer function, so far as ρ and Δq are small, as shown in Eq. (A. 4. 1).

$$\frac{\Delta q(s)}{\rho(s)}=G_R(s) \tag{A. 6. 1}$$

Teperatures ΔT_u, ΔT_s and ΔT_m, which appear in temperature coefficient feedback paths are represented as follows,

$$\begin{aligned}\Delta T_u &= G_{uq}(s)\Delta q+G_{ui}(s)\Delta T_{in}\\ \Delta T_s &= G_{sq}(s)\Delta q+G_{si}(s)\Delta T_{in}\\ \Delta T_m &= G_{mq}(s)\Delta q+G_{mi}(s)\Delta T_{in}\end{aligned} \tag{A. 6. 2}$$

where $G(s)$'s are transfer functions determined from Eqs. (3. 5).

Equation between reactivity and temperatures is,

$$\rho=\rho_{ex}+\alpha_u f\Delta T_u+\alpha_s f\Delta T_s+\alpha_m f\Delta T_m \tag{A. 6. 3}$$

Since response of q to ΔT_{in} is of interest, combination of Eqs. (A. 6. 1), (A. 6. 2), and (A. 6. 3) gives, setting ρ_{ex} equal to zero,

$$\Delta q=\frac{B(s)G_R(s)}{1-A(s)G_R(s)}\Delta T_{in} \tag{A. 6. 4}$$

$$A(s)=\alpha_u f G_{uq}(s)+\alpha_s f G_{sq}(s)+\alpha_m f G_{mq}(s) \quad \text{(A. 6. 5)}$$

$$B(s)=\alpha_u f G_{ui}(s)+\alpha_s f G_{si}(s)+\alpha_m f G_{mi}(s) \quad \text{(A. 6. 6)}$$

It can be seen from Eq. (A. 6. 4) that response of q is of a similar form upon introduction of similar ΔT_{in} disturbances with different magnitude. Consequently response of q to ΔT_{in} intersect abscissa at one point irrespective of the magnitude of ΔT_{in} disturbance, so far as ΔT_{in}'s are of the similar form.

It is also noted from Eq. (A. 6. 4) that this result holds for any type of ΔT_{in}, i. e., step change, ramp change and so forth.

The point where response of q to ΔT_{in} intersects abscissa depends upon the value of α_m as seen from analog computer solutions. This can be seen readily from Eqs. (A. 6. 5) (A. 6. 6) which includes α_m.

Conclusion stated above does hold, so far as the linearized assumption of Eq. (A. 6. 1) is justifiable, that is, ρ and Δq do not become so large. Analog computer solutions indicate that the above assumption is applicable under the conditions considered.

Appendix 7. Analysis Based on Revised Data for R-II.

Recently more detailed information concerning design and performance data for R-II was obtained. Based on these data, parameters for a dynamic analysis were evaluated and they are shown in the fifth column of TABLES 1 through 9, Appendix 2. Compared with the parameters used for the analysis of R-II, the several remarkable differences are noted as follows:

(1) Differences in nuclear constants such as β, λ and l.

(2) Differences in parameters for heat transfer and coolant flow, especially in gas velocity u_2. The coolant mass flow rate outside the sleeve is about 0. 44% of the total flow rate, and those for R-II and R-III have been assumed to be 1%.

(3) Difference in the magnitude of positive temperature coefficients.

The moderator temperature coefficient is 10.8×10^{-5}/°C, which is smaller than the value assumed for R-II and R-III, 15×10^{-5}/°C.

(4) Difference in coefficient of effectiveness of graphite sleeve to that of graphite moderator with respect to temperature coefficient.

The ratio of α_s to α_m is shown as a_V in TABLE 8. The value calculated from $\alpha_m=10.8\times10^{-5}$/°C and $\alpha_s=2.75\times10^{-5}$/°C is 0. 255 and much larger than the value assumed for R-II, $a_V=0.18$.

The transient behaviors based on the revised data are shown in **Figs. A. 7. 1** through **A. 7. 2** and comparison of the response to the step change in ρ_{ex} with those of R-II and R-III, in **Fig. A. 7. 3.** Incidentally the results are quite similar to those obtained for R-II. It should be noted, however, that the positive temperature coefficient is smaller for R-II (Rev.) as mentioned above. And in fact the response becomes curve B of **Fig. A. 7. 3** for $\alpha_m=15\times10^{-5}$/°C, which is considerably different from that of R-II. Its principal cause is the difference in a_V and, a_V made equal to the value assumed for R-II, the response becomes curve *C*. The effect of difference in nuclear constants is quite small, which is shown by the difference between curve *C* and *D*. Thus the difference between curve *D* and R-II should be attributed to the differences in thermal parameters, mentioned in item (2) above.

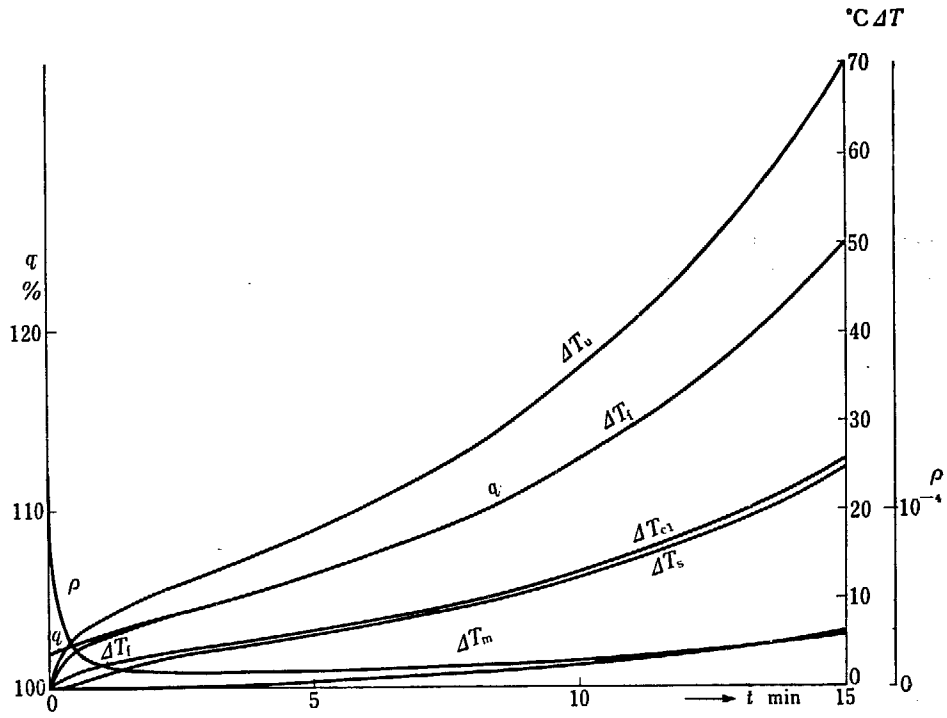

Fig. A. 7. 1. Response to step change in ρ_{ex} for R-II (Rev.)
$\rho_{ex}=1.2\times10^{-4}$, $\alpha_m=10.8\times10^{-5}$/°C

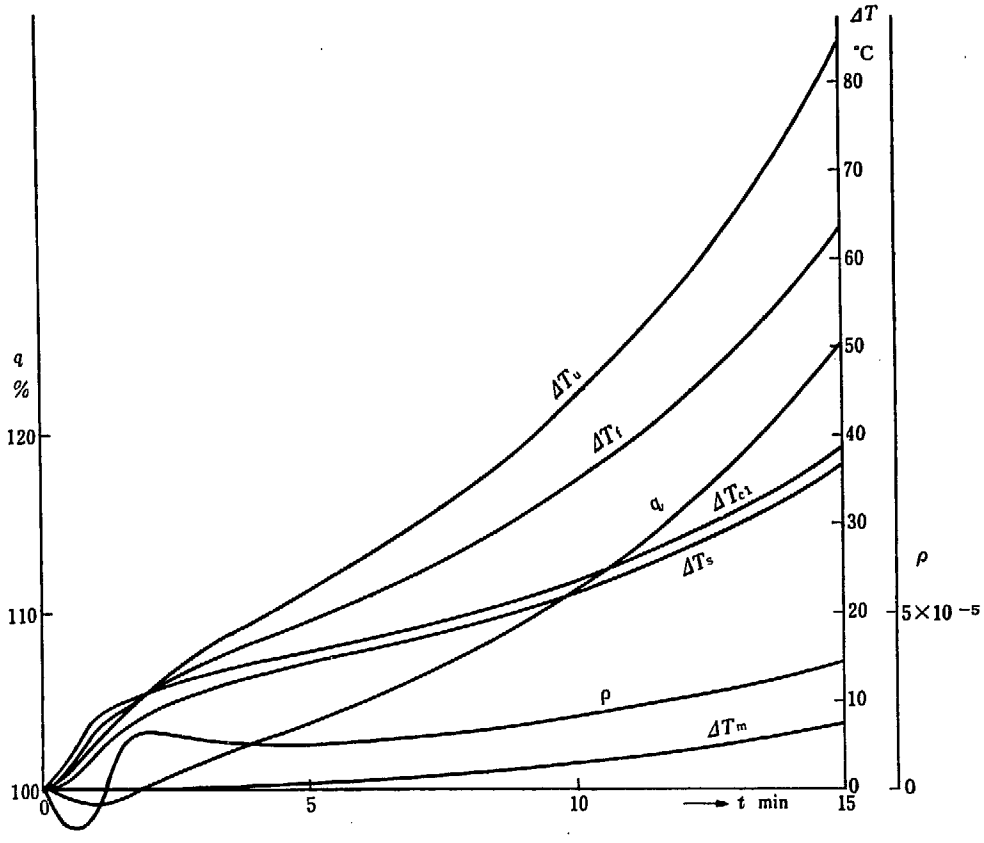

Fig. A. 7. 2. Response to ramp change in ΔT_{in} for R-II (Rev.)
$\Delta T_{in}=0.2$°C/sec×60 sec, $\alpha_m=10.8\times10^{-5}$/°C

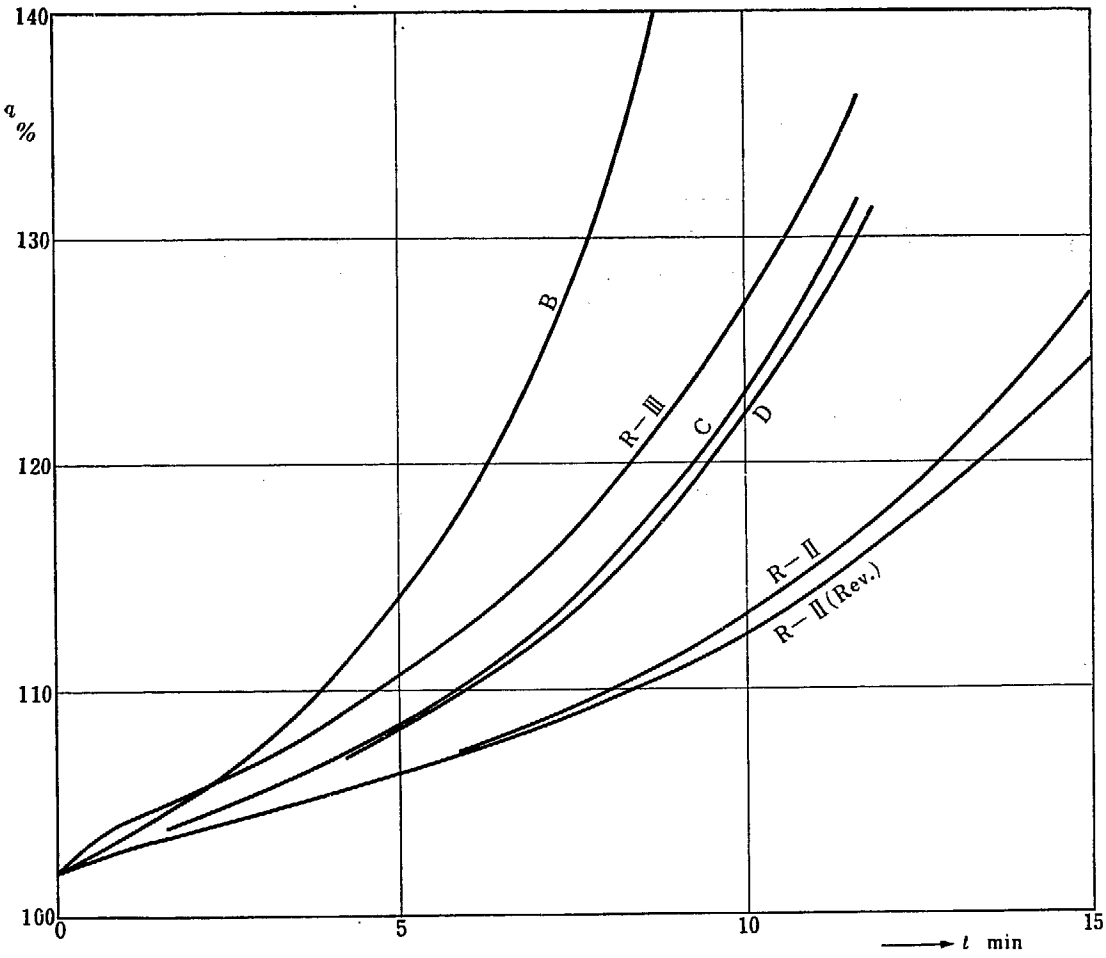

Fig. A. 7. 3. Comparison of responses to step change in ρ_{ex} for R-II, R-II (Rev.) and R-III
$\rho_{ex}=1.2\times10^{-4}$

Appendix 8. Remarks on the Analysis by a Distributed Parameter Heat Transfer Model.

In the analysis described thus far, the heat capacities of the fuel, the moderator, and of the coolant within the core were lumped respectively and the change in axial temperature distributions was not considered. Here a more rigorous method of simulating dynamic behavior of the reactor heat transfer system with a distributed parameter model is described, and a comparison is made with the lumped parameter model.

The heat production in the fuel is assumed to have a cosine distribution in the axial direction, and extrapolation distance was neglected for simplicity.

The rate of heat conduction in the solids is assumed to be zero in the axial direction and infinite in the radial direction.

The complete mixing of the coolant gas in the horizontal cross section is assumed.

With these assumptions, which are same as in the case of a lumped parameter model except slight modifications, the basic equations of dynamic behavior are obtained as follows

$$C_u\frac{\partial \Delta T_u(x,t)}{\partial t}=\mu_u \Delta Q(t)\sin\frac{\pi}{L}x-H_1\{\Delta T_u(x,t)-\Delta T_c(x,t)\}$$

$$C_c\left\{\frac{\partial \Delta T_c(x,t)}{\partial t}+u\frac{\partial \Delta T_c(x,t)}{\partial x}\right\}=H_1\{\Delta T_u(x,t)-\Delta T_c(x,t)\}+H_2\{\Delta T_m(x,t)-\Delta T_c(x,t)\}$$

$$C_m\frac{\partial \Delta T_m(x,t)}{\partial t}=\mu_m \Delta Q(t)\sin\frac{\pi}{L}x-H_2\{\Delta T_m(x,t)-\Delta T_c(x,t)\} \qquad \text{(A. 8. 1)}$$

Rewriting Eqs. (A. 8. 1) in the Laplace transforms and solving for $\Delta T_{out}(s)=\Delta T_c(L,s)$ with the boundary condition $\Delta T_c(0,s)=\Delta T_{in}(s)$,

$$\Delta T_{out}(s)=\left\{\frac{\mu_u}{\tau_u s+1}+\frac{\mu_m}{\tau_m s+1}\right\}\frac{\tau_0}{\pi C_c}\frac{1+e^{-LA(s)}}{1+\left\{\frac{L}{\pi}A(s)\right\}^2}\Delta Q(s)+e^{-LA(s)}\Delta T_{in}(s) \qquad \text{(A. 8. 2)}$$

where $\tau_u=C_u/H_1$, $\tau_m=C_m/H_2$, $\tau_0=L/u$

$$A(s)=\frac{s}{u}\left\{1+\frac{C_u/C_c}{\tau_u s+1}+\frac{C_m/C_c}{\tau_m s+1}\right\}$$

and further,

$$\Delta T_{cav}(s)=\frac{1}{LA(s)}\left[\left\{\frac{\mu_u}{\tau_u s+1}+\frac{\mu_m}{\tau_m s+1}\right\}\frac{2\tau_0}{\pi C_c}\Delta Q(s)-\{\Delta T_{out}(s)-\Delta T_{in}(s)\}\right]$$

$$\Delta T_{uav}(s)=\frac{1}{\tau_u s+1}\left\{\frac{2\mu_u}{\pi H_1}\Delta Q(s)+\Delta T_{cav}(s)\right\}$$

$$\Delta T_{mav}(s)=\frac{1}{\tau_m s+1}\left\{\frac{2\mu_m}{\pi H_2}\Delta Q(s)+\Delta T_{cav}(s)\right\} \qquad \text{(A. 8. 3)}$$

where subscript *av* means the averaged temperature in the axial direction.

From Eqs. (A. 8. 2) and (A. 8. 3), a block diagram of the reactor heat transfer system is obtained as shown in **Fig. A. 8. 1**.

The responses of ΔT_{out} to change in ΔQ and ΔT_{in} are examined for both the distributed parameter model described above and the lumped parameter model. and the results are shown in **Figs. A. 8. 2** and **A. 8. 3** in the form of vector locus. It is remarkable that the locus of $\Delta T_{out}(j\omega)/\Delta T_{in}(j\omega)$ is quite different for the two cases, especially in the high frequency region. This fact suggests that the lumped parameter model should be avoided to obtain the response of ΔT_{out} to ΔT_{in}, if the high frequency component to be included in the inlet gas temperature disturbances.

For more details on the distributed parameter model the Reference 10) should be consulted.

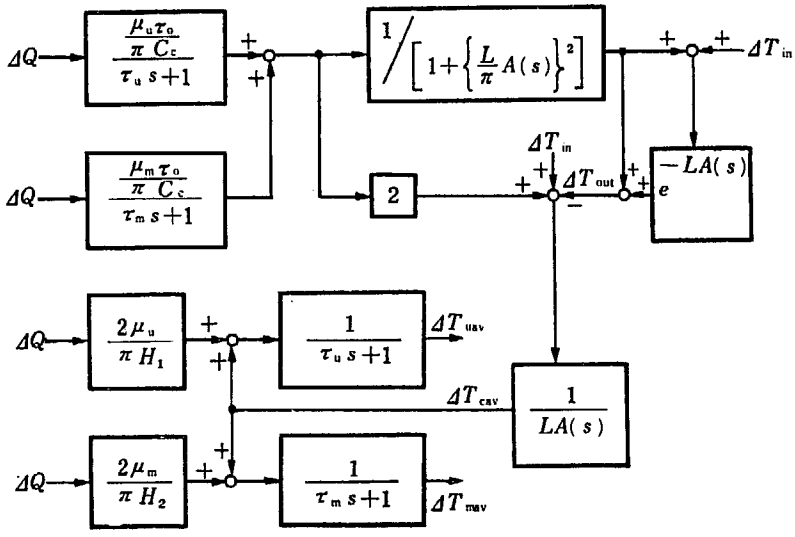

Fig. A. 8. 1. Block Diagram of Reactor Heat Transfer System (Distributed Parameter Model)

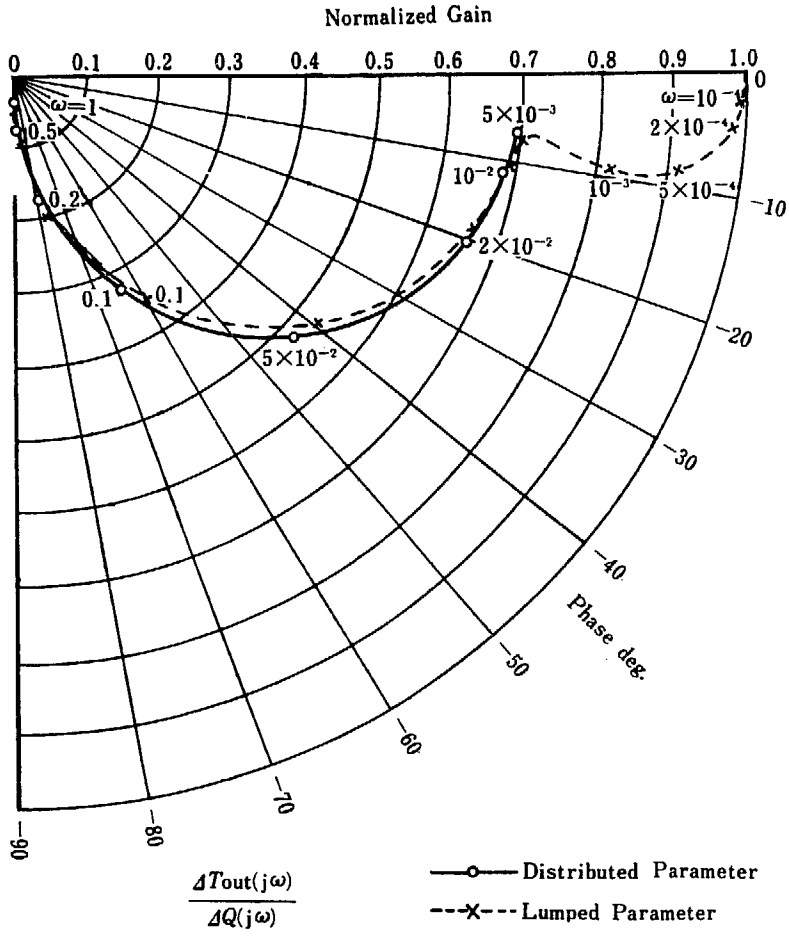

Fig. A. 8. 2. Frequency Response of ΔT_{out} to Change in ΔQ (A Comparison between a Distvibuted Parameter Model and a Lumped Parameter Model)

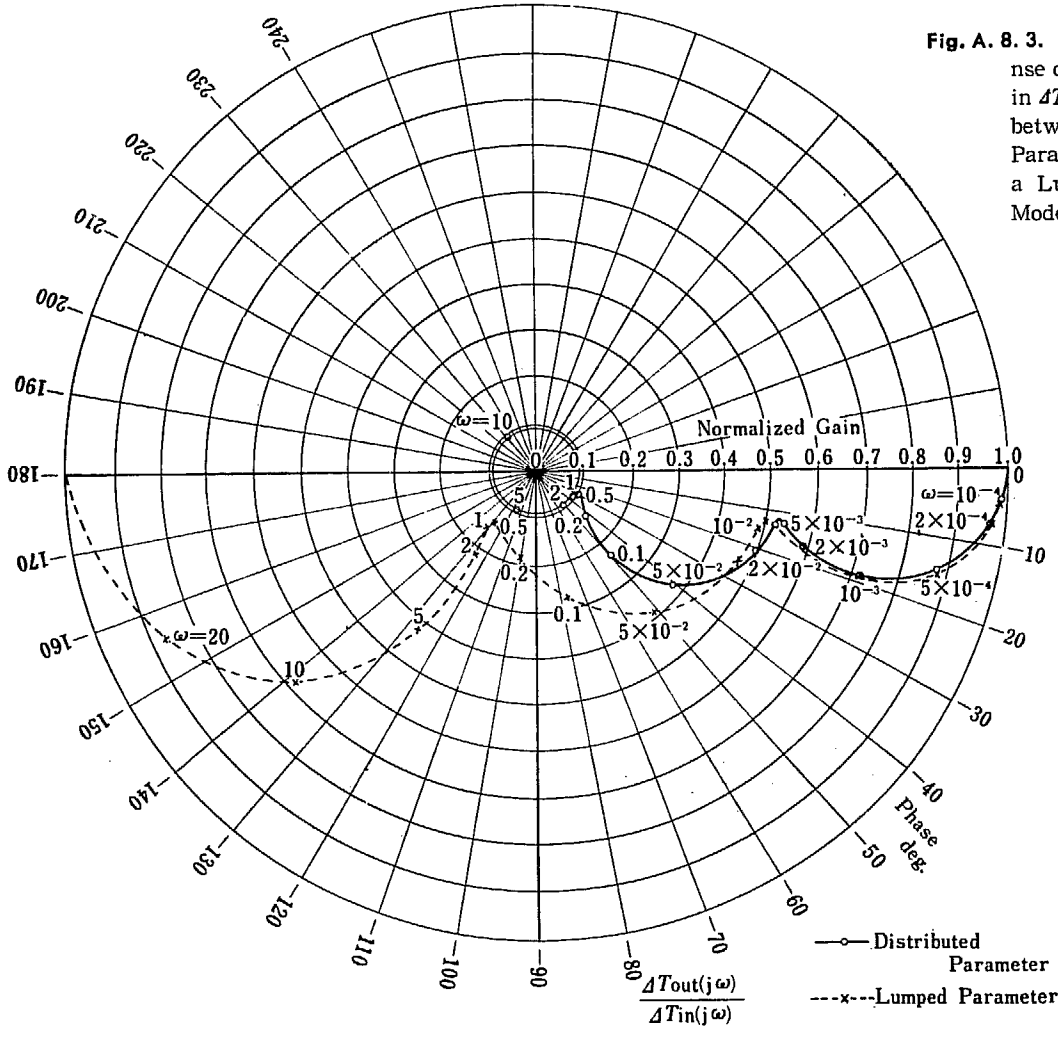

Fig. A. 8. 3. Frequency Response of ΔT_{out} to Change in ΔT_{in} (A Comparison between a Distributed Parameter Model and a Lumped Parameter Model)

List of Computer Results

Fig No.	Page	Parameter	Variables Recorded
(R-I)			
Fig. 2.2		$\rho_{ex}=1.2\times10^{-4}$ step, $\alpha_m=15\times10^{-5}$/°C	ρ, q, ΔT_u, ΔT_c, ΔT_m
Fig. 2.3		$\Delta T_{in}=0.02$°C/sec ramp, $\alpha_m=12.5\times10^{-5}$/°C	ρ, q, ΔT_u, ΔT_c, ΔT_m
Fig. 2.4		$\Delta T_{in}=-15$, -10, -5, 0, 5, 10, 15°C step, $\alpha_m=12.5\times10^{-5}$/°C	q
Fig. 2.5		$\Delta u=-0.5\,u_0$ step, $\alpha_m=12.5\times10^{-5}$/°C	ρ, q, ΔT_u, ΔT_c, ΔT_m
(R-II)			
Fig. 3.2		$\rho_{ex}=1.2\times10^{-4}$ step, $\alpha_m=15\times10^{-5}$/°C	ρ, q, ΔT_u, ΔT_f, ΔT_s, ΔT_{c1}, ΔT_{c2}, ΔT_m
Fig. 3.3		$\Delta T_{in}=0.02$°C/sec×60 sec ramp, $\alpha_m=15\times10^{-5}$/°C	ρ, q, ΔT_u, ΔT_f, ΔT_{fm}, ΔT_s, ΔT_{c1}, ΔT_{c2}, ΔT_m, ΔT_{in}
Fig. 3.4		$\Delta u=-0.02\,u_0$/sec×30 sec ramp, $\alpha_m=15\times10^{-5}$/°C	ΔT_u, ΔT_s, ΔT_f, ΔT_{fm}, ΔT_{c1}, ΔT_{c2}, ΔT_m
Fig. 3.5		$\Delta u=-0.02\,u_0$/sec×30 sec ramp, $\alpha_m=15\times10^{-5}$/°C	u, ρ, q
(R-III)			
Fig. 4.1.a		$\rho_{ex}=3\times10^{-4}$, 1.2×10^{-4} step, $\alpha_m=-5\times10^{-5}$/°C	q
Fig. 4.1.b		$\rho_{ex}=3\times10^{-4}$, 1.2×10^{-4} step, $\alpha_m=-5\times10^{-5}$/°C	ρ
Fig. 4.1.c		$\rho_{ex}=1.2\times10^{-4}$ step, $\alpha_m=-5\times10^{-5}$/°C	ΔT_u, ΔT_{fm}, ΔT_{c1}, ΔT_m
Fig 4.2		$\rho_{ex}=1.2\times10^{-4}$ step, $\alpha_m=15\times10^{-5}$/°C, $a=1.8$	$\alpha_u\Delta T_u$, $\alpha_s\Delta T_s$, $\alpha_m\Delta T_m$
Fig. 4.3		$\rho_{ex}=1.2\times10^{-4}$ step, $\alpha_m=15\times10^{-5}$/°C, $a=1.15$	$\alpha_u\Delta T_u$, $\alpha_s\Delta T_s$, $\alpha_m\Delta T_m$
Fig. 4.4		$\rho_{ex}=1.2\times10^{-4}$ step, $\alpha_m=15\times10^{-5}$/°C, $a=1.8$, 1.15	ΔT_{fm}
Fig. 4.5		$\rho_{ex}=3\times10^{-4}$, 1.2×10^{-4} step, $\alpha_m=15\times10^{-5}$/°C	q (with and without sleeve)
Fig. 4.6		$\rho_{ex}=1.2\times10^{-4}$ step, $\alpha_m=15\times10^{-5}$/°C	ΔT_u, ΔT_{fm}, ΔT_s, ΔT_{c1}, ΔT_m (with and without sleeve)
Fig. 4.7		$\rho_{ex}=3\times10^{-4}$, 1.2×10^{-4} step, $\alpha_m=15\times10^{-5}$/°C	ρ (with and without sleeve)
Fig. 4.8		$\Delta T_{in}=0.2$°C/sec×60 sec ramp, $\alpha_m=15\times10^{-5}$/°C	ρ, q, ΔT_u, ΔT_{fm}, ΔT_s, ΔT_{c1}, ΔT_{c2}, ΔT_m
Fig. 4.9		$\Delta T_{in}=0.2$°C/sec×60 sec $\alpha_m=-5\times10^{-5}$/C°	ρ, q, ΔT_u, ΔT_f, ΔT_{fm}, ΔT_{c1}, ΔT_{c2}, ΔT_m
Fig. 4.10		$\rho_{ex}=1.2\times10^{-4}$ step, $\alpha_m=-5\times10^{-5}$/°C, $\Delta T_{in}=\mu\Delta T_{out}(t-20)$, $\mu=0$, 0.5, 0.75, 0.9, 1.0	q
Fig. 4.11		$\rho_{ex}=1.2\times10^{-4}$ step, $\alpha_m=-5\times10^{-5}$/°C, $\Delta T_{in}=\mu\Delta T_{out}(t-20)$, $\mu=0$, 0.5, 0.75, 0.9, 1.0	ρ
Fig. 4.12		$\rho_{ex}=1.2\times10^{-4}$ step, $\alpha_m=15\times10^{-5}$/°C, $\Delta T_{in}=\mu\Delta T_{out}(t-20)$, $\mu=0$, 0.5, 0.75, 0.9, 1.0	q
Fig. 4.13		$\Delta u=-1\%$/sec×60 sec, -2%/sec×30 sec, -2%/sec×15 sec, -4%/sec×7.5 sec ramp, $\alpha_m=15\times10^{-5}$/°C	q
Fig. 4.14		$\Delta u=-0.02\,u_0$/sec×30 sec ramp, $\alpha_m=15\times10^{-5}$/°C	ρ
Fig. 4.15		$\Delta u=-1\%$/sec×60 sec, -2%/sec×30 sec, -2%/sec×15 sec ramp, $\alpha_m=-5\times10^{-5}$/°C	ΔT_u, ΔT_{fm}, ΔT_{c1}, ΔT_m
Fig. 4.16		$\Delta u=-1\%$/sec×60 sec, -2%/sec×30 sec, -2%/sec×15 sec ramp, $\alpha_m=-5\times10^{-5}$/°C	q
Fig. 4.17		$\Delta u=-2\%$/sec×30 sec, $\alpha_m=-5\times10^{-5}$/°C	ρ
Fig. 4.18		$\rho_{ex}=1.2\times10^{-4}$ step, $\alpha_m=15\times10^{-5}$/C	ΔT_u, ΔT_{fm}, ΔT_{c1}, ΔT_m
Fig. 5.1.1		$\rho_{ex}=1.2\times10^{-4}$ step, $\alpha_m=15\times10^{-5}$/°C	q (R-I, R-II, R-III)
Fig. 5.1.2		$\rho_{ex}=1.2\times10^{-4}$ step, $\alpha_m=-5\times10^{-5}$/°C	ΔT_{fm} (R-II, R-III), ΔT_u (R-I)
Fig. 5.1.3		$\rho_{ex}=1.2\times10^{-4}$ step, $\alpha_m=-5\times10^{-5}$/°C	q (R-II, R-III)
Fig. 5.1.4		$\Delta T_{in}=0.02$°C/sec, $\alpha_m=12.5\times10^{-5}$/°C (R-I)	ΔT_{fm} (R-II, R-III)
Fig. 5.1.5		$\Delta T_{in}=0.02$°C/sec×60 sec, $\alpha_m=15\times10^{-5}$/°C (R-II, R-III)	q (R-I, R-II, R-III)

Fig. No.	Page	Parameter	Variable Recorded
Fig. 5. 1. 6		$\Delta T_{in}=0.02$°C/sec ramp, $\alpha_m=12.5\times10^{-5}$/°C (R-I) $\Delta T_{in}=0.02$°C/sec×60 sec ramp, $\alpha_m=15\times10^{-5}$/°C (R-II, R-III)	ΔT_u (R-I), ΔT_{fm} (R-II, R-III)
Fig. 5. 1. 7		$u=-0.5\,u_0$ step, $\alpha_m=12.5\times10^{-5}$/°C (R-I) $u=-2\%u_0$/sec×30 sec ramp, $\alpha_m=15\times10^{-5}$/°C (R-II, R-III)	q (R-I, R-II, R-III)
Fig. 5. 1. 8		$u=-0.5\,u_0$ step, $\alpha_m=12.5\times10^{-5}$/°C (R-I) $u=-2\%u_0$/sec×30 sec ramp, $\alpha_m=15\times10^{-5}$/°C (R-II, R-III)	ΔT_u (R-I), ΔT_{fm} (R-II, R-III)
Fig. 5. 1. 9		$u=-2\%u_0$/sec×30 sec ramp, $\alpha_m=-5\times10^{-5}$/°C (R-II, R-III)	q (R-II, R-RIII)
Fig. 5. 1. 10		$u=-2\%u_0$/sec×30 sec ramp, $\alpha_m=-5\times10^{-5}$/°C (R-II, R-III)	ΔT_{fm} (R-II, R-III)
Fig. 5. 2. 3(a)		$\rho_{ex}=1.2\times10^{-4}$ step, $\alpha_m=15\times10^{-5}$/°C	q (R-II)
Fig. 5. 2. 3(b)		$\rho_{ex}=1.2\times10^{-4}$ step, $\alpha_m=15\times10^{-5}$/°C	ΔT_u, ΔT_s, ΔT_m (R-II)
Fig. 5. 2. 4(a)		$\rho_{ex}=1.2\times10^{-4}$, 3×10^{-4} step, $\alpha_m=15\times10^{-5}$/°C	q (R-III)
Fig. 5. 2. 4(b)		$\rho_{ex}=1.2\times10^{-4}$ step, $\alpha_m=15\times10^{-5}$/°C	ΔT_u, ΔT_s, ΔT_m (R-III)
Fig. 5. 2. 5		$\rho_{ex}=1.2\times10^{-4}$ step, $\alpha_m=15\times10^{-5}$/°C $\delta_u\times1.3$ $\delta_u\times0.7$, $\delta_s\times0.7$, $\delta_s\times1.3$, $\delta_m\times0.7$, $\delta_m\times1.3$	q (R-III)
Fig. 5. 2. 6		$\rho_{ex}=1.2\times10^{-4}$ step, $\alpha_m=15\times10^{-5}$/°C $K_u\times1.3$, $K_u\times0.7$, $K_s\times0.7$, $K_s\times1.3$, $K_m\times0.7$, $K_m\times1.3$	q (R-III)
Fig. 5. 2. 7		$\rho_{ex}=1.2\times10^{-4}$ step, $\alpha_m=15\times10^{-5}$/°C (R-II, R-III)	q (R-II, R-III)
Fig. 5. 2. 8		$\rho_{ex}=1.2\times10^{-4}$ step, $\alpha_m=15\times10^{-5}$/°C, $V_s/(V_s+V_m)=0.13$, 0.1	q (R-III)
Fig. 5. 3. 2		$\rho_{ex}=1.2\times10^{-4}$ step, $\alpha_m=0.5\times10^{-5}$, 2×10^{-5}, 3×10^{-5}, 3.5×10^{-5}, 4×10^{-5}, 4.5×10^{-5}/°C	q (R-I)
Fig. 5. 3. 3		$\rho_{ex}=1.2\times10^{-4}$ step, $\alpha_m=0.5\times10^{-5}$, 2×10^{-5}, 3×10^{-5}, 3.5×10^{-5}, 4×10^{-5}, 4.5×10^{-5}/°C	ΔT_u (R-I)
Fig. 5. 3. 4		$\rho_{ex}=1.2\times10^{-4}$ step, $\alpha_m=-1\times10^{-5}$, 0, 1×10^{-5}, 2×10^{-5}, 2.5×10^{-5}, 3×10^{-5}, 4×10^{-5}/°C	q (R-III)
Fig. 5. 3. 5		$\rho_{ex}=1.2\times10^{-4}$ step, $\alpha_m=10^{-5}$, 2.5×10^{-5}, 3×10^{-5}/°C	ΔT_u (R-III)
Fig. A. 5. 1		$\rho_{ex}=1.2\times10^{-4}$ step, $\alpha_m=15\times10^{-5}$/°C, Analog Comp., Digital Comp.	q (R-II)
Fig. A. 5. 2		$\rho_{ex}=1.2\times10^{-4}$ step, $\alpha_m=15\times10^{-5}$/°C, Analog Comp., Digital Comp.	T_{fm} (R-II)
Fig. A. 7. 1		$\rho_{ex}=1.2\times10^{-4}$ step, $\alpha_m=10.8\times10^{-5}$/°C	ρ, q, ΔT_u, ΔT_f, T_{c1}, ΔT_s, ΔT_m for R-II (Rev.)
Fig. A. 7. 2		$\Delta T_{in}=0.2$°C/sec×60 sec ramp, $\alpha_m=10.8\times10^{-5}$/°C	〃
Fig. A. 7. 3		$\rho_{ex}=1.2\times10^{-4}$ step	q (R-II, R-II (Rev.), R-III)